

# Role of XIAP in ubiquitin mediated regulation of Cdc42 and other Rho GTPases

## **Dissertation**

Zur Erlangung des Grades  
Doktor der Naturwissenschaften

Am Fachbereich Biologie  
Der Johannes Gutenberg-Universität Mainz

**Arun Murali**  
**Geb. am 22.10.1989 in Coonoor, India**

Mainz, 2017

Dekan:

1. Berichterstatter:
2. Berichterstatter:

Tag der mündlichen Prüfung: 3<sup>rd</sup> May,  
2018

## Table of Contents

Abbreviations	5
Abstract	8
Zusammenfassung	10
<b>1. INTRODUCTION</b>	<b>12</b>
<b>1.1 INHIBITOR OF APOPTOSIS PROTEINS</b>	<b>12</b>
1.1.1. Discovery and History of IAPs	12
1.1.2. Anatomy of IAPs	14
1.1.3. IAPs and apoptosis	16
1.1.4. IAPs and ubiquitin	18
1.1.4.1. Ubiquitin	18
1.1.4.2. Auto and cross-ubiquitination of IAPs	20
1.1.4.3. IAPs, ubiquitin and the NF- $\kappa$ B pathway	21
1.1.4.3.1. <i>Canonical NF-<math>\kappa</math>B signaling pathway</i>	22
1.1.4.3.2. <i>Non-canonical NF-<math>\kappa</math>B signaling pathway</i>	23
1.1.5. IAPs and their role in tumorigenesis and tumor progression	24
1.1.6. IAPs and cellular differentiation	25
1.1.7. IAPs and cell migration	26
<b>1.2 RHO GTPASES</b>	<b>27</b>
1.2.1. Introduction	27
1.2.2. Discovery of Rho GTPases	28
1.2.3. Anatomy of Rho GTPases	30
1.2.3.1. G-domain	30
1.2.3.2. Insert region	33
1.2.3.3. C-terminal domain	33
1.2.4. Regulation of Rho GTPases	34
1.2.4.1. Regulation of Rho GTPases by GEFs, GAPs and RhoGDI	34
1.2.4.2. Post-translational regulation of Rho GTPases	36
1.2.4.2.1. Lipid modifications	36
1.2.4.2.2. Phosphorylation of Rho GTPases	39
1.2.4.2.3. SUMOylation and Ubiquitination	40
1.2.4.2.4. Other post-translational modifications	41
1.2.5. Rac1 and the WAVE2 complex	43
1.2.6. RhoA and RhoB	45
1.2.7. Cdc42	47
1.2.8. Rho GTPases and cell migration	49
1.2.9. Rho GTPases, IAPs and cell migration	51
<b>2. MATERIALS AND METHODS</b>	<b>54</b>
<b>2.1 CELL BIOLOGY METHODS</b>	<b>54</b>
2.1.1. Cell lines	54
2.1.2. Production of Lentiviruses	55
2.1.3. Transfection of siRNAs	55
2.1.4. Cell Culture and Transfection	56
<b>2.2 MOLECULAR BIOLOGY METHODS</b>	<b>56</b>
2.2.1. Vectors, cDNAs and constructs	56
2.2.2. Site-directed mutagenesis	57
2.2.3. RT-PCR	58
<b>2.3 BIOCHEMICAL METHODS</b>	<b>59</b>
2.3.1. Antibodies	59
2.3.2. SDS-PAGE and Western Blotting	60
2.3.3. Protein-protein interaction assays	61

2.3.4.	Immunoprecipitation	62
2.3.5.	HIS-TUBE pull down	63
2.3.6.	F-actin assay - FACS analysis	63
<b>2.4</b>	<b>PROTEOMICS</b>	<b>64</b>
2.4.1.	Determination of ubiquitin sites on proteins	64
2.4.2.	Whole Proteome Analysis	65
<b>2.5</b>	<b>PHENOTYPICAL STUDIES</b>	<b>66</b>
2.5.1.	Immunofluorescence and counting of filopodia	66
2.5.2.	Wound healing assay	66
2.5.3.	Lung colonization experiments	67
<b>2.5</b>	<b>APPENDIX- MATERIAL</b>	<b>67</b>
<b>3.</b>	<b>RESULTS</b>	<b>69</b>
<b>3.1</b>	<b>UBIQUITIN-MEDIATED REGULATION OF CDC42 BY XIAP</b>	<b>69</b>
3.1.1	Role of XIAP in regulating Cdc42 stability and activity	69
3.1.1.1	Depletion of XIAP leads to Cdc42 upregulation	69
3.1.1.2	XIAP contributes to the proteostasis of Cdc42	71
3.1.1.3	Depletion of XIAP leads to basal & EGF induced Cdc42 activation	72
3.1.2	Role of XIAP in filopodia formation	73
3.1.2.1	Depletion of XIAP enhances number of filopodia	73
3.1.2.2	XIAP regulates filopodia formation through Cdc42	75
3.1.2.3	EGF stimulation mimics XIAP depletion	76
3.1.3	Molecular mechanisms of XIAP-mediated Cdc42 degradation	77
3.1.3.1	XIAP directly binds to Cdc42	77
3.1.3.2	XIAP is an E3 ubiquitin ligase of Cdc42	78
3.1.3.3	XIAP ubiquitinates Cdc42 on Lysine 166	82
3.1.3.4	Molecular modeling of the XIAP-Cdc42 interface	83
3.1.4	Role of XIAP in tumor cell metastases	85
<b>3.2</b>	<b>REGULATION OF RHOA, RAC1 AND RHOB BY IAPs</b>	<b>86</b>
3.2.1	XIAP binds to but does not ubiquitinate RhoA	86
3.2.2	Control of Rac1 and WAVE2 complex by IAPs	87
3.2.2.1	clAP1 synthesises K11/K48 polyubiquitin chains on Rac1	87
3.2.2.2	IAP-mediated cell morphology is dependent on the WAVE regulatory complex	88
3.2.2.3	Depletion of IAPs promote actin polymerization	90
3.2.2.4	IAP depletion influences WAVE2 phosphorylation	92
3.2.3	RhoB stability is influenced by XIAP	93
<b>4.</b>	<b>DISCUSSION</b>	<b>96</b>
4.1	Loss of XIAP promotes filopodia formation in a Cdc42 dependent manner	96
4.2	XIAP directly binds to Cdc42	98
4.3	XIAP is a direct E3 ligase of Cdc42	101
4.4	Loss of XIAP promotes tumor cell metastases in vivo	106
4.5	Synergistic activation of WAVE complex upon IAP depletion	107
4.6	Outlook and Future Perspectives – IAPs and Rho GTPases	110
5.	References	114
6.	List of Publications	115
7.	Curriculum Vitae	133
8.	Acknowledgements	136

## Abbreviations

ATP	Adenosine triphosphate
APS	Ammonium persulfate
ARTS	Apoptosis-related protein in the TGF- $\beta$ signaling pathway
Bad	Bcl-2 antagonist of cell death
Bak	Bcl-2 homologous antagonist killer
Bax	Bcl-2 associated X protein
Bcl-2	B-cell lymphoma 2
Bid	BH3 interacting-domain death agonist
BIR	Baculoviral IAP repeat
BRUCE	BIR containing ubiquitin conjugating enzyme
BSA	Bovine serum albumin
$^{\circ}\text{C}$	degree Celsius
CARD	Caspase recruitment domain
cDNA	copy DNA
Cdc42	Cell division control protein 42 homolog
CHX	Cycloheximide
clAP1	Cellular IAP1
clAP2	Cellular IAP2
CMV	Cucumber mosaic virus
CO <sub>2</sub>	Carbon dioxide
CpGV	<i>Cydia pomonella</i> granulosis virus IAP
C-terminal	Carboxy-terminal
CR	Conserved regions
C-RAF	RAF kinase C isoform
DAPI	4'-6-Diamidino-2-phenylindole
ddH <sub>2</sub> O	Double distilled water
Diablo	Direct IAP binding protein with low Pi
DIAP1	Drosophila IAP protein 1
DIAP2	Drosophila IAP protein 2
DMEM	Dulbecco's modified Eagle's medium
DMSO	Dimethylsulfoxide
DNA	Deoxyribonucleic acid
DTT	Dithiothreitol
DUBs	Deubiquitinating enzymes
E1	Ubiquitin activating enzyme
E2	Ubiquitin conjugating enzymes
E3	Ubiquitin ligating enzyme
EDTA	Ethylenediamine tetra-acetic acid
ECM	Extracellular matrix
<i>E.coli</i>	<i>Escherichia coli</i>
EGF	Epidermal growth factor
EGFR	Epidermal growth factor receptor
EMT	Epithelial to Mesenchymal transition
ER	Endoplasmic Reticulum
ERK1/2	Extracellular-regulated kinase 1/2

EV	Empty Vector
FADD	Fas-associated death domain
FAK	Focal adhesion kinase
FCS	Fetal calf serum
GAP	GTPase activating protein
GDP	Guanosine diphosphate
GEF	Guanine nucleotide exchange factor
GFP	Green fluorescent protein
GPCR	G-protein-coupled receptor
GSH	Glutathione
GST	Glutathione-S-transferase
GTP	Guanosine triphosphate
h	hours
HCC	Hepatocellular carcinoma
HECT	Homologous to the E6-AP Carboxyl Terminus
His	Histidine
HEPES	2-[4-(2-hydroxyethyl)piperazin-1-yl]ethanesulfonic acid
IAC	IAP antagonist compound
IAP	Inhibitor of apoptosis
IBM	IAP-binding motif
IgG	Immunoglobulin G
ILP2	IAP like protein 2
IP	Immunoprecipitation
kb	Kilobase pairs
kDa	Kilodalton
LB	Luria-Bertani medium
MAPK	Mitogen-activated protein kinase
MAP2K	MAPK kinase
MAP3K	MAPK kinase kinase
MEF	Mouse Embryonic Fibroblasts
MEK1/2	MAPK/ERK kinase 1/2
MEKK2	Mitogen-activated protein kinase kinase kinase 2
MEKK3	Mitogen-activated protein kinase kinase kinase 3
MET	Mesenchymal to Epithelial Transition
ML-IAP	Melanoma IAP (Livin)
MP 1	MEK partner 1
M2PK	Pyruvate kinase isoenzyme type M2
min	minute
MMP	Matrix metalloproteinase
mRNA	Messenger RNA
MS	Mass spectrometry
MW	Molecular weight
no.	Number
NAIP	Neural Apoptosis Inhibitory Protein
NP-40	Nonidet P40
N-terminus	Amino terminus
NOD	Nucleotide-binding and oligomerization domain
NSCLC	Non-small-cell lung carcinoma
N-terminal	Amino-terminal
Omi/HtrA2	High temperature requirement protein A2

OpiAP	<i>Orygia psuedogata</i> nuclear polyhedrosis virus IAP
PAK	p21-activated protein kinase
PARP-1	Poly-[ADP-ribose]-polymerase 1
PBD	PAK binding domain
PBS	Phosphate buffered saline
PCD	Programmed Cell Death
PCR	Polymerase chain reaction
PI3K	Phosphatidylinositol 3-kinase
PMSF	Phenylmethylsulfonylfluorid
Rac1	Ras-related C3 botulinum toxin substrate 1
RAF	Rapidly accelerated fibrosarcoma
Ras	Rat sarcoma
RBD	Ras binding domain
RBR	Ring between Ring
RhoA	Ras homolog gene family, member A
RhoB	Ras homolog gene family, member B
RhoC	Ras homology gene family, member C
RING	Really Interesting New Gene
Rip	Receptor-interacting protein
RNA	Ribonucleic acid
ROCK	Rho-associated, coiled coil containing protein kinase
RPMI	Roswell Park Memorial Institute medium
SDS	Sodium dodecyl sulphate
SDS-PAGE	SDS-Polyacrylamide gel electrophoresis
shRNA	small hairpin ribonucleic acid
siRNA	small interfering RNA
Smac	Second mitochondrial activator of caspases
SUMO	Small-ubiquitin-related modifier
TAB1	TAK1 binding protein 1
TAK1	TGF beta-activated kinase 1
TEMED	N,N,N,N- Tetramethylethyldiamine
TGF- $\beta$	Transforming growth factor-beta
TNF	Tumor necrosis factor
TNF-R1	Tumor necrosis factor alpha receptor 1
TLR	Toll-like receptors
T <sub>m</sub>	Melting temperature
TRAF	TNFR-associated factor
TRAF1	TNFR-associated factor 1
TRADD	TNFR-associated death domain
TRAIL	TNF-alpha-related apoptosis inducing ligand
Tris	Tris-hydroxymethyl-aminomethane
Ub	Ubiquitin
UBA	Ubiquitin-associated domain
UV	Ultra Violet
VEGFR	Vascular endothelial growth factor receptor
WAVE2	WASP family Verprolin-homologous protein 2
WASP	Wiskott-Aldrich syndrome protein
WT	Wild Type
XAF1	X-linked inhibitor of apoptosis-associated factor 1
XIAP	X-linked apoptosis protein (BIRC4)

## **Summary**

Inhibitor of Apoptosis proteins (IAPs) are evolutionarily conserved, multifunctional proteins characterized by the presence of a baculoviral IAP repeat (BIR) domain. Initially discovered as endogenous inhibitors of apoptosis, recent studies have identified these proteins at the heart of various cellular processes. IAPs were shown to be integral in modulating cellular morphology and migration by regulating C-Raf kinase and Rac1, a Rho GTPase involved in cell shape and migration, the latter by targeting it for proteasomal degradation.

This thesis aimed to further uncover the role of IAPs in the regulation of actin cytoskeleton and the dynamics of tumor cell migration. We discover that XIAP negatively regulates Cdc42 proteostasis as loss of XIAP led to an increase in Cdc42 protein levels. Further, the levels of GTP bound Cdc42, the active form of the Rho GTPase is found to be increased in XIAP depleted cells. Depletion of XIAP enhances filopodia formation in a Cdc42 dependent manner and this phenomenon phenocopies the effect of EGF stimulation. XIAP binds to Cdc42 and directly conjugates poly ubiquitin chains to the Lysine 166 of Cdc42 targeting it for proteasomal degradation. Finally, XIAP depletion promotes lung colonization of tumor cells in mice in a Cdc42 dependent manner. To conclude, these observations suggest that XIAP is a direct E3 ubiquitin ligase of Cdc42. We further studied the downstream components of the Rac1 pathway, namely the WAVE (WASP family verprolin-homologous protein) complex in the context of IAP-regulated cell migration. As expected, integrity of the WAVE2 complex is required for elongated morphology as well as enhanced migration upon IAP depletion. We showed that XIAP depletion leads to WAVE2 phosphorylation as well as enhanced actin polymerization. We could also demonstrate that XIAP does not indiscriminately ubiquitinate Rho GTPases – while Cdc42 and Rac1 were ubiquitinated by XIAP, RhoA was not.

Finally, by employing quantitative mass spectrometry based approaches we identified several factors that are regulated by XIAP. Preliminary validation of



these results revealed that XIAP influence the stability of RhoB, another member of the Rho GTPase family.

Taken together, these observations reaffirm and extend the role of XIAP in the regulation of cell shape and migration. Rho GTPases work in cohorts both spatially and temporally in influencing cell migration and are primarily regulated by Guanine nucleotide exchange factors (GEFs) and GTPase activating proteins (GAPs). However, recent advances in the field have identified ubiquitin mediated degradation as a novel, non-canonical way of regulating these Rho GTPases and this study sheds molecular insights into this ubiquitin dependent regulation of Rho GTPases and the actin cytoskeleton.

## **Zusammenfassung**

„Inhibitor of apoptosis proteins“ (IAPs) sind evolutionär konservierte, multifunktionelle Proteine, die durch die Anwesenheit einer baculoviralen IAP-Wiederholungsdomäne (engl.: baculoviral IAP repeat (BIR)) gekennzeichnet sind. Ursprünglich als endogene Apoptose-Inhibitoren entdeckt, konnte in neueren Studien gezeigt werden, dass diese Proteine eine tragende Rolle in zahlreichen zellulären Prozessen spielen. Unter anderem konnte gezeigt werden, dass IAPs durch die Regulierung der CRAF- Proteinkinase sowie Rac1, eine für die Zellausprägung essentielle Rho GTPase, wesentlich an Zellmorphologie- und Zellmigrationsprozessen beteiligt sind. Dabei wird Letztere durch IAPs für den proteasomalen Abbau markiert.

Das Ziel dieser Arbeit war die Untersuchung der Rolle von IAPs in der Regulierung des Aktin-Zytoskeletts und der Tumorzellmigration. Da der Verlust von XIAP zu einem erhöhten Proteingehalt an Cdc42 führt, konnte hierdurch gezeigt werden, dass XIAP die Cdc42 Proteostase negativ reguliert. Weiterhin konnte gezeigt werden, dass der Gehalt an GTP-gebundenem Cdc42, der aktiven Form der Rho-GTPase, in XIAP-defizienten Zellen erhöht ist. Diese XIAP-Defizienz führt außerdem zu einer verstärkten Filopodien-Bildung in einem Cdc42-abhängigen Mechanismus, was ebenfalls bei der EGF-Stimulation zu sehen ist. XIAP bindet an Cdc42, wodurch Polyubiquitinketten an das Lysin 166 von Cdc42 konjugiert werden, was dieses für den proteasomalen Abbau markiert. Außerdem kommt es in Mäusen durch die Depletion von XIAP zur Einwanderung von Tumorzellen in die Lungen. Dieser Prozess ist ebenfalls Cdc42-abhängig. Diese Beobachtungen zeigen, dass XIAP eine direkte E3-Ubiquitin-Ligase von Cdc42 ist. Weiterhin wurden die „downstream“-Komponenten des Rac1-Signalwegs, insbesondere der „WASP family verprolin-homologous protein“ (WAVE)- Komplex im Kontext einer IAP-regulierten Zellmigration untersucht. Bei einer IAP-Defizienz wird die Unversehrtheit des WAVE2-Komplexes sowohl für die Zellmorphologie als auch für eine gesteigerte Migration benötigt. Es konnte gezeigt werden, dass eine Depletion von XIAP zu einer

Phosphorylierung von WAVE2 und einer gesteigerten Aktin-Polymerisierung führt. Außerdem wurde in dieser Arbeit gezeigt, dass XIAP ausschließlich spezifische Rho-GTPasen ubiquitiniert- während Cdc42 und Rac1 von XIAP ubiquitiniert werden, wird es RhoA beispielsweise nicht.

Schließlich konnten mithilfe von massenspektrometrischen Untersuchungen einige Faktoren identifiziert werden, die durch XIAP reguliert werden. Erste Ergebnisse dieser Untersuchungen zeigten, dass XIAP die Stabilität von RhoB, einem weiteren Mitglied der Rho-GTPase-Familie, beeinflusst.

Zusammenfassend lässt sich sagen, dass in dieser Arbeit die Rolle von XIAP in der Regulation der Zellmorphologie und -migration bestätigt werden konnte. Die Rho-GTPasen interagieren bei zellmorphologischen Prozessen sowohl räumlich als auch zeitlich miteinander und werden hierbei primär durch „Guanine nucleotide exchange factors“ (GEFs) und „GTPase activating proteins“ (GAPs) reguliert. Zusätzlich konnte der Ubiquitin-abhängige Abbau als Möglichkeit der Regulierung dieser Rho-GTPasen und des Aktin-Zytoskeletts identifiziert werden.

# 1. Introduction

## 1.1 Inhibitor of Apoptosis Proteins

### 1.1.1 Discovery and History of IAPs

Inhibitor of Apoptosis Proteins (IAPs) are a highly conserved class of multifunctional proteins. IAPs were discovered in the early 90's in the laboratory of Lois Miller through the genetic screening of baculoviruses *Orgyia pseudotsugata* nuclear polyhedrosis virus (OpMNPV) and *Cydia pomonella* granulosis virus (CpGV)<sup>1,2</sup>. The Miller lab employed an assay in which infection by a mutant strain of a third baculovirus, *Autographa californica* nuclear polyhedrosis virus (AcMNPV) results in unconstrained host (lepidopteran SF-21 cells) cell apoptosis. Using this technique, the CpGV and the OpMNPV genomes were screened for loci which would suppress this cell death, resulting in the identification of founding members of a new class of anti-apoptotic genes encoding CpiAP and OpiAP, two proteins which share both homology and the ability to block apoptosis via a wide number of apoptotic triggers in insect cells.

Since their discovery, numerous homologues of these proteins have been identified and characterized in a wide range of species. The first mammalian IAP protein, Neuronal Apoptosis Inhibitory Protein (NAIP/BIRC1) was discovered in 1995 by N. Roy and her colleagues in an effort to determine the genetic basis of Spinal Muscular Atrophy (SMA), a neurodegenerative disease<sup>3</sup>. Soon after this discovery of NAIP, other IAPs were discovered by employing genetic and biochemical screens as well as by the presence of conserved domains among its members (Please see section 1.1.2). Eight IAPs have been identified in mammals - BIRC1 (neuronal IAP/NAIP – Neuronal Apoptosis Inhibitory Protein), BIRC2 (cellular IAP1/cIAP1/HiAP2), BIRC3 (cellular IAP2/cIAP2/HiAP1), BIRC4 (X-linked IAP/XIAP/hILP), BIRC5

(Survivin), BIRC6 (BIR containing ubiquitin conjugating enzyme/BRUCE/Apollon), BIRC7 (Melanoma IAP/ML-IAP/Livin) and BIRC8 (IAP-like protein 2/hILP2/Ts-IAP).

While IAPs were originally thought to function as caspase inhibitors, they have been shown to play a major role in a multitude of other cellular processes in recent years. Due to the elevated expression of some IAPs in tumors, IAP antagonist compounds (IAC) have been designed to target them. Further, IAPs have been implicated in the Ubiquitin dependent signaling machinery controlling both canonical and non canonical pathways of NF $\kappa$ B activation, which controls important cellular processes like inflammation, cell survival and immune responses<sup>4</sup>. A study by Bertrand et al. identified cIAP1 and cIAP2 as important effectors of innate immunity, mediating critical steps in Nucleotide-binding oligomerization domain-containing protein (NOD) signaling<sup>5</sup>. Labbe et al. reported that the cIAPs were critical effectors of the inflammasomes and were required for efficient caspase-1 activation<sup>6</sup>. Dagenais et al. reported that cIAP2-deficient mice had impaired activation of the regenerative inflammasome–interleukin-18 (IL-18) pathway<sup>7</sup>. The cIAPs were shown to attenuate TNF signaling during hepatitis B infection, and they restrict the death of infected hepatocytes, thus allowing viral persistence<sup>8</sup>. Work from our lab revealed yet another side of IAPs in the regulation of tumor cell shape, migration and differentiation. IAPs, specifically XIAP, cellular IAP1 (cIAP1) and melanoma inhibitor of apoptosis protein (ML-IAP) were discovered to negatively regulate the stability of CRAF kinase through the Hsp90 protein quality-control machinery and thus regulate the Mitogenic Activated Protein Kinase (MAPK) cascade responsible for driving cell migration<sup>9,10</sup>. Further, XIAP and c-IAP1 have been shown to function as the direct E3 ubiquitin ligases of the Rho GTPase Rac1<sup>11</sup>. Recently, it was also shown that XIAP plays a novel role in regulating human myoblast differentiation. XIAP and cIAP1 ubiquitinate MEKK2 and MEKK3 and interfere with the ERK5 signaling cascade<sup>12</sup>. These studies attest to the growing realization in the field that IAPs are extremely pleiotropic proteins.

### 1.1.2. Anatomy of IAPs

IAPs are characterized by the presence of evolutionarily conserved **B**aculoviral **I**AP **R**epeat (BIR) domain - a zinc finger domain of approximately 70 amino acid residues, containing the characteristic sequence CX<sub>2</sub>CX<sub>16</sub>HX<sub>6</sub>C. They are arranged in three stranded  $\beta$ -sheets surrounded by four short  $\alpha$ -helices that coordinate a zinc ion by one histidine and three cysteine residues<sup>13–15</sup>. Containing both hydrophobic and hydrophilic residues on its surface, this BIR domain core is responsible for mediating protein-protein interactions. They can be sub-classified into two groups – type I and type II domains. While type II BIR domains are able to bind to the IAP-binding motifs (IBMs) via their hydrophobic binding cleft, the type I BIR domains only contain a shallow surface groove<sup>16–18</sup>. The IBMs are N-terminal tetrapeptides with A-(V/T/I)-(P/A)-(F/Y/I/V) consensus sequence<sup>19</sup>. Also, known inhibitors of the IAPs like Smac/Diablo and Omi/HtrA2 contain the AVPI consensus sequence<sup>20</sup>. XIAP, c-IAP1 and c-IAP2 each contain one type I domain (BIR1) and two type II domains (BIR2 and 3)<sup>18</sup>. Small structural changes in the grooves of BIR domains confer their specificity for a particular IBM and thus, to a particular IBM containing protein. For example, the type I BIR domain of cIAPs (BIR1) binds to tumor necrosis factor receptor (TNFR)-associated factor 1 (TRAF1) and TRAF2 whereas that of XIAP mediates interaction with transforming growth factor- $\beta$  (TGF $\beta$ )-associated kinase (TAK1) binding protein, TAB1<sup>21–23</sup>. The BIR2 domain and the preceding linker region of XIAP bind to IBMs of caspase-3 and caspase-7, effector caspases of the apoptotic pathway and the BIR3 binds to IBM of caspase-9, which is an initiator caspase. Binding of XIAP to caspase-3 and 7 prevents substrate entry and thereby results in inhibition of the catalytic activity of the caspases<sup>24,25</sup>. In the case of caspase-9, the BIR3 domain of XIAP binds to the homo-dimerization surface of the protein resulting in inactivation, as caspase-9 requires a dimerization induced conformational change to generate a productive catalytic pocket<sup>26</sup>.

Three of the IAPs – XIAP, cIAP1 and cIAP2 contain an evolutionarily conserved Ubiquitin-associated (UBA) domain which exhibits Ubiquitin binding properties and binds to both poly ubiquitin as well as mono ubiquitin (Figure 1) <sup>27,28,15,29</sup>. Like other UBA domains, it has a compact structure consisting of three  $\alpha$ -helices. This interaction with Ubiquitin is based on the interplay of the classical hydrophobic patch surrounding Ile<sub>44</sub> of Ubiquitin, the highly conserved MGF hydrophobic binding loop and the LL motif of the UBA domain <sup>27,29,30</sup>. In c-IAPs, the mutation of the MGF motif or deletion of the entire UBA domain leads to impaired NF- $\kappa$ B activation and defective 26S proteasomal degradation of IAPs. Further, the UBA domains of c-IAP1 and 2 enhance ubiquitylation by facilitating E2-Ub conjugate recruitment. Mutation of the MGF and LL motifs cause unfolding of c-IAP1 and consequently increased multi-monoubiquitylation <sup>31</sup>.

Of the eight IAPs, five of them – cIAP1, cIAP2, XIAP, ML-IAP and ILP2 also contain a Really Interesting New Gene (RING) zinc-finger carboxy terminal domain which confers them with E3 ubiquitin ligase activity (Figure 1) <sup>32,33</sup>. Probably the most important feature of this 40 amino acid zinc-coordinating domain is the recruitment of E2 ubiquitin conjugating enzymes <sup>32</sup>. While individual IAPs have unique E2 partners, the RING domains of IAP proteins show a preference for the Ubch5 family of E2 enzymes <sup>34</sup>. The RING domains of IAPs have been shown to be responsible for auto-ubiquitination, cross-ubiquitination of other IAPs and substrate ubiquitination. Studies with IAC and other small molecule inhibitors of IAPs suggest that IAP E3 ligase activity might be affected by closed conformation of the BIR3-RING domains. Disruption of this interaction leads to enhanced RING-RING dimerization, E3 ligase activity and autoubiquitylation and proteasomal degradation of these IAPs <sup>35</sup>. Ubiquitination is discussed in more detail in section 1.1.4.

Finally, cIAP1 and cIAP2 also contain an evolutionarily conserved caspase recruitment domain (CARD) whose function is not fully understood till date. Typically, these domains mediate oligomerization with other CARD containing proteins. A study in 2011 suggested that the closed conformation of cIAP1 is

stabilized by the CARD and BIR3 domain of the protein. Consequently, this prevents E2 binding and suppresses the activation of the E3 ligase activity of cIAP1 mediated by the RING domain<sup>36</sup>.

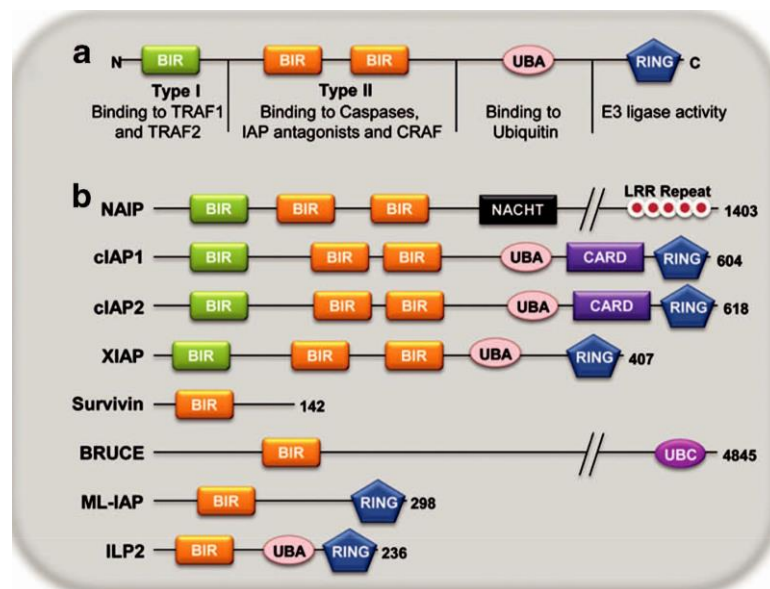


**Figure 1:** a) The prototypical IAP is depicted showcasing its Type I and II BIR domains, the Ubiquitin Binding Domain (UBA) and the RING domain. The function of each domain is mentioned below. b) Each mammalian IAP is depicted along with the functional domains they contain. Figure adapted from Oberoi-Khanuja, Murali, Rajalingam, 2013. See text for details

### 1.1.3. IAPs and apoptosis

Apoptosis was a term first used in the now-seminal paper by Kerr, Wyllie and Currie in 1972 to describe a morphologically distinct form of cell death<sup>37</sup>. In the years since, apoptosis has since been recognized as a distinct and important form of programmed cell death (PCD) that occurs in multicellular organisms. Apoptosis is a genetically controlled, highly regulated process consisting of a cascade of signaling events culminating in the activation of executioner enzymes known as caspases (**c**ysteine **a**spar**tate** specific **p**rote**a**ses) that cleave hundreds of substrates to effect the morphological features. There are four entwined pathways described for caspase activation: (1) Death receptor pathway (Extrinsic Pathway) induced by death ligand binding (FasL, TNF, etc.) to their receptors, (2) Mitochondrial pathway (Intrinsic Pathway) induced by release of cytochrome *c* and pro-apoptotic proteins from the mitochondria due to mitochondrial outer membrane permeabilization, (3) Endoplasmic reticulum (ER) stress-induced pathway and



(4) the apoptotic pathway induced via cytotoxic T cells and NK cells by granzyme B mediated cleavage and activation of caspases<sup>38,39</sup>.

Caspases reside in proteolytic cascades that are usually started by initiator caspases, such as caspase-9, caspases-2 and caspase-8. These initiator caspases cleave and activate downstream effector caspases, like caspase-3 and caspase-7<sup>40,41</sup>. Following this activation, certain members of the IAP family can regulate caspases<sup>42</sup>. This is valid even in *Drosophila* where loss of DIAP1 leads to spontaneous caspase-mediated apoptosis<sup>43–46</sup>. While most IAPs have a role in caspase inhibition, mammalian XIAP is the only direct inhibitor of caspases<sup>47</sup>. XIAP directly binds to and inhibits caspases-3, -7, and -9 by different mechanisms. In the case of caspases -3 and -7, apoptotic induction first leads to partial caspase cleavage. This exposes their N-terminal IBM motif that is targeted by XIAP through its BIR2 domain. While the BIR2 domain itself plays little direct role in the inhibitory mechanism, it is nevertheless crucial as it makes contacts with the residues outside the caspase catalytic pocket. In fact, it is the linker region preceding the BIR2 domain that plays a key role as it directly obstructs the catalytic pocket of the caspases, thus preventing substrate entry<sup>24,25</sup>. Caspase-9 inhibition works differently as this caspase requires dimerization to generate the catalytic pocket for substrate cleavage. XIAP binds to the homodimerization surface thus interfering with the conformational changes required for caspase activation<sup>26</sup>. However, it is not just the BIR domains that are important for caspase inhibition and there have been studies that show that the RING domains of the IAPs also play a vital role in this inhibitory process. Expression of the RING-deletion XIAP mutant did not compensate for the deficiency of XIAP in stem cells and thymocytes and increased caspase-3 activity and apoptosis<sup>48</sup>. Further, XIAP has been observed to induce the K48 ubiquitination of active caspases leading to their degradation<sup>49</sup>.

Constant crosstalk among apoptotic pathways and their regulators ensures an appropriate outcome, be it cell death or survival. In certain cell types, death receptor stimulation results in caspase-8 cleavage that isn't an IAP substrate.

Activated caspase-8 then cleaves and activates Bid, a pro-apoptotic Bcl-2 family member. This stimulates the formation of Bax and Bak pores in the Mitochondrial Outer Membrane, resulting in the activation of the mitochondrial pathway, thus releasing pro-apoptotic proteins like IAP antagonists. This clearly shows how IAPs are placed at a crucial pivot between cell death and survival.

#### **1.1.4. IAPs and Ubiquitin**

##### **1.1.4.1. Ubiquitin**

Ubiquitylation is a covalent post-translational modification where Ubiquitin (Ub), a 76 amino acid protein is attached to target proteins. This can have profound effects on the stability of the target protein, localization or interactions with other proteins. This process is achieved by the sequential actions of an E1 Ub-activating enzyme, an E2 Ub-conjugating enzyme and an E3 Ub ligase<sup>50,51</sup>. The first step in this cascade is the ATP-dependent activation of Ub by the E1 (Figure 2), which links the C-terminal glycine residue of Ub via a thioester bond to a cysteine residue within the E1 active site<sup>52</sup>. The second step involves the transfer of the activated Ub intermediate to the catalytic cysteine residue of an E2 enzyme. The E3 ligase finally conjugates the Ub via an isopeptide bond to the  $\epsilon$ -amino group of the target lysine (K) of the substrate<sup>53</sup>. The incredible amount of complexity and specificity of this process is put to effect by the diversity of its constituent enzymes: two known E1, 39 E2s and hundreds of E3s<sup>54</sup>. An extension to this process is by E4 enzymes, or ubiquitin-chain elongation factors, which add pre-formed poly ubiquitin chains to substrates<sup>55</sup>.

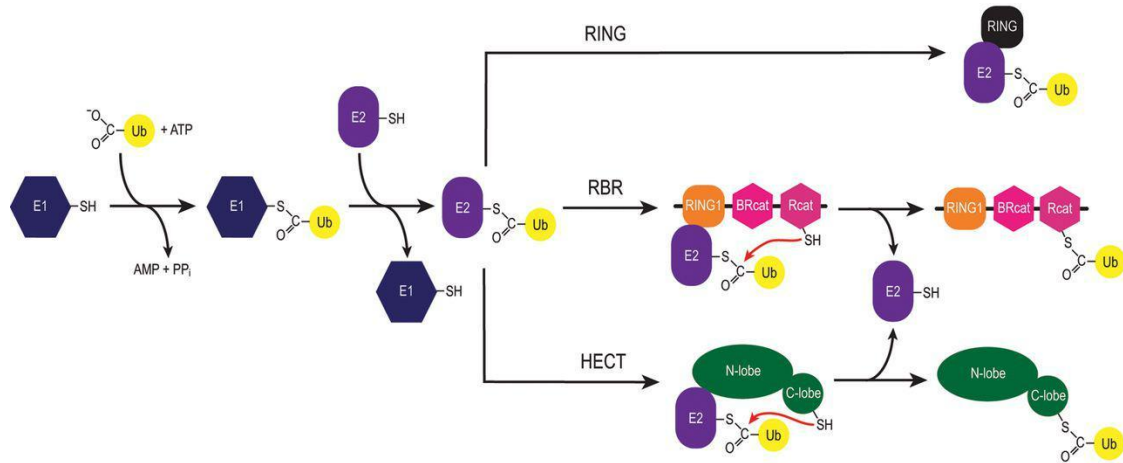


**Figure 2:** The ubiquitination pathway with the different types of E3 ligases. Starting with an E1 enzyme which activates ubiquitin, the E2 conjugates it and transfers the ubiquitin to the E3. The E3 then ubiquitinates its substrates by different mechanisms. Adapted from Spratt et. al 2015. See text for details

Based on their catalytic domain structure and mode of catalysis, E3 ligases are classified primarily into 3 types – the HECT E3 ligases which temporarily accept activated Ub, RING E3 ligases which catalyse the direct transfer of Ub from the E2 to the substrate, and the RBR family (Figure 2), which catalyse the transfer of Ub by a RING/HECT hybrid-like mechanism<sup>56</sup>. A fourth category of E3 ligases is the U box E3 ligase family. It contains a 70 amino acid conserved U box motif that behaves as a modified RING domain wherein salt bridges and hydrogen bonds were proposed to have replaced the zinc-cysteine-histidine coordination of the RING domain (Yee, Goring 2009). Depending on the lysine residue within Ub utilized to anchor the subsequent Ub molecule, Ub chains of different types and lengths can be obtained. Linkages can occur on M1, K6, K11, K27, K29, K33, K48 or K63 of Ub<sup>57</sup>. M1 chains, also called linear ubiquitin chains are unique in that they are the only ubiquitin chains formed without a Lysine residue involved<sup>58</sup>. All these polyubiquitin chain topologies are observed physiologically, leading to the plethora of biological effects observed as a result of this post-translational modification. The removal of Ub(s) attached to target proteins is called deubiquitylation and is catalyzed by deubiquitinating enzymes (DUBs)<sup>59</sup>. Approximately 100 Deubiquitinases (DUBs) are known at present, contributing to complexity of the ubiquitin system by removing ubiquitin adducts.

#### **1.1.4.2. Auto and cross-ubiquitylation of IAPs**

As outlined in 1.1.2., five of the eight human IAPs contain a RING domain, meaning that they catalyse the direct transfer of Ub from the E2 to the substrate. Moreover, IAPs can be post-translationally modified by addition of ubiquitin chains themselves. The RING domain of c-IAP1 has been reported to mediate the degradation of other RING domain containing IAPs<sup>60</sup>. Structural and biochemical studies have revealed that under normal conditions, cIAP1 sequesters its RING domain within a compact, monomeric structure that blocks its dimerization. Upon binding of IAC to the BIR3 domain, crucial BIR3-RING interactions are disrupted, causing conformational changes in the molecule leading to its RING-RING dimerization, enhanced E3 ligase activity, ubiquitylation and degradation (Figure 3)<sup>61</sup>.

XIAP can autoubiquitinate itself at Lysine 322 and Lysine 328, both lysine residues in the BIR3 domain of the protein<sup>62</sup>. Work by Yang and colleagues in 2000, it emerged that XIAP could be degraded through the ubiquitin-proteasome pathway<sup>29</sup>. However, the mechanism of autoubiquitination of XIAP is unclear and studies have focused on using XIAP-interacting IBM-motif containing proteins to confer a structural change in XIAP that triggers autoubiquitylation. In mammalian cells, the prototype of such proteins is Smac/DIABLO, a mitochondrial protein that is released into the cytosol along with cytochrome *c* during apoptotic induction<sup>63</sup>. However, whether the binding of Smac/DIABLO merely occludes XIAP's caspase binding activity or whether autoubiquitination of XIAP occurs as a result is not clear<sup>64–67</sup>. Conversely, there have been reports of IAP-RING mediated ubiquitination and degradation of Smac and another IAP antagonist, ARTS<sup>68–71</sup>.

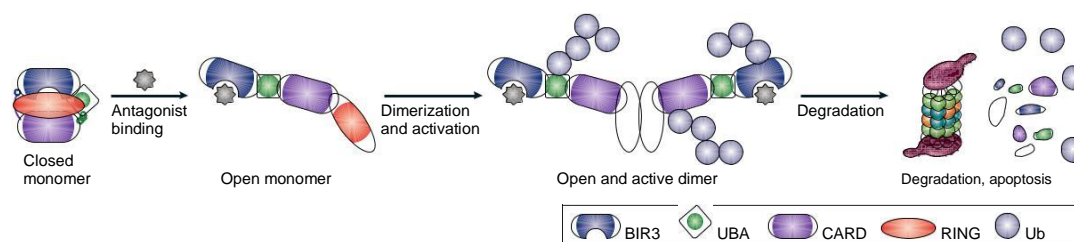


**Figure 3: Model of IAC binding to IAPs leading to autoubiquitination.** Upon antagonist binding, the IAP opens its conformation allowing the IAC to bind to the BIR3 domain. This leads to ubiquitination and subsequent proteasomal degradation. Adapted from Vucic et al, 2012. See text above for details

*In vitro* and *in vivo* ubiquitylation and degradation of XIAP was blocked by binding to the transactivation domain of Notch, which interacts directly with the RING region of XIAP to block the binding of E2<sup>72</sup>. X-linked inhibitor of apoptosis-associated factor 1 (XAF1) activates E3 activity of XIAP and targets Survivin degradation by direct ubiquitylation through formation of a XIAP-XIAF1-Survivin complex<sup>73</sup>.

#### 1.1.4.3. IAPs, ubiquitin and the NF- $\kappa$ B pathway

The IAPs also play crucial roles as E3 ligases in the NF- $\kappa$ B pathway. NF- $\kappa$ B signalling cascades are ubiquitin dependent signalling complexes regulated by ubiquitin ligases, Ub receptors and deubiquitinases. NF- $\kappa$ B is an important regulator of cell growth and motility and NF- $\kappa$ B transcription factors (RELA (p65), RELB, CREL, NF- $\kappa$ B1 (p105) and NF- $\kappa$ B2 (p100)) are important regulators of genes vital for cell survival and proliferation as well as innate and adaptive immune responses. Constitutive activation of NF- $\kappa$ B and chronic inflammation plays a major role in both solid and liquid tumor development<sup>74</sup>. IAPs have slowly emerged as central regulators of NF- $\kappa$ B signalling, thereby consolidating the interest in IAP antagonist compounds (IAC) as anti-cancer therapy. XIAP, cIAP1 and cIAP2 have been implicated in NF- $\kappa$ B activation as well as regulation and a positive feedback loop is initiated by further induction of XIAP, cIAP1 and cIAP2 expression by NF- $\kappa$ B. XIAP serves as an E3 ligase for COMMD1, which is a negative regulator of NF- $\kappa$ B. COMMD1 is also involved in copper homeostasis thus indirectly implicating XIAP in this process

<sup>75</sup>. Depending on the mechanism of activation, NF- $\kappa$ B signaling can be categorized into canonical and non-canonical pathways.

#### ***1.1.4.3.1. Canonical NF- $\kappa$ B signaling pathway***

The cIAPs play a prominent role in activating the canonical pathway in response to TNFR1. Trimeric TNF $\alpha$  binds to TNFR1 leading to recruitment of adaptor protein TRADD (TNFRSF1A-associated via death domain), Ub ligases TRAF2, TRAF5, cIAP1, cIAP2 and protein kinase RIPK1. This leads to the formation of what is commonly known as Complex I at the plasma membrane <sup>76</sup>. cIAPs ubiquitinate RIPK1, a component of Complex I, this triggers ubiquitin mediated recruitment of the linear ubiquitin assembly complex (LUBAC), kinase complexes TAK1-TAB2-TAB3 and IKK $\gamma$ -IKK $\alpha$ -IKK $\beta$  through the ubiquitin binding domains of HOIP, TAB2 and IKK $\gamma$ , respectively <sup>77-79</sup>. LUBAC then promotes linear polyubiquitination of IKK $\gamma$  (NEMO) as well as other Complex I components, resulting in its stabilization <sup>77,80</sup>. IKK $\beta$  in turn phosphorylates inhibitor of NF- $\kappa$ B- $\beta$  (I $\kappa$ B) targeting it for ubiquitin-mediated degradation. This allows NF- $\kappa$ B (p65) to translocate to the nucleus and induce the target gene expression. As an E3 ligase, cIAP1 synthesises K63 ubiquitin chains on RIPK1 thus mediating activation of the canonical pathway as well as cell survival. Loss of both cIAP1 and cIAP2 is observed to strongly impair TNF $\alpha$ -mediated NF- $\kappa$ B activation <sup>77,81-83</sup>. In the absence of cIAPs, TNF $\alpha$  stimulates the formation of Complex-II, a complex containing RIPK1, Fas-associated via death domain (FADD) and caspase-8 <sup>84,85</sup>. This results in the rapid activation of caspase-8 and induces apoptosis. Figure 4 provides an overview of this process.

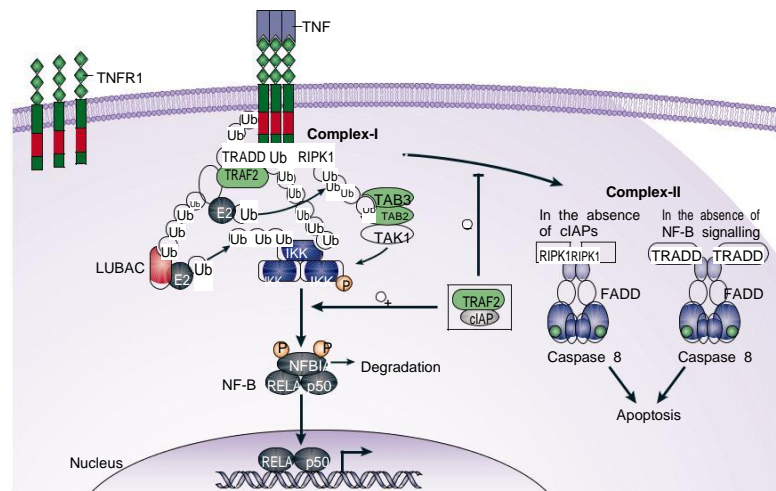


**Figure 4: Canonical NF- $\kappa$ B signaling pathway.** Activation of TNFR1 stimulates Complex-I. The cIAP1s ubiquitinate several members of this complex, leading to recruitment of LUBAC, TAK1-TAB2-TAB3 complex and the IKK $\gamma$ -IKK $\alpha$ -IKK $\beta$  complex. In addition, cIAPs impede the formation of the death inducing complex-II, which is the activation platform for caspase-8. Figure adapted from Hansen and Meier, Nature Reviews 2010.

#### 1.1.4.3.2. Non-canonical NF- $\kappa$ B signaling pathway

This pathway is predominantly activated in response to ligands of the TNF receptor superfamily such as CD40L, B cell activating factor (BAFF) and TNF-related weak inducer of apoptosis (TWEAK)<sup>86–88</sup>. Constitutive degradation of NF-kappa-B-inducing kinase (NIK) through an Ub-ligase complex consisting of TRAF3-TRAF2-cIAP1 and/or cIAP2 ensures that this pathway is normally shut down in cells<sup>87,88</sup>. TRAF3 directly binds to and recruits NIK to TRAF2-cIAP1 complex. TRAFs act as adaptor proteins bringing NIK to cIAPs for its ubiquitin mediated proteasomal degradation. Unlike in the canonical pathway, cIAP1/2 mediate K48 ubiquitination on NIK and cause degradation of the protein (Varfolomeev et al, 2007). NIK phosphorylates IKK $\alpha$  at Ser176 and Ser180, and p100 at Ser866 and Ser870. IKK $\alpha$  can then heteromerize and phosphorylate additional residues on p100, leading to its ubiquitination and partial proteasomal processing to mature p52. Genetic and pharmacological deletion of components of the TRAF2, TRAF3 or cIAP1/2 ubiquitination complex results in the accumulation and consequent activation of NIK protein levels, resulting in the constitutive activation of non-canonical NF- $\kappa$ B pathway,



which in turn leads to TNF $\alpha$  production and thus, canonical NF- $\kappa$ B pathway activation<sup>4</sup>. Multiple genetic alterations have been identified in regulating NIK levels within the cells<sup>89–92</sup>. This provides ample evidence that unrestrained non-canonical NF- $\kappa$ B activation substantially contributes to tumorigenesis. As IAPs prevent accumulation of NIK, it can be surmised that IAPs might suppress NIK-mediated tumor development in a cell type dependent manner. Figure 5 shows an overview of this process.

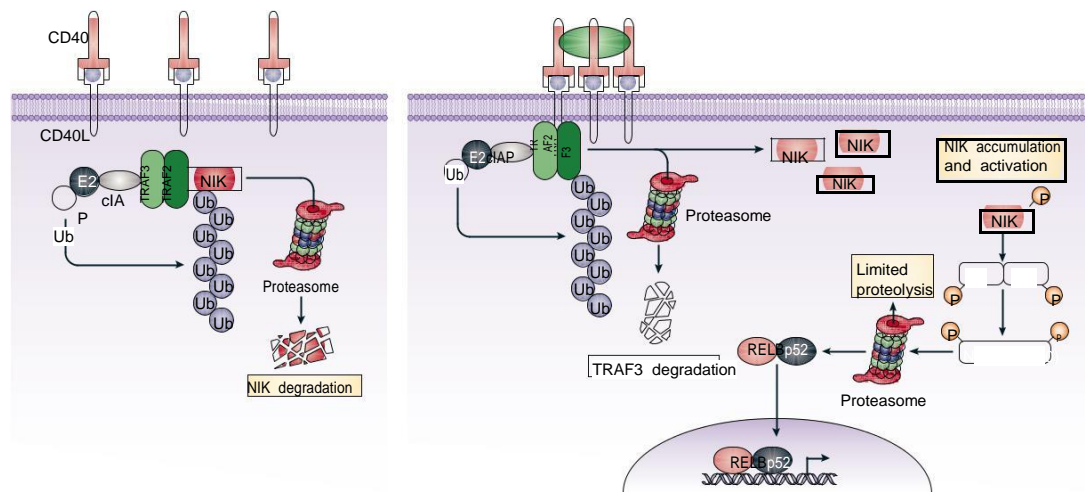


**Figure 5: Non-canonical NF- $\kappa$ B signaling pathway.** To the left is the resting condition in the cell wherein the TRAF-cIAP1 complex constitutively targets NIK for degradation. The right hand side depicts the activated state, wherein NIK levels are high due to cIAP1-mediated ubiquitination of TRAF3. Figure adapted from Hansen and Meier, Nature Reviews 2010.

### 1.1.5. IAPs and their role in tumorigenesis and tumor progression

The role of IAPs as tumor modulators has been explored in depth and has been substantiated by the differential expression of IAP family members in numerous malignancies. Crucial signaling molecules sitting at the intersection of various cell death and survival pathways, IAPs have been observed to be elevated in different tumor types. Consequently, anti-tumor therapeutics, especially small molecule inhibitors against IAPs have been designed and 6 IAP antagonist compounds have entered clinical trials to date<sup>35,93,94</sup>. However, there are opposing prognostic implications for IAPs in different tumor types, thus strongly suggesting a context and cell type dependent



function of IAP signalling and sounds a note of caution before we move towards the use of IAP mediated therapeutics. Various genetic studies have identified cIAPs as candidate proto-oncogenes. cIAP1, cIAP2 and YAP (Yes-associated protein) are a part of the 11q21-11q23 amplicons and they are detected in a variety of cancers like esophageal carcinoma, hepatocellular carcinoma, medulloblastoma, glioblastoma, gastric carcinoma, renal cell carcinoma and Non-Small Cell lung carcinoma<sup>35,95-98</sup>. XIAP was also shown to inhibit apoptosome activation of apoptotic cascade in human NSCLC cell lines and treatment with XIAP antagonist or XIAP antisense led to sensitization of cells to apoptosis<sup>99,100</sup>. However, a study by Ferreira et. al. contradicted these findings and reported that high XIAP levels correlated with lower proliferation rate and longer survival, suggesting it as a positive prognostic factor for NSCLC<sup>101</sup>.

#### 1.1.6. IAPs and cellular differentiation

Several anti-apoptotic proteins like Bcl-2, FAIM-s and FLIP have been shown to modulate neurite growth and neuronal differentiation in different neuronal types through the regulation of the Trk/MEK/ERK pathway, leading to the suggestion that XIAP could have an analogous function<sup>102-104</sup>. In a study by Fadó and colleagues, XIAP was observed to regulate neurite outgrowth in neuronal cells. They showed that Nerve Growth Factor (NGF) treatment induced a reduction of endogenous XIAP concomitant with the induction of neuronal differentiation. Further, XIAP overexpression prevented NGF-induced neuronal differentiation and these effects of XIAP are mediated by the MEK/ERK signaling pathway<sup>105</sup>.

More recently, work from our lab implicated XIAP in myoblast differentiation<sup>12</sup>. We showed that XIAP negatively regulates ERK5 activation by direct interaction and ubiquitination. ERK5 (Extracellular-signal-regulated kinase 5) is a unique, conserved member of the Mitogen activated protein kinase family and is activated through a three-tier cascade constituting MEK5 and MEKK2/3. XIAP and cIAP1 were observed to conjugate predominantly K63-

linked ubiquitin chains to MEKK2 and MEKK3 impeding the interaction between MEK5 and ERK5 in a trimeric complex, thus leading to ERK5 inactivation (Figure 6). ERK5 regulates neuronal and muscle differentiation via the MEF2 transcription factors <sup>106,107</sup>. Depletion of XIAP was observed to promote myoblast differentiation in a MEKK2/3-ERK5 dependent manner <sup>12</sup>.

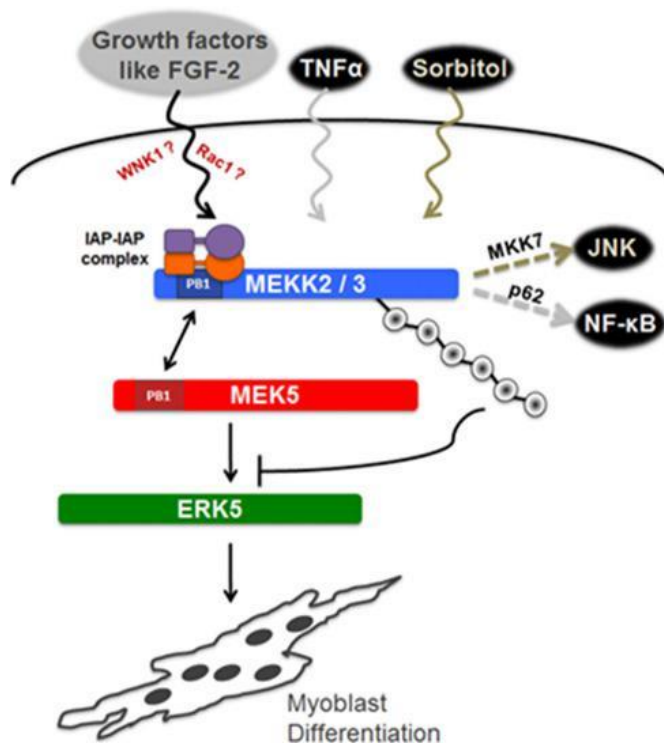


**Figure 6: IAPs and their role in promoting myoblast differentiation.** XIAP and cIAP1 ubiquitinate MEKK2 and 3 thus impeding interaction between ERK5 and MEK5. This leads to ERK5 inactivation and impedance of myoblast differentiation. Figure adapted from Takeda et al, 2014

### 1.1.7. IAPs and Cell Migration

IAPs play an important role in modulation of cell migration. Normally working in tandem with a family of proteins called Rho GTPases, there have been several studies linking IAPs with a crucial role in cell migration. This will be discussed in detail in the coming sections after Rho GTPases, a central component of this thesis are introduced and discussed.

## 1.2 Rho GTPases

### 1.2.1. Introduction

Rho GTPases are small (21-25kDa), evolutionarily conserved proteins which belong to and constitute a unique subfamily within the Ras superfamily of small GTPases. Guanine nucleotide binding proteins, also called G-proteins are mediators of extracellular signals, using secondary signaling pathways to convert said signals into intracellular responses <sup>108,109</sup>. G-proteins are divided into large G-proteins and small G-proteins. Large G-proteins, also called heterotrimeric G proteins are activated by G protein-coupled receptors (GPCRs) and are made up of alpha ( $\alpha$ ), beta ( $\beta$ ) and gamma ( $\gamma$ ) subunits <sup>110</sup>. The  $\beta$  and  $\gamma$  subunits are referred to as the beta -gamma complex and this complex is released from the  $\alpha$  subunit upon activation of the GPCR. This complex can then act as a signaling molecule, either by activating secondary messengers or by direct gating of ion channels. The  $G\beta\gamma$  complex when bound to histamine receptors, can activate phospholipase A2 <sup>111</sup>. They are also involved in the cAMP response induced by the stimulation of the histamine H1 receptor <sup>112</sup>.  $G\beta\gamma$  complexes can also bind to muscarinic acetylcholine receptors thus directly opening G protein-coupled inward rectifying potassium channels (GIRKs) <sup>113</sup>.

Small GTPases are a family of hydrolase enzymes that can act as molecular switches by specifically binding to and hydrolysing guanosine triphosphate (GTP). They are found in the cytosol and are homologous to the  $\alpha$  subunit of heterotrimeric G-protein. However, unlike the  $\alpha$  subunit of G proteins, a small GTPase can function independently as a hydrolase enzyme that binds to and hydrolyzes a guanosine triphosphate (GTP) to form guanosine diphosphate (GDP). The best known members of this family of small GTPases are the Ras family of GTPases, hence the title of Ras "superfamily". There are over 150 members in the Ras superfamily and can be broadly divided into 5 families - Ras, Rho, Ran, Rab and Arf GTPases. Despite considerable structural and biochemical similarities, these proteins are versatile and key regulators of

virtually every fundamental cellular process. As a result, their dysfunction plays a crucial role in the pathogenesis of serious human diseases, including cancer and various developmental syndromes <sup>114</sup>.

Proteins from the Rho family of GTPases are crucial regulators of cell shape and migration and they play a central role in the remodeling of actin cytoskeleton <sup>115</sup>. Activation of Rho GTPases also triggers various pathways that influence other cellular processes including cell division, proliferation, gene expression <sup>116</sup> and transcriptional regulation, microtubule organization, cell adhesion, invasion, metastasis and wound healing <sup>117</sup>. The best-characterized members of this family are Rac1, RhoA and Cdc42, all of which will be covered in extensive detail in this thesis.

### 1.2.2. Discovery of Rho GTPases

Rho GTPases were first identified and later extensively studied beginning in the 1980's. RhoA was the first member of the family to be identified in 1985. It was discovered serendipitously in Richard Axel's group while they searched for Ras-related genes in a low stringency cDNA screen in marine snail, *Aplysia californica* <sup>118</sup>. This led to the discovery of RhoA, RhoB and RhoC in humans as well as Rho1 and Rho2 in yeast. Four years later, two more members, Rac1 and Rac2 were identified as a substrate of botulinum toxin. Isolated from a differentiated cDNA library, Rac1 and Rac2 cDNA clones were found to share significant homology with both the previously discovered Rho family members. This landmark study further suggested that the Rac family of proteins were plasma membrane associated GTP binding proteins, a result that is today considered integral to Rho GTPase biology <sup>119</sup>. The very next year, Cdc42 was discovered in *Saccharomyces cerevisiae* and was shown to be important for budding and polarity <sup>120,121</sup>. Later that year, work in the group of P. Polakis connected Cdc42 to G25K, a low molecular mass GTP-binding protein that had been identified in several mammalian tissues <sup>122–125</sup>. They noticed that this protein was highly homologous to sequences contained in the *CDC42* gene product of *Saccharomyces cerevisiae* <sup>120</sup>. Eight additional

mammalian Rho members were identified from biological screens in the 1990s, which were a turning point in biology due to availability of complete genome sequences that allowed full identification of gene families. After the initial discoveries, numerous counterparts of these proteins were also discovered in diverse organisms like *S. cerevisiae* (7 genes), *C. elegans* (9 genes), *D. melanogaster* (9 genes) and *Homo sapiens* (23 genes)<sup>126</sup>.

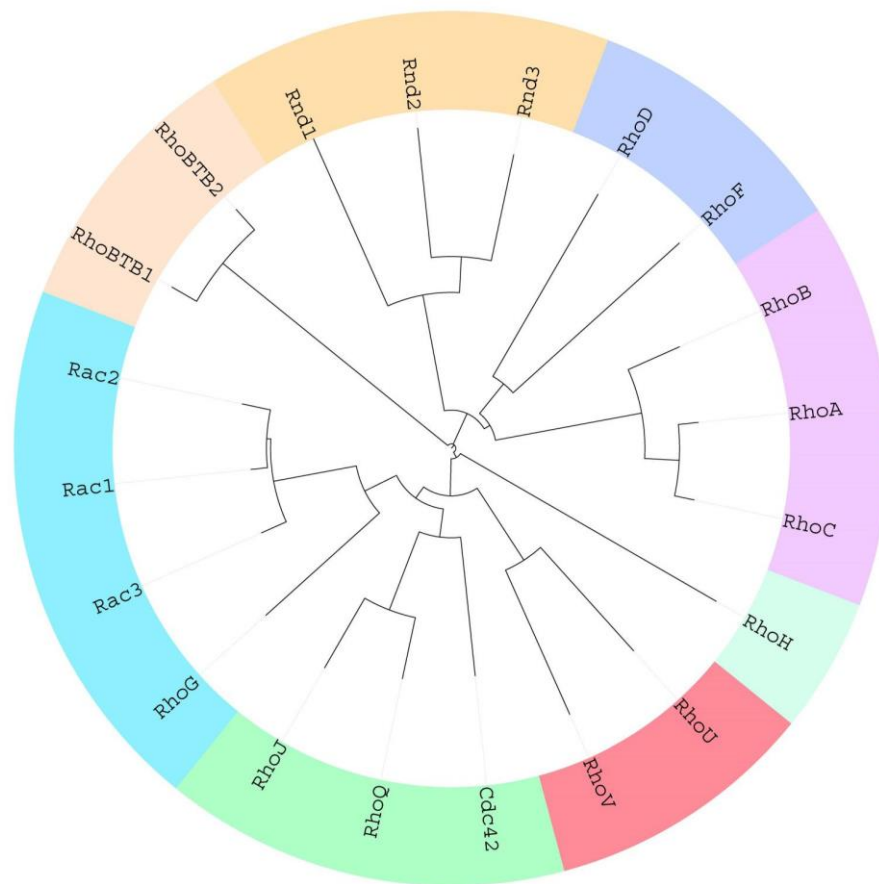


**Figure 7: Phylogenetic tree of Rho GTPases** – A family tree showing the evolution of Rho GTPases over time. The family of 20 Rho GTPases is split into 8 sub families based on evolution, sequence homology and function. Figure adapted from Murali et al, 2014. See text for details

Today, the Rho family of GTPases comprises of 20 proteins in mammals, which are further divided into eight sub-groups based on their primary amino acid identity, structural motifs and biological function (Figure 7). The eight sub-groups are - Rac proteins (Rac1, Rac2, Rac3 and RhoG), Rho proteins (RhoA, RhoB and RhoC), Cdc42 proteins (Cdc42, RhoQ, and RhoJ), Rnd

proteins (Rnd1, Rnd2/RhoN, and Rnd3/RhoE), RhoBTB proteins (RhoBTB1, RhoBTB2), RhoH, RhoUV (RhoU (Wrch) and RhoV (Chp)), and the RhoF subfamily (RhoD and RhoF).

### **1.2.3. Anatomy of Rho GTPases**

#### **1.2.3.1. The G domain**

A hallmark of the structure of Rho GTPases and other members of the Ras superfamily is the presence of the highly conserved G domain <sup>127</sup>. Rho GTPases also contain a short insert region and a hypervariable C terminal region. In general, there is a high sequence similarity in the primary structures of small GTPases due to the presence of the structurally conserved G domain <sup>128</sup>. They share 30% similarity with members of the Ras superfamily and 40-95% sequence similarity is shared between members of the Rho GTPase family. <sup>129</sup>. The G domain mediates nucleotide binding and over the years, crystal structures of multiple members of the Rho GTPase family including Rac1, RhoA and Cdc42 have been deciphered <sup>130-134</sup>. Crystallographic analysis of the G domain revealed the presence of a Rossmann fold - 6-stranded  $\beta$  sheets surrounded by 5  $\alpha$  -helices <sup>135</sup>. The domain also contains two functional elements – Switch I and Switch II that undergo conformational changes when bound to GTP. Figure 8 shows the different domains as well as the structural similarities between various members of the Rho GTPase family.

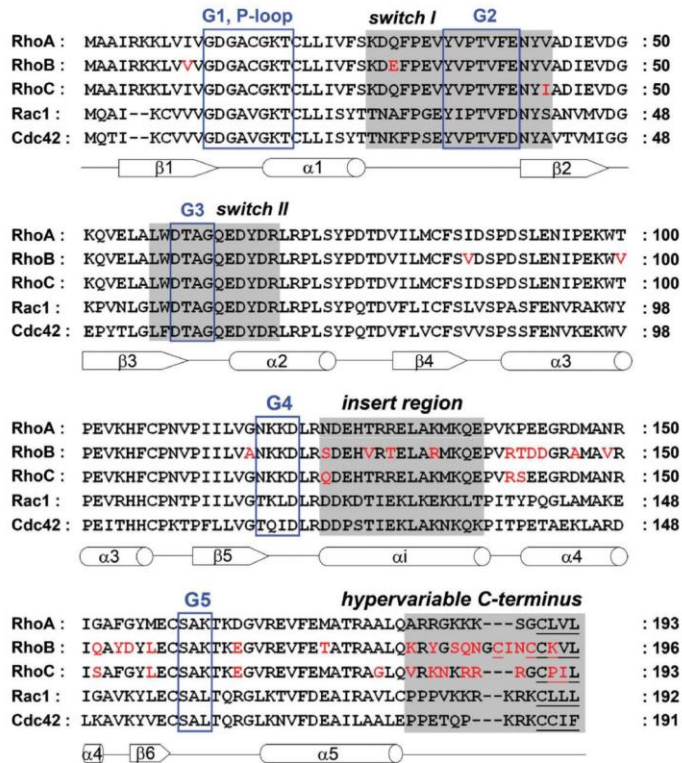


**Figure 8: Alignment of RhoA, RhoB, RhoC, Rac1 and Cdc42 – Different motifs marked with different colours. G-motifs marked with a blue box, the switch regions, insert region and the C-terminus highlighted in gray, underlined letters are sites of lipid modification and sequence differences are highlighted in red. Secondary structures below the sequences are with RhoA as a template. Figure adapted from Schaefer et. al, 2014**

The switch I region is important for effector function, with mutations in this region impairing interaction between the Rho GTPase and downstream partners<sup>136</sup>. RhoA, RhoB and RhoC have an identical sequence in the switch I and switch II regions (residues 27-43 and 57-68 in RhoA respectively) except for the positions 29 and 43, both of which are in the Switch I region. While RhoA and RhoC contain a glutamine at position 29, RhoB interestingly contains a negatively charged glutamate residue. RhoA and RhoB have a Valine at residue 43 while RhoC encodes isoleucine, another hydrophobic but significantly bulkier amino acid. The latter plays a crucial role in effector binding and also with activators of Rho GTPases.

The switch II region (57-68 in RhoA) plays more of a mechanistic role, coordinating the nucleophilic water that is required for both intrinsic as well as GTPase activity mediated by GTPase activating proteins, also called GAPs<sup>137,138</sup>. It contains a highly conserved glutamine (position 61 in Rac1 and Cdc42, 63 in RhoA/B/C) that performs the above role and is remarkably conserved between all Rho GTPases. Mutation of this glutamine residue to an alanine or a leucine renders it constitutively active. Various studies have shown that cytotoxic necrotizing factor 1 (CNF1) toxin from bacteria



uropathogenic *E. coli* can catalyze deamidation of this glutamine to glutamic acid, reducing the GTPase activity and thus, promoting permanent activation of the Rho GTPase<sup>139,140</sup>. Another toxin, DNT (dermonecrotic toxin) of *Bordetella bronchiseptica* can also modify Q61 of Rac1 leading to its persistent activation. Structurally, the mechanism of binding to GDP or GTP is called the 'loading-spring mechanism' and is universal to all small GTPases<sup>137,141</sup>. In detail, the main chain NH groups of Thr37 (switch I) and Gly62 (switch II) in RhoA form 2 hydrogen bonds with the oxygen of the  $\gamma$ -phosphate in the nucleotide.  $\gamma$ -phosphate is only present in GTP and not GDP, so when it is lost during GTP hydrolysis, the hydrogen bonds are disrupted leading to the relaxation of the switch I and switch II regions.

The G domain is characterized by 5 conserved sequence motifs G1-G5. These motifs form the nucleotide-binding site and dictate nucleotide specificity and affinity<sup>138</sup>. The G1 motif is also called the phosphate binding loop or P-loop due to its crucial role in coordinating the bound nucleotide's  $\beta$ -phosphate. It is located between  $\beta 1$ - $\alpha 1$  and also coordinates a  $Mg^{+2}$  ion that is required for nucleotide binding<sup>142</sup>. Further, the P-loop works in conjunction with the switch I and switch II regions to form a binding surface for GAPs<sup>138</sup>. While the switch II region contains the Q61 (in Rac1/Cdc42 and 63 in RhoA/B/C), which leads to constitutive activation when mutated, the P-loop contains a similar Glycine at position 12 (in Rac1/Cdc42 and 14 in RhoA/B/C) which when mutated into a Valine causes a steric hindrance in the structure of the protein leading to constitutive activation of the protein. Conversely, the threonine at position 17 (in Rac1/Cdc42 and 19 in RhoA/B/C) upon mutation into an Asparagine results in a low nucleotide affinity consequently leading to a high affinity binding with Guanine nucleotide exchange factors (GEFs). This causes the mutant to become dominant negative. Both these mutants as well as the switch II mutant have been commonly used in cell biological experiments to identify specific interaction partners and explore different biological activities of GTPases upon changes to activity<sup>142</sup>.



In contrast to the G1 motif, which is highly conserved, other motifs like G4 and G5, which mediate interaction with the guanine base show low sequence homology amongst Rho GTPase family members<sup>142</sup>.

### **1.2.3.2. Insert region**

Another characteristic domain present in all Rho GTPases is the Rho insert domain that is located within the 5<sup>th</sup>  $\beta$  strand and the 4<sup>th</sup>  $\alpha$  helix. It is located between the G4 and G5 motif and extends the G domain by 13 residues. While this Rho insert domain has no significant impact on the structure in GDP and GTP bound forms, it is involved in GEF binding<sup>143</sup>. While the insert region of RhoA and RhoC are identical, RhoB differs from the other two members in four amino acids. However, the sequences of the insert regions of RhoA, Cdc42 and Rac1 have no similarity. It is this unique feature that confers isoform-specific binding and activation to several effector proteins like NADPH oxidase, IQGAP, ROCK and mDia<sup>144–147</sup>.

### **1.2.3.3. C-terminal region**

The C-terminal end of the Rho GTPases is called the hypervariable region, and as the name suggests is a big reason for the overall mediocre sequence homology between members of the Rho family. This region provides a binding surface for specific downstream effectors as well as interaction with chaperones called guanine nucleotide dissociation inhibitors (RhoGDIs), cytosolic proteins that retain Rho GTPases in their inactive conformation. The hypervariable region consists of two major components – the first is a stretch of adjacent lysine and arginine residues, called the polybasic region (PBR). This region controls the membrane binding of the Rho GTPases as well as subcellular localization and specific effector binding<sup>148</sup>. The (K(K/R)X(K/R)) sequence functions as a nuclear localization signal in various members of the family<sup>149</sup>. All members of the family contain a PBR except RhoB, RhoD and the RhoBTB members<sup>115</sup>. The second component is the C-terminal CAAX box (C is a cysteine, A is an aliphatic residue and X is any residue), a

tetrapeptide motif that is conserved in most Rho GTPases (all Rho GTPases except RhoBTB1 and 2 contain the CAAX box<sup>150</sup>). The CAAX box is usually the site for post various post translational modifications like farnesylation and geranyl-geranylation<sup>151</sup>. These lipophilic post translational modifications are vital for appropriate subcellular localization and regulation<sup>152,153</sup>. Members of the RhoUV family contain an incomplete CAAX box<sup>154,155</sup>. Between the polybasic region and CAAX box is a CXXC tetrapeptide motif, which is involved mainly in plasma membrane targeting<sup>156</sup>. In some Rho GTPases, a third kind of post-translational modification called palmitoylation occurs on the cysteine residue preceding the CAAX box. This modification helps recruitment of the GTPase to appropriate membranes<sup>157</sup>. Post-translational modifications will be discussed in detail in the upcoming sections.

#### 1.2.4. Regulation of Rho GTPases

##### 1.2.4.1. Regulation of Rho GTPases by GEFs, GAPs and RhoGDI

Rho GTPases, like other members of the GTPase superfamily cycle between an inactive GDP bound state and an active GTP bound state. Due to their key role in regulation of cytoskeletal structure, 3 types of proteins tightly regulate this cycling. **G**uanine nucleotide **e**xchange **f**actors (GEFs) catalyze the conversion of Rho GTPases from the inactive GDP bound form to the active GTP bound form. They catalyze nucleotide exchange by reducing the affinity to GDP and transiently stabilize the nucleotide-free intermediate till it binds GTP<sup>158</sup>. While GTP levels are higher in the cell, the spontaneous conversion of GDP bound Rho GTPases to a GTP bound form is prevented by elevated levels of cytosolic  $Mg^{+2}$ <sup>159</sup>. In essence, the dissociation rates of Rho GTPases are very slow (hours in the case of GDP) in the presence of  $Mg^{+2}$  and the binding affinities between the GTPases and guanine nucleotides are in the nanomolar/picomolar range<sup>158</sup>. GTPases, as the name indicates, have an intrinsic but weak GTPase activity, thus hydrolyzing GTP to GDP at a very slow rate. To speed this process up, proteins called GTPase activating proteins (GAPs) accelerate the intrinsic GTPase activity and re-form the GDP

bound state. GAPs stabilize the charged intermediate and facilitate proper positioning of the hydrolytic water molecule and consequently reduce the activation barrier for GTP hydrolysis <sup>160</sup>. Lastly, guanine nucleotide dissociation inhibitors (GDIs) are a family of regulators that interact with the inactive GTPase domains and any covalently attached lipid post-translational modifications. This sequesters the Rho GTPase in its inactive GDP bound form in the cytosol, inhibits GTPase activity and prevents access to downstream targets. This interaction between GDIs and the lipid moiety of the Rho GTPase controls the sub cellular distribution of Rho GTPases <sup>138</sup>. This led to the simplified dogma that active proteins are localized to the membranes while the inactive proteins are sequestered in the cytosol. However, the relationship between their activity and localization is much more complicated than assumed as a series of papers by Pozo and Schwartz <sup>161–163</sup> showed that Rac1 activation and membrane localization could be dissociated. While Rho proteins are believed to persist in the GDP bound inactive state in resting cells, for example, imaging experiments reveal that 95% of RhoA is cytosolic and is sequestered by RhoGDIs <sup>164</sup>, recent qualitative analysis showed that RhoD and RhoF exist in a GTP bound state due to relatively higher GDP dissociation as well as low GTP hydrolysis <sup>165</sup>.

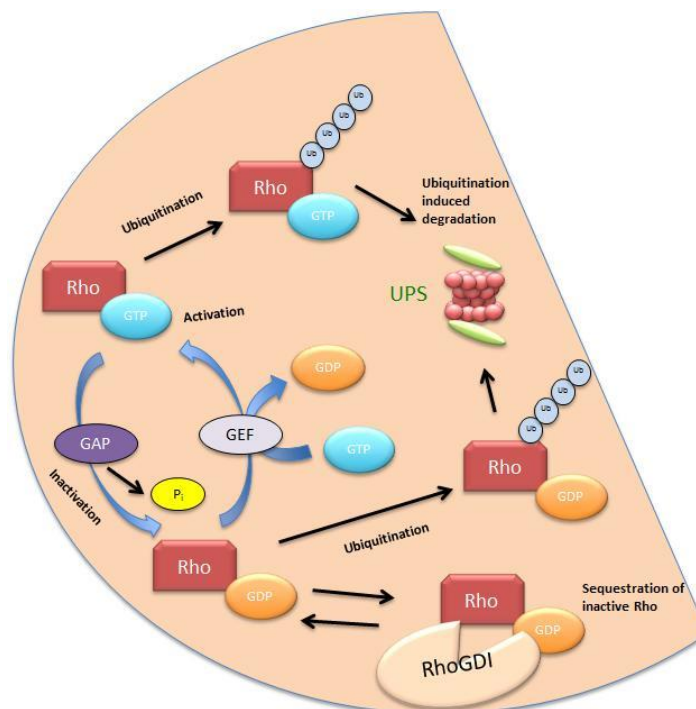


**Figure 9: Regulation of Rho GTPases.** Rho GTPases primarily cycle between an inactive GDP and an active GTP state. RhoGDI sequesters inactive Rho GTPases in the cytosol and both GDP and GTP bound Rho GTPases are subject to ubiquitin mediated degradation. Figure adapted from Murali et al, 2014.

#### **1.2.4.2. Post-translational regulation of Rho GTPases**

*Various post-translational modifications influence Rho GTPase activity, with covalent attachment of lipid groups and phosphorylation being among the best-studied modifications in this family of proteins. While regulation by GEFs, GAPs and GDIs is important for maintaining protein homeostasis in cells, post-translational modifications have shown to be essential for regulation of Rho GTPase activity under both physiological and pathological conditions <sup>166,167</sup>. Figure 12 summarizes these modifications.*

##### **1.2.4.2.1. Lipid modifications**

*Lipid post-translational modifications (PTMs) that commonly occur on Rho GTPases are isoprenylation and palmitoylation. Isoprenylation involves the transfer of either a farnesyl or a geranyl-geranyl moiety to C-terminal cysteine(s) of the target protein. There are three enzymes that carry out prenylation in the cell. They are - farnesyl transferase, CAAX protease and geranylgeranyl transferase I <sup>168</sup>. Farnesylation is a type of isoprenylation, a post-translational modification of proteins by which an isoprenyl group is added to a cysteine residue. Farnesyltransferase (FTase) and Geranylgeranyltransferase I (GGTase I) are two similar proteins that recognize the CAAX box at the C-terminus of the target protein. FTase recognizes CAAX boxes where X is a Threonine, Serine, Alanine, Cysteine or a Glutamine. GGTase I recognizes CAAX boxes where X is a Leucine, Phenyl Alanine, Valine or an Isoleucine <sup>169</sup>. Interestingly, Methionine has been found to trigger both geranylgeranylation and farnesylation. Palmitoylation is the covalent attachment of fatty acids, to cysteine and occasionally to serine and threonine residues of proteins, which are typically membrane proteins <sup>170</sup>.*

---

---

Palmitoylation enhances the hydrophobicity of proteins and contributes to their membrane association.

Isoprenylation of the Ras superfamily of proteins was originally demonstrated in a series of papers from Hancock and colleagues where they showed that Ras proteins are farnesylated in order to facilitate attachment with lipid membranes<sup>171–175</sup>. These studies were eventually extended to Rho family proteins as well<sup>176,177</sup>. In the Rho family of GTPases, 16 of the 20 members harbor a functional CAAX motif with RhoU and RhoV containing an incomplete CAAX box and RhoBTB proteins being the only members not have a CAAX box at all<sup>153</sup>. Rac1, Rac2, Rac3, RhoG, RhoA, RhoC and Cdc42 are all geranylgeranylated, while RhoB has both a palmitoyl anchor as well as a geranylgeranyl or a farnesyl group attached<sup>176</sup>. While most Rho GTPases contain the palmitoylation site between the PBR and the CAAX box, Rac1 is the only member that has a palmitoylation site before the PBR – at Cysteine 178<sup>178</sup>. This palmitoylation site was shown to be essential for membrane spreading and organization as well as migration. Palmitoylation has also been described for the brain-specific splice variant of Cdc42 (bCdc42). The bCdc42 isoform terminates with a CCIF sequence and, upon prenylation at Cys188, bypasses C-terminal proteolysis and carboxymethylation and undergoes palmitoylation at the adjacent Cys189 residue<sup>179</sup>.

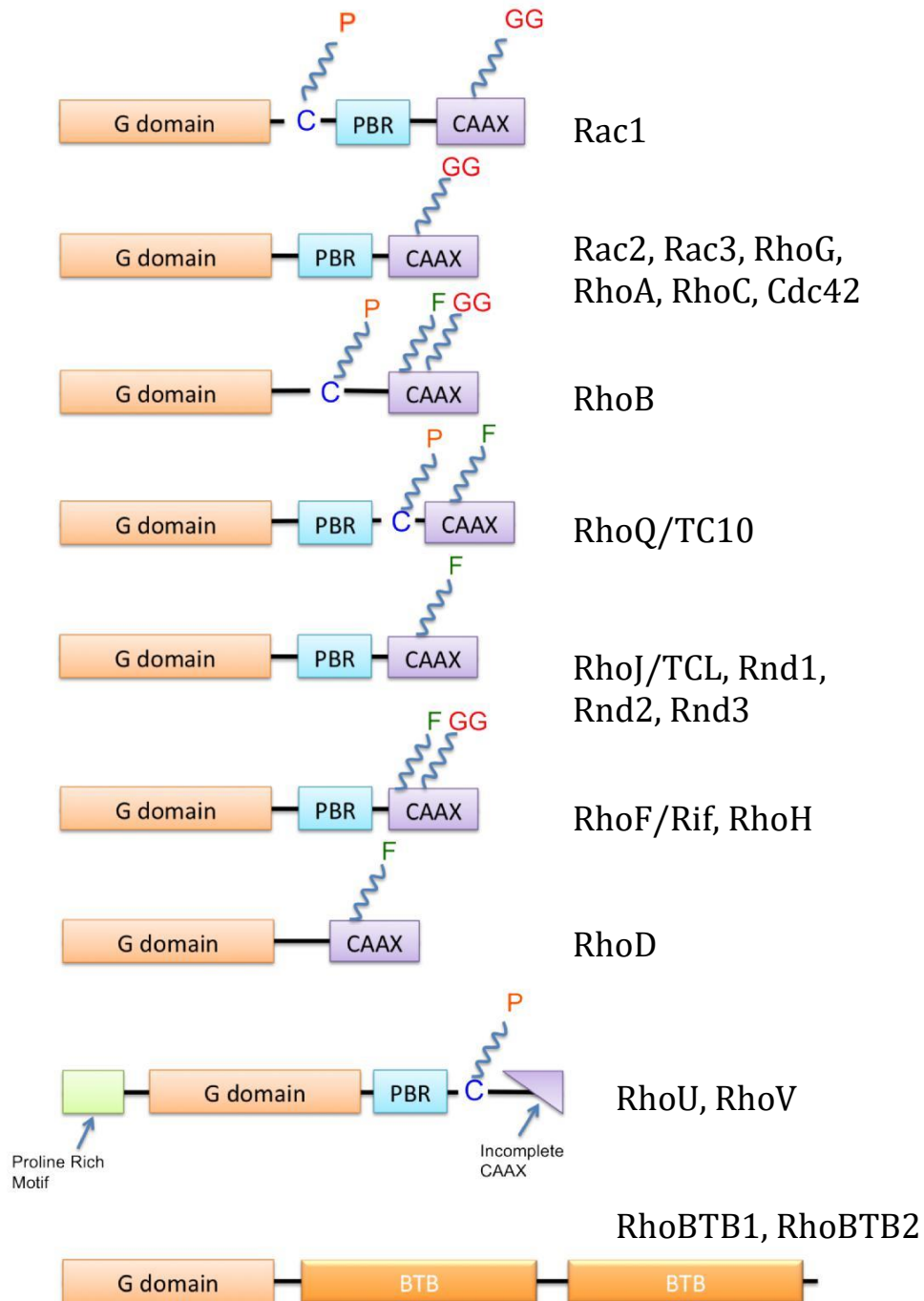


**Figure 10: Post-translational modifications on Rho GTPases.** Structural depiction of Rho GTPases and their post-translational modifications. Rho GTPases are subject to various PTMs, sometimes on the same C terminus and this contributes towards their membrane localization as well as stability. Figure adapted from Murali et al, 2014.

It is speculated that one side effect of Rho protein isprenylation may be to favour their misfolding in aqueous solution and consequent degradation. This generates a unique dilemma at the heart of the Rho switch where on the one

hand, isoprenylation is required for proper localization of Rho proteins, but on the other, this disturbs their folding in solution thus triggering their degradation<sup>180</sup>.

#### **1.2.4.2.2. Phosphorylation of Rho GTPases**

The second most common PTM after lipid-based PTMs of Rho GTPases is phosphorylation. Phosphorylation is a PTM widely used to regulate proteins in a reversible manner. Site-specific and mass spectroscopy methods have been used to map the phosphorylation sites in the catalytic domain and the regulatory sites<sup>181</sup>. The best-studied phosphorylation event on Rho GTPases is Ser188 on RhoA. Cdc42 has a functionally equivalent serine at position 185 and this is phosphorylated by PKA. This phosphorylation, much like the Ser188 on RhoA increases Cdc42 affinity for RhoGDI<sup>182</sup>. RhoG has a similar functional serine in the hypervariable region that has been reported phosphorylated, however its function is as yet unclear<sup>183</sup>. Recent studies showed that RhoC, but not RhoA is phosphorylated on Ser73 by the kinase Akt in breast cancer cells<sup>184</sup>. Interestingly, this serine is conserved across all 3 Rho-isoforms, but this RhoC specific phosphorylation is required for downstream signaling and invasiveness, contrasting with the inactivating phosphorylation on RhoA. RhoB is phosphorylated by CK1 on Ser185 leading to impeded actin stress fiber organization and epidermal growth factor stabilization<sup>185</sup>.

Finally, Rac1 and Cdc42 phosphorylation has been reported both *in vitro* and in cells: Ser71 by PKB/Akt on Rac1 and Tyr64 by Src on Cdc42 as well as Ser71 on Cdc42<sup>186,187</sup>. This phosphorylation of Rac1 could play a role in microbial pathogenesis<sup>188</sup>. Phosphorylation of Rac1 has also been reported on Thr108 by extracellular signal-related kinase (ERK1/2) in response to epidermal growth factor (EGF) which causes Rac1 to translocate to the nucleus<sup>189</sup>.



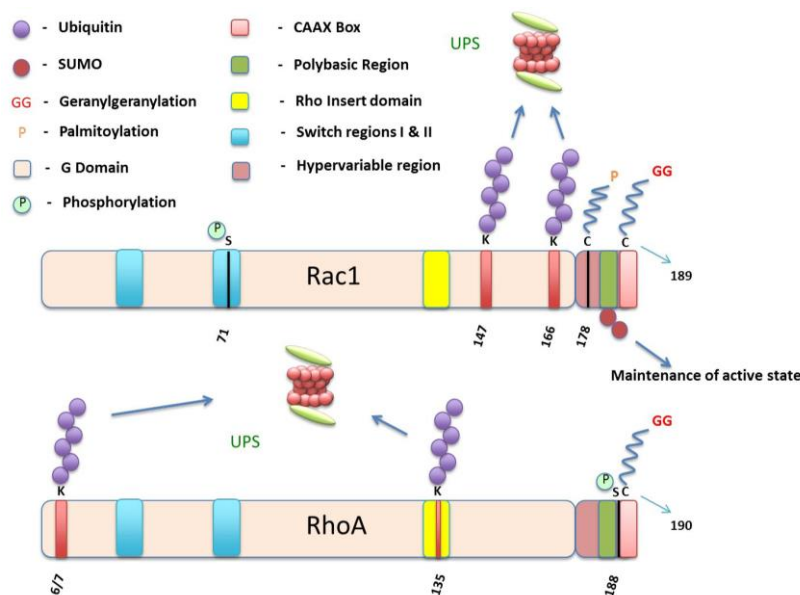
### 1.2.4.2.3. SUMOylation and Ubiquitylation

Another layer of modulation of Rho protein activation is by a PTM called SUMOylation. SUMOylation is a process in which small-ubiquitin-like modifier (SUMO) proteins 1, 2, and 3 are covalently conjugated to specific lysine residues on target proteins. It is a reversible modification catalyzed by a family of SUMO specific proteases called SENPs. Angeliki Malliri's group provided the first and to date only evidence of Rho GTPase SUMOylation when they showed that Rac1 SUMOylation in the PBR is required for sustained activation of the protein, and consequently for optimal cell migration<sup>190</sup>. It is expected that other Rho family proteins be also regulated by similar PTMs.

Ubiquitylation, in recent years has emerged as another level of inactivating Rho GTPases by targeting them for proteasomal degradation. Ubiquitylation and degradation of Rho GTPases was first witnessed during host-pathogen interactions. As mentioned in earlier sections, Cytotoxic necrotizing factor 1 (CNF1) constitutively activated Rac1, Cdc42 and RhoA by deamidating the glutamine at Gln61 (Gln63 in RhoA)<sup>139,140</sup>. This triggered the degradation of the proteins in a proteasome-mediated manner in various cell types<sup>191</sup>. Consequently, studies to identify E3 ligases of these proteins gained steam and the first breakthrough was made with RhoA. The HECT domain-containing E3 ligase Smurf1 was identified as a specific E3 ligase by ubiquitinating Lys6/7 on RhoA, targeting it for proteasomal degradation<sup>192,193</sup>. The second E3 ligase identified for RhoA was CUL3<sup>BACURD</sup>. It belongs to the Cullin-RING multi-subunit ubiquitin ligase family (CRL). BACURD1/2 are evolutionarily conserved BTB-domain containing proteins that function as RhoA receptors<sup>194</sup>. They specifically bind to RhoA and use the scaffold CUL3 to link RhoA to E3 ligases. Depletion of CUL3 or BACURD1/2 stimulates assembly of actin stress fibres in HeLa cells by increasing RhoA levels<sup>195</sup>. Finally **Skp1-Cul1-Fbox** (SCF) FBXL19 (SCF<sup>FBXL19</sup>) was identified as an E3 ligase for RhoA in lung epithelial cells<sup>196</sup>.

Rac1 is also ubiquitinated by a range of E3 ligases. Two studies in 2011/2012 unveiled the E3 ligases on Rac1 <sup>11,197</sup>. The first study, by Oberoi and colleagues showed that XIAP and cIAP1 directly bind to Rac1 and conjugate polyubiquitin chains to Lysine 147, thus targeting it for degradation. Down-regulation of XIAP and cIAP1 resulted in an elongated morphology and enhanced cell migration in both normal and tumor cells. The second study showed that Hace1, a HECT domain-containing protein also ubiquitylated Rac1 at Lysine 147. The key difference between the IAPs and Hace1 was that Hace1 only targeted active Rac1 while the IAPs bound to Rac1 in a nucleotide independent manner. A third E3 ligase for Rac1 is SCF<sup>FBXL19</sup>, which ubiquitinates Rac1 on Lysine 166.

This thesis will explore in detail novel ubiquitination sites on Rho GTPases as well as extend our knowledge on the kinds of ubiquitin chains on already discovered substrates.



#### 1.2.4.2.4. Other post-translational modifications

While phosphorylation and isoprenylation regulate the function of Rho proteins by altering their localization, other PTMs can directly alter their

**Figure 11: Regulation of Rac1 and RhoA by ubiquitination and SUMOylation.** Rac1 and RhoA depicted with their post-translational modifications, with a specific focus on SUMOylation and ubiquitination. Rac1 is known to be SUMOylated in the Polybasic region and ubiquitinated at both Lysine 147 and 166 while RhoA has Lys 6/7 and 135 for ubiquitination sites. These are discussed in detail in the text, figure adapted from Murali et al, 2014

biochemical activity. One such PTM is redox-mediated oxidation of cysteine residues in certain Rho proteins that has been described to stimulate nucleotide exchange in the absence of GEFs<sup>198</sup>. The cysteine in question is Cys18 in Rac1 and Cys20 in RhoA, a cysteine in the P-loop of the protein. This cysteine can be oxidized in the presence of reactive oxygen or nitrogen species (ROS and RNS respectively), altering the nucleotide-binding pocket and triggers release of the nucleotide. As this reaction is reversible in cells, reduction of the protein restores nucleotide-binding ability, which is usually GTP due to the higher concentration of GTP than GDP in cells. ROS mediated oxidation is slightly more complex in RhoA as RhoA also contains a Cys16 residue that can also be oxidized at higher levels of ROS. This leads to a formation of a disulphide bridge, an irreversible reaction in cells, thus leading to the constitutive activation of the oxidized RhoA molecule<sup>199,200</sup>. Thus, activation of the Rho protein is facilitated in a GEF-independent manner.

Pathogenic bacteria produce a variety of virulence factors and toxins that covalently modify Rho GTPases. These factors induce different PTMs on Rho GTPases like adenylation, ADP ribosylation, deamination, glucosylation, proteolytic cleavage and transglutamination. Two Arginine residues in Rac1, Arg66 and Arg68 are ADP-ribosylated by Exoenzyme S secreted by *Pseudomonas aeruginosa*. This leads to persistent activation and relocalization of Rac1 to the membrane<sup>201</sup>. Furthermore, T35 of Rac1 can be AMPylated by VopS, an effector of *V. parahaemolyticus* and promotes inactivation of Rac1 causing cytoskeletal disruption<sup>202</sup>. The *Clostridium difficile* toxin B<sup>203</sup> attaches a glucose group to a serine of Cdc42, Rac1 and other Rho GTPases, thus non-selectively blocking membrane association and downstream signaling. Rac1 can be modified at residue T35 in the switch I region by various *Clostridium* toxins that lead to disruption of its binding to effectors and thus, disruption of actin cytoskeleton<sup>204</sup>.

### 1.2.5. Rac1 and the WAVE2 complex

Four Rho GTPases constitute the Rac subfamily – Rac1, Rac2, Rac3 and RhoG (**Figure 7**). Sharing over 80% sequence homology, this family of proteins has been traditionally associated with formation of lamellipodia and membrane ruffles in activated cells. Rac1 is the most well studied member of the family and has been implicated in various cellular functions like cell migration, proliferation, tumorigenesis, intercellular adhesion, endocytosis and phagocytosis <sup>115</sup>. Rac1 regulates tumor cell function through various proteins like JNK <sup>205</sup>, cAMP <sup>206</sup> and phospholipase C $\gamma$ 1 (PLC $\gamma$ 1) <sup>207</sup>.

Rac1 promotes cytoskeletal reorganization through two main pathways. The first pathway involves the WASP-family verprolin-homologous protein (WAVE) complex that is directly downstream of Rac1. The WASP superfamily proteins are defined by characteristic domain architecture: a proline-rich stretch followed by a conserved C-terminal sequence called the VCA region. The VCA region acts as a platform to simultaneously bind to both an actin monomer and the Arp2/3 complex, bringing them into close proximity. The WAVE complex is a pentameric protein complex consisting of Nap, Sra1, Abi1/2, HSPC300 and WAVE2. WAVEs, unlike WASPs, do not possess the CRIB domain and thus cannot bind directly to Rac1. Instead, insulin receptor substrate (IRS) p53 has been identified as a linker molecule connecting Rac1 and WAVEs. WAVE2 has a number of regulatory phosphorylation sites that are characterized targets of various kinases like PKA, ERK2, Src and Abl <sup>208</sup>. ERK2 is the terminal kinase of the classical MAP kinase cascade and is known to phosphorylate Ser308, Ser343, Ser351 and Thr346 in the Proline-rich domain (PRD) of WAVE2 <sup>209–211</sup>. Activation of the WAVE complex can happen via activating phosphorylations on WAVE2 or Abi and leads to translocation towards the plasma membrane and activation of Arp2/3, a seven-subunit protein complex that serves as a nucleation site for new actin filaments. Arp2/3 binds to existing actin filaments and initiates growth of new filaments at a 70° angle to the parental one <sup>212</sup>. The Arp2/3 complex induced actin protrusions are essential for cell motility and migration during various

crucial processes like neurite extension, wound healing, cancer metastasis and development<sup>213</sup>.

The second mechanism by which Rac1 regulates cytoskeletal organization is via the p21-activated kinase (Pak). The Paks are a family of 6 serine/threonine kinases which bind to both Rac1 and Cdc42 and primarily modulate cytoskeletal reorganization by phosphorylation of various proteins including myosin light chain kinase (MLC), LIM kinase as well as the Arpc1b subunit of the Arp2/3 complex<sup>214–216</sup>. Pak1 is the best studied amongst the Paks and is crucial in the context of cell motility, survival and cell cycle progression<sup>217</sup>. It is highly up-regulated in ovarian, breast and bladder cancers<sup>218</sup>.

Rac1 knockout results in embryonic lethality<sup>219</sup>, as a result conditional knockout mice are studied to learn more about the tissue-specific roles of Rac1<sup>220–224</sup>. In recent times, the development of a photoactivatable Rac1 has allowed insights into the spatio-temporal dynamics of Rac1 in moving cells<sup>225</sup>. These studies showed that localized activation of Rac1 leads to inhibition in RhoA activity in a spatially controlled manner<sup>226</sup>. In border cells of the *Drosophila* ovary, localized activation of Rac1 leads to a response in other cells of the cluster, leading to the suggestion that cells sense direction as a group rather than on an individual basis<sup>226,227</sup>. Optogenetic technology enables to evaluate the spatiotemporal activation of photoactivatable Rac1 (PA-Rac1) in living cells. Notably, PI(3,4,5)P3 and WAVE2 were localized in the extending lamellipodium in a PI3K-dependent manner. These results suggest that Rac1-induced lamellipodial motility consists of two distinct activities, PI3K-dependent outward extension and PI3K-independent ruffling<sup>228</sup>. Studies have also demonstrated that Rac1 diffusion in cells is not uniform *in vivo* and varies depending on whether Rac1 is bound to actin or not<sup>229</sup>. Specifically, Rac1 activity peaks 40 seconds after and 2µm away from the protrusion event<sup>230</sup>. Further, Rac1 diffuses slower at the leading edge of the cells than elsewhere due to its high interaction with actin at this edge. Finally,

various FRET biosensors have been employed as well to understand Rho GTPase dynamics<sup>142</sup>.

Rac1 overexpression, much like RhoA, has been reported in a variety of cancers including breast cancer, testicular cancer, gastric cancer, prostate cancers, oral squamous cell carcinoma and lung cancers<sup>231–236</sup>.

Recent studies have identified a recurrent somatic mutation in Rac1 in melanomas<sup>237,238</sup>. Both studies suggested that UV induced a mutation in the Pro29 residue (P29S), which usually sits in the hydrophobic pocket of the Switch I region mutation. This proline is mutated into a serine and alters the conformation of the protein significantly. This gain-of-function mutation is shown to increase proliferation and migration, possibly due to increased binding to Pak1 and induced Rac1 accumulation in ruffling membranes, a hallmark of Rac1 activation<sup>237,238</sup>. In fact, this mutation is so common in melanomas that Rac1 is now recognized as the 3<sup>rd</sup> most commonly mutated protooncogene after B-raf and N-Ras in these cancers<sup>239</sup>.

### 1.2.6. RhoA and RhoB

The Rho subfamily consists of three highly conserved proteins – RhoA, RhoB and RhoC. While RhoA and RhoC are frequently up-regulated in human tumors, RhoB is observed to have pro-apoptotic functions<sup>240,241</sup>. However, all three members of the family have a role in stress fiber formation as well as in focal adhesion complexes.

RhoA, the best-studied isoform of the three has been implicated in various stages of cancer progression. The functional divergence is a consequence of differences at the C-terminal end where a set of 15 amino acids plays an important role in mediating interaction with effector molecules. The three major effectors of RhoA are ROCK, PIP5K and mDia. Induction of RhoA-ROCK signaling leads to blebbing, thus causing amoeboid migration<sup>242</sup>. RhoA is also responsible for mediating thrombin-induced inflammatory response. This is accomplished through XIAP, as when XIAP is silenced, it

inhibits RhoA activation<sup>243</sup>. Several studies have observed and correlated RhoA activation with the rear of the cell. However, there have also been studies showing RhoA at the front of randomly migrating cells<sup>244–246</sup>. Specifically, RhoA protrusion was detected during the initial protrusive phase of membrane ruffling which requires Cdc42 activation and Rac1 inactivation. Spatio-temporal analyses of RhoA activity showed that RhoA activity is localized to within 2µm of the cell edge<sup>230</sup>. RhoA has an antagonistic relationship with Rac1 and is shown to reduce migratory polarity through ROCK2-mediated suppression of Rac1 activity in lamellipodia<sup>247</sup>. RhoA and RhoC are both required for ROCK2 mediated promotion of centrosome duplication<sup>248</sup>.

Elevated levels of RhoA expression are observed in numerous forms of cancer, most notably in breast, colon, and lung cancers<sup>249</sup>. Increased RhoA expression in the liver correlated with increased protein activity, poor prognosis and recurrence<sup>250</sup>. Elevated RhoA levels also corresponded to progression of other cancer including ovarian<sup>251</sup>, bladder<sup>252</sup>, gastric<sup>235</sup> esophageal squamous cell<sup>253</sup>, and testicular cancer<sup>236</sup>. Taken together, data from human patients strongly suggest an important function of RhoA in malignant progression of various tumors.

RhoB is known to regulate trafficking of growth factor tyrosine kinase receptors through endosomes. This includes epidermal growth factor receptor (EGF) and vascular endothelial growth factor (VEGF) receptor. It also influences the trafficking of Src, a tyrosine kinase to the plasma membrane<sup>254,255</sup>. Loss of RhoB in macrophages reduces integrin levels on the cell surface<sup>256</sup>. It has been implicated in cell spreading and inhibits stable lamellipodium extension. This is effected downstream of Rac1 as it is known that Rac1 plays a key role in these phenomenon. Interestingly, it promotes migration though it impairs persistence and directionality<sup>257</sup>. Further, depletion of RhoB also reduces cell adhesion in epithelial cells leading to the hypothesis that RhoB downregulation in epithelial cancers could lead to weakening of cell-cell junctions during tumor progression<sup>258</sup>. RhoB



expression is also frequently induced by stress stimuli and by growth factors, thus potentially modulating cell shape changes as well as migration in response to these treatments<sup>240</sup>. RhoB stimulates NF- $\kappa$ B activation through ROCK1<sup>259</sup>. Although RhoB is considered as a tumor suppressor, there have been reports of RhoB regulating the uPAR signaling pathway which plays a key role in promoting cancer cell adhesion, migration and invasion<sup>260</sup>.

### 1.2.7. Cdc42

The Cdc42 subfamily consists of 3 members – Cdc42, RhoJ and RhoQ. Of the three members, Cdc42 is easily the most studied and has been implicated in various crucial cellular processes. All three members of the family are known to stimulate filopodia formation and maintaining cell polarity. Apart from these two well-known phenotypes, Cdc42 has also been known to regulate various process in the nervous system like cell motility, cytoskeletal reorganization, neuronal cell polarity and morphology as well as cell cycle progression. Cdc42 is responsible for axon myelination in glial cells<sup>261</sup>, is essential for axon generation in hippocampal neurons<sup>262</sup> and also plays a critical role in innate immune signaling<sup>263</sup>. Similar to Rac1, germline deletion of Cdc42 is embryonic lethal, so conditional knockouts have been generated to elucidate tissue specific roles of Cdc42.

Probably the most well known phenotype associated with Cdc42 is that of filopodia formation. Unlike lamellipodia, filopodia are stiff rods made of parallel bundles of actin filaments that extend beyond the leading edge of lamellipodia forming “finger-like” protrusions. Filopodia are very important when it comes to directional migration, guidance based on chemotropic cues, as well as substrate surface probing for adhesion sites. Myosin X usually transports integrins to the filopodial tips and the subsequent adhesion promotes cell migration<sup>264</sup>. It also localizes to filopodia tips and has potent filopodia-inducing activity<sup>265</sup>. As a result of its functions, filopodia find themselves integral to a variety of processes like wound healing, angiogenesis<sup>266</sup> and embryonic development. The driving force for the elongation and consequent



movement of the cells is the same for filopodia as lamellipodia – barbed end actin filaments that can be used as a starting point for polymerization towards the plasma membrane.

While Cdc42 has been the major Rho GTPase linked with filopodia formation the exact molecular mechanisms remains unclear despite intense investigations. Both Arp2/3 as well as mDia proteins, also called formins that are effectors downstream of Cdc42 could play a key role in formation of filopodia. Two different models have been proposed for filopodia initiation and extension, namely a) the convergent elongation model and b) the tip nucleation model. The convergent elongation model involves an obligatory role for Arp2/3, while the tip nucleation model primarily argues for a role for formins in filopodia initiation. Expression of dominant negative Rac1 in cultured fibroblasts <sup>267</sup>, as well as in *Drosophila* pupae <sup>268</sup> resulted in an inhibition of filopodium, thus supporting the convergent elongation model and the involvement of Arp2/3 in the formation of these F-actin rich protrusions. In-vitro studies also showed that Fascin and Arp2/3 mediate the reorganization of actin filaments from branched to parallel bundles <sup>269,270</sup>. However the presence of filopodia even in the absence of Arp2/3 <sup>271</sup> is one of the reasons an alternative model was proposed – the tip nucleation model, which proposes that formins, which can nucleate, elongate and protect the filaments from capping are primarily responsible for filopodia formation under these settings <sup>272–274</sup>.

While all Rho GTPases have been visualized at the leading edge of cell migration depending on the stage, Cdc42 and Rac1 are usually known to work in tandem at the front of the cell. It is also suggested that Cdc42, in tandem with Rac1 may be essential in strengthening and stabilization of protrusions <sup>230</sup>.

High Cdc42 levels correlate with testicular cancer progression and consequently poorer outcome <sup>236</sup>. Cdc42 is also overexpressed in breast cancers <sup>249</sup>, lung cancer and cutaneous melanoma and has been suggested

as a disease marker and prognosis parameter in the latter case <sup>275</sup>. Recently, it has been shown that Cdc42 activity is critical for transendothelial migration and lung metastasis formation *in vivo* in a  $\beta$ 1 integrin dependent fashion <sup>276</sup>.

### 1.2.8. Rho GTPases and cell migration

Cell migration is a complex biological process that underlies key phenomenon like tissue formation and maintenance, regeneration as well as pathological conditions like invasion of tumor cells leading to metastasis. While there are various factors that influence cell shape and migration like cell-cell and cell-matrix adhesions, pericellular proteolysis, polarity, as well as the extracellular matrix (ECM), the key feature driving this process is the actin cytoskeleton, and by extension, the Rho GTPases. The seminal paper by Lauffenburger and Horwitz in 1996 proposed a 5-step model for 2D cell migration: Lamellipodium extension, formation and stabilization of focal adhesion complexes, proteolysis of the ECM using surface proteases, contraction of the cell body, and finally, the retraction of the tail (Lauffenburger et al., 1996). While initial studies focused on cell migration in a 2D setting, recent studies have employed 3D models of the ECM to visualize cells. These studies have dismantled the dogma prevailing in the field regarding cell migration. In fact, these studies have showcased the importance of factors like ECM porosity, crosslinking and topography in influencing 3D cell migration <sup>277</sup>. 2D cell migration mainly spoke of lamellipodia and filopodia based cell migration strategies, however 3D migration introduced new actin rich complexes like lobopodia, which are blunt, cylindrical protrusions formed due to intracellular pressure <sup>278</sup>. Cells are also capable of forming actin-rich structures that proteolytically degrade the ECM – invadopodia and podosomes, all of which significantly contribute to 3D cell migration <sup>279</sup>. In 2D cell migration, ECM molecules are presented as a flat sheet of globular molecules without any appreciable fibrillar structure, whereas 3D migration results in a fibrillar topography that prevents lateral spreading. As a consequence, apico-basal polarity is not imposed on the actin cytoskeleton in 3D migration unlike in 2D

models <sup>280</sup>. Thus, utmost care should be taken in comparing results between 2D and 3D migration models.

Mesenchymal migration is characterized by elongated cell morphology, focalized cell–matrix interactions with high attachment to the ECM, high contractility as well as established cell polarity and the secretion of proteases to degrade the ECM to move in a fibroblast-like manner. Amoeboid migration is usually seen in cells with a rounded morphology, such as leukocytes, hematopoietic stem cells, and cancer cells. This type of movement is largely independent from any matrix contact and proteolytic degradation is avoided, as the cells tend to squeeze through gaps in the extracellular matrix rather than degrading it. This results in a faster form of migration with speeds up to 10  $\mu\text{m}/\text{min}$  <sup>281</sup>. However, for many cancer types, histomorphologically, the most frequently observed invasion unit is a group of cells that together define a malignant function <sup>282,283</sup>. Rho GTPases play a key role in all forms of migration and **Figure 12** summarizes all these activities succinctly.

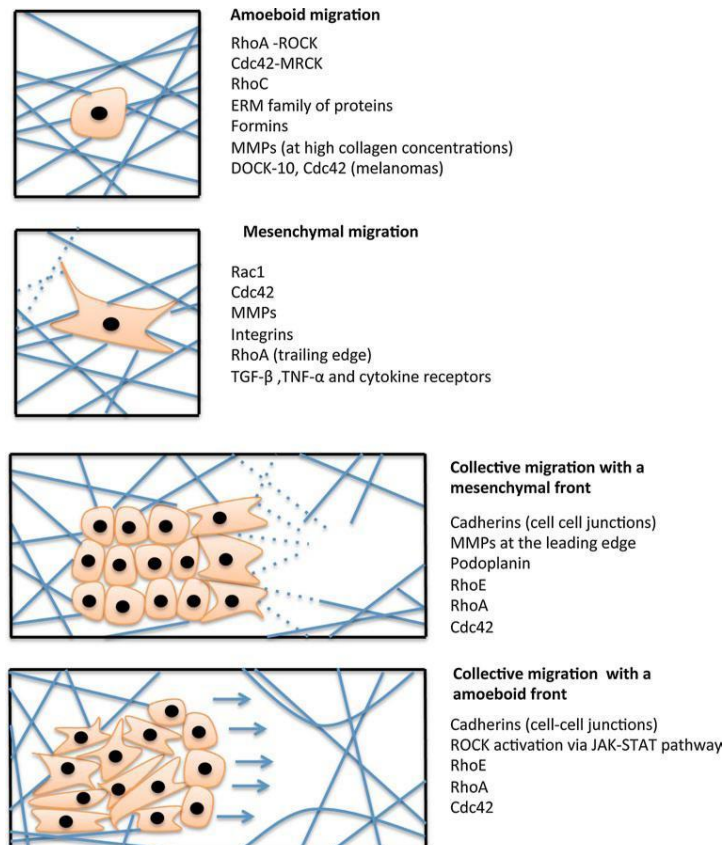


**Figure 12: Different modes of migration visualized.**

Rho GTPases involved in each form of migration are mentioned alongside each form of migration. It is clear from this that while certain Rho GTPases are exclusive to particular forms of migration, like Rac1 (mesenchymal), some Rho GTPases participate in different steps and at different points spatially in the cell to facilitate either amoeboid or mesenchymal migration (like Cdc42). Figure adapted from Murali et al, 2014.

It is becoming increasingly evident that changes to the microenvironment or intrinsic cell properties result in cells adapting to the new conditions by genomic and epigenetic alterations. Modulating various proteins, receptor expression levels and the presence of different cytoskeletal regulators responsible for cell–cell and cell–matrix adhesion ultimately leads to a change in the mode of migration of the cell. This ability of cells to adapt to their environment and change their migration styles instead of completely abandoning them is referred to as cell plasticity. One such transition is the epithelial-to-mesenchymal transition (EMT). EMT is involved in many developmental processes as well as in invasive tumors, where immotile epithelial cells lose their cell–cell contacts, polarity, and acquire mesenchymal traits like motility and invasiveness, thus allowing them to move away from their location<sup>284</sup>.

While amoeboid and mesenchymal forms of movement are discussed as two distinct types, it is prudent to see them as the two extremes in a spectrum modulated by various signaling pathways as well as environmental cues, all of which influence the decision of the cell to switch between one mode to the other. Thus, plasticity of cell migration needs to be considered duly while designing inhibitors targeting one particular form of migration. Utilizing combinations of inhibitors as well as identifying potential master switches in the signaling pathways regulating migration remains an aim for the future.

### **1.2.9. Rho GTPases, IAPs and cell migration**

Geisbrecht and Montell demonstrated in 2004 for the first time that IAPs could play a role in influencing Rho GTPase function and cell migration. They worked on the phenomenon of border cell migration in ovaries during oogenesis and showed that overexpression of DIAP1 compensated for the inhibition of migration caused by dominant negative Rac1 expression. They further showed that DIAP1 interacted with Rac1 in a nucleotide independent manner as well as profilin, an actin-binding protein<sup>285</sup>. Interestingly, Oberoi and colleagues observed contradictory results in both mammals as well as

zebrafish models <sup>11</sup>. While they demonstrated that XIAP and cIAP1 can directly bind to Rac1, this binding led to subsequent K48-ubiquitylation and proteasome-mediated degradation of the Rho GTPase. Loss of the two IAPs stabilized Rac1 levels and promoted a mesenchymal mode of migration in many primary and tumor cell lines <sup>11</sup>. This was extended to a zebrafish model where enhanced expression of DrXIAP in cerebellar granule neurons (CGNs) led to a loss of cell polarity in a Rac1 dependent manner. More recently, Marivin and colleagues showed that cIAP1 binds directly to Cdc42, Rac1 and RhoA. In contrast to Rac1 that requires XIAP for degradation in response to RhoGDI silencing, cIAP1 stabilizes the inactive form of Cdc42 by strengthening its interaction with RhoGDI1 <sup>286</sup>. cIAP1 was required for the activation of Cdc42 and consequent filopodia formation in response to TNF $\alpha$ , while it was also important for Cdc42 activation upon EGF stimulation or oncogenic H-Ras expression. Thus, IAPs have been shown to perform both pro as well as anti-migratory functions in tumor cells, some of which are discussed in the following paragraphs.

Lopez and colleagues showed in 2011 that the CARD domain of cIAP1 could play a role in regulating cell migration. cIAP1 cooperates with Myc to drive cell proliferation – it does this by ubiquitylating and degrading Mad1, a myc antagonist. The study observed that the CARD deletion mutant of cIAP1 showed enhanced E3 ligase activity. They also demonstrated that the cIAP1 mutant showed enhanced migration compared to the WT cIAP1 cells <sup>36</sup>. However, a later study by Blankenship et al. suggested a role for the linker region between the BIR3 domain and the CARD domain for maintaining cIAP1 stability <sup>27</sup>. Similarly, another study speculated that the BIR3-RING interactions could determine the E3 ligase activity of cIAP1, rather than the CARD domain <sup>61</sup>. In addition, another study reported that XIAP-mediated cancer cell migration was RING domain dependent in HCT116 cells, and that depletion of XIAP led to diminished migration in these cells <sup>287</sup>. XIAP prevented the SUMOylation of RhoGDI at Lys138, interfering with the actin cytoskeleton and cell motility <sup>288,289</sup>. Yet another study showed that down-regulation of XIAP affected recruitment of Focal Adhesion Kinase (FAK) to the

focal adhesion sites, thus disrupting FAK-Src contact, preventing shear-stress induced Src-mediated-FAK phosphorylation and Erk1/2 activation thus inhibiting cell migration<sup>290</sup>.

For every report of IAPs playing a pro-migratory role, there have been parallel reports stating the exact opposite. Studies by our group showed that IAPs regulate the stability of C-RAF kinase, a central kinase of the classical MAP kinase cascade that plays a vital role in tumorigenesis downstream of Ras<sup>9,10</sup>. Loss of IAPs led to enhanced actin protrusions and led to enhanced C-Raf dependent cell migration. Further work along these lines demonstrated that using IAP antagonists at sub lethal doses led to cells exhibiting an elongated morphology as well as enhanced Rac1- and MAP kinase-dependent cell migration. This phenotype was recapitulated by employing cIAP1<sup>-/-</sup> as well as XIAP<sup>-/-</sup> Mouse Embryonic Fibroblasts (MEFs)<sup>11,286</sup>. It is likely that many of the contradictory migratory phenotypes associated with the IAPs are due to differences in cell types employed, this also fits in with the bigger picture where IAPs are seen to play both oncogenic and tumor suppressive roles in various cancers. Finally, IAPs, as discussed in earlier sections, play a crucial role in both the canonical and non-canonical NF-κB pathway and various studies have shown that treatment of cells with IACs can trigger the pro-migratory and invasive properties of NF-κB signaling.

One crucial unanswered issue is that of cross regulation between IAPs influencing cell migration and other related phenomenon. While cIAP1<sup>-/-</sup> MEFs showed elongated morphology, a cIAP1<sup>-/-</sup>/cIAP2<sup>-/-</sup> MEFs are more rounded cells with lesser protrusions. It has already been documented that IAPs exist in heteromeric protein complexes<sup>291,292</sup>, however while a lot is known about individual contributions, not much is known about how these complexes work in the context of regulating cell shape and migration.

## 2. Materials and Methods

### 2.1 Cell biology methods

#### 2.1.1. Cell lines

Cell Line	Description	Culture medium
HeLa	Cervical Cancer cells	DMEM
MDA-MB231	Metastatic Breast Cancer cells	DMEM
NCI-H226	Lung Cancer cells	RPMI
BT474	Breast Cancer cells	DMEM
HMEC	Primary mammary epithelial cells	MEGM
HMEC-T	Tert-immortalized mammary epithelial cells	MEGM
293T	Human Embryonic kidney cells	DMEM

To ensure assay accuracy, cells were always counted prior to seeding as described in the sections below. Cells were counted by use of TC 20™ automated cell counter (BioRad #145-0101) whereby counts have been obtained for suspension cells grown as adherent cells at concentrations up to  $1 \times 10^7$  cells/ml. 10  $\mu$ l of cell suspension in the presence of trypan blue (Sigma, #T8154) have been used for determining cell viability and count. HeLa cells, 293T, BT474 and MDA-MD231 cells were cultured in Dulbecco's modified Eagle (DMEM) medium (GIBCO) supplemented with 10 % FCS and 0.2 % Penicillin (100U/ml)/streptomycin (100 $\mu$ g/ml) (Gibco) at 37°C in 5 % CO<sub>2</sub>. NCIH226 cells were cultured in RPMI (Gibco) medium supplemented with 10% FCS and antibiotics, while HMEC and HMEC-T cells were cultured in MEGM medium (Lonza) supplemented with growth factors as recommended



by the company (CC-4136 SingleQuot kit) including Hydrocortisone solution, GA-1000, Recombinant human insulin 0.5 %, BPE High Protein and hEGF at a concentration of 10 µg/ml).

### 2.1.2. Production of lentiviruses

shRNAs directed against human Cdc42 (**NM\_001791**) were obtained from Sigma. Cells were infected by lentiviral particles and subsequently selected for resistance to puromycin (2.5 µg/ml) until a stable knockdown culture was achieved.

The lentiviral particles with Cdc42 shRNAs used for stable knockdown in HeLa cells was: Cdc42 shRNA, Sequence: CCGGCCTGATATCCTACACAACAACTCGAGTTTGTGTGTAGGATATCA GGTTTTTG

### 2.1.3. Transfection of siRNAs

To silence XIAP, cIAP1, Cdc42 or Rac1 translation by siRNA interference, about 75,000 cells per well were seeded on 12-well plates at least 20 h before transfection. siRNAs directed against mRNAs of interest or a scrambled control siRNA as a negative control were transfected into cultures using Saint Red (Synvolux), Lipofectamine RNAiMAX (Invitrogen, #13778-150) or HiPerfect (Qiagen) at a final concentration of 60 nM. For co-transfection experiments, both siRNAs were transfected at a final concentration of 60 nM. Unless otherwise stated, cells were lysed 48 h after transfection to test knockdown efficiency by immunoblots. The siRNAs used in this study were purchased from Qiagen;

XIAP3'-UTR siRNA: Target Sequence: CTGACTGATCTAATTGTATTA (Qiagen),

XIAP siRNA-2: Target Sequence: GAAGGAGAUACCGUGCGGUGCUUUA (Invitrogen),

XIAP siRNA-3: Target Sequence: AAGTGCTTTCACCTGTGGAGGA (Qiagen),

Control siRNA: Target Sequence: AATTCTCCGAACGTGTACAGT(Qiagen),



Cdc42 siRNA-1: Target Sequence: CATCAGATTTGAAATATTTAA (Qiagen),  
Cdc42 siRNA-2: Target Sequence: GGCGATGGTGCTGTTGGTAAA  
(Qiagen)

#### **2.1.4. Cell culture and transfection**

All cells were grown at 37° C at 5 % CO<sub>2</sub> containing air. After reaching confluency, the cells were passaged at regular intervals. Where indicated, cells were treated with DMSO (Applichem #A3672), BV6 (Syngene), UO126 (Calbiochem, # 662005), and NSC23766 (Calbiochem, CAS 1177865-17-6) in the presence of serum for the times and at the concentrations (ranging from 0.1 to 10 mM) indicated in the figures. For treatment with Epidermal Growth Factor (EGF) (Labgen), a stock concentration of 25 ng/μl was used. MG132 treatment (Calbiochem CAS 133407-82-6) was performed 5 h before lysing of cells at a concentration of 10 μM. Cycloheximide chases were performed with InSolution Cycloheximide (Calbiochem) at a final concentration of 100 μg/ml. For overexpression experiments, unless otherwise stated, HeLa and 293T cells were transiently transfected with various plasmids amounting to 1 μg of DNA, using polyethylenimine/ PEI (Polysciences Inc., #23966) at a concentration of 10 mM. In the case of Cycloheximide chases post overexpression, the chase experiments were started 40 h post transfection so as to lyse cells at 48 h post transfection.

## **2.2. Molecular biology methods**

### **2.2.1. Vectors, cDNAs and constructs**

Vectors:

pGEX-6T1

pcDNA3.1/*myc*-HisB (Invitrogen)

pGEX4T

pRK5 *myc*

cDNAs:

pRK5 *myc*-Cdc42WT

pRK5 myc-Cdc42Q61L  
pRK5 myc-Cdc42T17N  
pRK5 myc-Cdc42Q61LK166A  
pGEX Cdc42WT  
pGEX Cdc42Q61L  
pGEX Cdc42T17N  
pGEX-6T1 XIAP  
pCMV XIAP-Flag  
pCMV XIAPH467A-Flag

cDNAs used for lentivirus production (viral plasmids):

HDM VSV-G  
HDM Hgpm2  
HDM tat 1b  
RC CMV-Rev

### 2.2.2. Site-directed mutagenesis

The K166A point mutation in different Cdc42 mutants was generated with the Site-Directed Mutagenesis Kit (Agilent) following manufacturer's instructions. Depending on the type of mutation desired, the number of PCR cycles used in the cycling parameters varied between 16 and 18. The contents and timings for mutant strand synthesis- PCR are listed as followed, but were modified according to vector and insert length:

	Final concentration (50µl reaction volume)	Temperature	Time	
10x Pfu buffer	1x	1. Initial denaturation	95°C	1 min
dNTPs 2mM	0.2 mM	2. Denaturation	95°C	45 s
forward primer 10 pM	1 pM	3. Annealing	58°C	1 min
reverse primer 10pM	1 pM	4. Extension	68°C	7 min
Template DNA	25ng	5. Final extension	68°C	10 min
Pfu polymerase 2.55U/µl	2.5	6. Cool down	4°C	unlimited
ddH <sub>2</sub> O	add to final volume			

} 18x

Annealing temperature was determined according to the melting temperature of primers ( $T_m - 5^\circ\text{C}$ ) and extension time was calculated depending on the length of amplified DNA fragment (2 min per kb of DNA). After endonuclease

*Dpn I* –treatment to digest parental DNA template and to select for mutation-containing synthesized DNA, the PCR product was heatshock transformed into chemocompetent *E. coli* bacterial cells as followed: Incubation of DNA with *E. coli* for 30 min on ice, followed by heat shock at 42 °C for 90 s, placed on ice again for 5 min before 500 µl of antibiotic-free LB-medium (Applichem, #A4425) was added. After incubation at 37 °C for 45 min, the transformed bacteria were selected on antibiotic containing LB-agar plates. The selection marker of the pRK5 vector is Ampicillin (Applichem, #A0839). Single colonies were then expanded in appropriate antibiotic containing LB- medium at 37 °C for >16 h and used for DNA preparation, which was achieved by use of the GeneJET- DNA purification kit (Thermo Scientific) following manufacturer's instructions. The fidelity of mutagenesis was confirmed by DNA sequencing (Eurofins MWG Operon). The pLenti4V5-DEST™ Gateway® Vector system (Invitrogen) was used for lentiviral-based expression of a target gene in dividing and non-dividing mammalian cells.

### 2.2.3. RT-PCR

Total RNA was extracted from cells using Trizol (Ambion/Thermo Fisher) or an RNA isolation kit (ThermoFisher). Briefly, cells were resuspended in Trizol, Chloroform was then added to the cell suspension and cells were vortexed for 15 seconds. They were then spun down at 14,000 rpm for 15 min at 4 °C. The aqueous upper phase is then transferred to sterile tubes containing Isopropanol. After incubating this mix at RT for 10 min, the samples are again spun down at 14,000 rpm for 15 min at 4 °C. They are then washed with 75 % Ethanol and spun down at 10,000 rpm for 5 min at 4 °C. The pellet is air dried and resuspended in 50 µl of RNase free dH<sub>2</sub>O. The amount of RNA was subsequently measured via NanoDrop (Thermo Fisher). When using the RNA isolation kit, standard protocol was followed. cDNA was synthesized using the RevertAid RT kit (Thermo Scientific) and manufacturer's instructions were followed. For PCR amplification, the following primers were used: Cdc42-For-1 – AGTGGTCTGCACTTACACAGAAAG, Cdc42-Rev-1 – CTGCGGCTCTTCTTCGGT, Cdc42-For-2 –

AGGCTGTCAAGTATGTGGAGTG,	Cdc42-Rev-2	–
GGCTCTTCTTCGGTTCTGG,	Cdc42-For-3	–
CATCGGAATATGTACCGACTGTT,	Cdc42-Rev-3	–
TGCAGTATCAAAAAGTCCAAGAGTA,	GAPDH-For-1	–
TGCACCACCAACTGCTTAGC,	GAPDH-Rev-1	–
GGCATGGACTGTGGTCATGAG,	RPS13-For-1	–
CGAAAGCATCTTGAGAGGAACA,	RPS13-Rev-1-	
TCGAGCCAAACGGTGAATC		

The qPCR machine was programmed as follows: 1 cycle at 50 °C – 2 min, 50 cycles at 95 °C – 15 min, 95 °C – 15 s, 57 °C – 15 s, 72 °C – 15 s and finally 1 cycle at 95 °C – 1 min.

## 2.3 Biochemical methods

### 2.3.1. Antibodies

Antibody	Antibody type	Source	Dilution employed
Anti-Cdc42	Primary	BD Transduction	1:500
Anti-beta Actin (HRP)	Secondary	Abcam	1:20000
Anti-beta Actin	Primary	Sigma	1:1000
Anti-XIAP	Primary	BD Pharmingen	1:500
Anti Flag (HRP)	Secondary	Sigma	1:10000
Anti-c-Myc	Primary	Santa Cruz	1:500
Anti-GST	Primary	Santa Cruz	1:1000
Anti-pERK1/2 Thr202/Tyr204	Primary	CST	1:500
Anti-pCRAF S338	Primary	CST	1:500
Anti-pMEK1/2	Primary	CST	1:500
Anti-WAVE2	Primary	CST	1:1000
Anti-pWAVE2 Ser308	Primary	CST	1:500
Anti-pWAVE2 Thr346	Primary	CST	1:500

Anti-Rac1	Primary	BD Pharmingen	1:500
Mouse IgG	Primary	Santa Cruz	1:3000
Rabbit IgG	Primary	Santa Cruz	1:3000
Anti-Tubulin	Primary	Sigma	1:2000

### 2.3.2. SDS-PAGE and Western blotting

Proteins were separated by electrophoresis on the basis of mass in a polyacrylamide gels\* under denaturing conditions disrupting nearly all non-covalent interactions (SDS-page). Cells were lysed in 5X Laemmli Buffer (60 mM Tris-base (pH 6.89), 10 % Glycerol, 3 % SDS and 5 %  $\beta$  - Mercapthoethanol, bromophenolblue) and boiled at 100 °C for 5 min before loading them on the polyacrylamide gels. After separation by SDS-PAGE, the proteins were transferred to either nitrocellulose (Whatman Protran BA83 #10401396) or PVDF membranes (GE Healthcare Life Sciences). Following the transfer, membranes were then blocked using 5 % low fat milk (Carl Roth, #T145.2) in either Phosphate-Buffered Saline or TBST or 3 % BSA + TBST for 1 h at room temperature. They were subsequently incubated overnight with various primary antibodies diluted in 3 % blocking buffer, 3 % BSA + TBST or 1 % BSA + TBST. Horseradish peroxidase coupled secondary antibodies followed by chemiluminescence (Amersham Biosciences, Millipore #RPN2209) were used to detect the antigen antibody complexes. They were finally visualised on X-ray films (Agfa Cronex, #ECOAA). Quantification of the obtained Western Blots was performed by densitometry on ImageJ (NIH).

\*The polyacrylamide gels used in this work were composed of two layers: a 6–15 % separating gel (pH 9) that separates the proteins according to size and a lower percentage (5 %) stacking gel (pH 6.8) that ensures simultaneous protein entry into the separating gel at the same height.

### 2.3.3. Protein-protein interaction assays

#### Purification of recombinant proteins

Recombinant XIAP, Cdc42 Wild Type, Cdc42Q61L and Cdc42T17N were expressed as GST fusion proteins in BL-21 *Escherichia coli* strain (Stratagene, Cedar Creek, TX) according to manufacturer's instructions. The proteins were purified using standard protocols. Briefly, Protein Purification Buffer (50 mM HEPES, pH 7.5, 150 mM NaCl, 1 mM EDTA, 5 % Glycerol and 0.1 % NP-40) was used to lyse the bacteria which were then sonicated for three cycles, lasting 10 s each. GST beads were added to specifically pull our protein of interest down and multiple incubations and wash steps were performed to purify the protein. Samples were collected at each step and run on an SDS PAGE gel to check for loss during subsequent washing steps. Proteins were then cleaved, if required from their GST tag by using Thrombin (1U) (GE Healthcare). Thrombin cleavage was performed using manufacturer's instructions.

#### CRIB Pull down Assays

For the pulldown assays, GST-PAK-PBD (Cytoskeleton) was added to the in vitro Ubiquitylation reaction of Cdc42 and the mix was incubated at 4 °C for 2 h on the rotator. 10 µl of Glutathione Sepharose Beads (GE Healthcare Life Sciences) which were first washed thrice with Binding Buffer (25 mM Tris-HCl pH 7.2, 150 mM NaCl, 0.5 % NP-40, 1 mM MgCl<sub>2</sub>, 5 % Glycerol) were then added to the reaction mix and was incubated for 1.5 h at 4 °C on the rotator. The beads were then washed thrice with 500 µl of Binding Buffer and pelleted down at 2500 rpm for 1 min. 50 µl of Sample Buffer was added before boiling the samples at 100°C for 5 minutes. The interaction between the proteins of interest was then observed by SDS-PAGE and subsequent western blot analysis.

### **Interaction between Cdc42 and XIAP mutants**

293T cells were transfected with Cdc42 Wild Type plasmid and cells were harvested. 72 h post transfection. RIPA Buffer supplemented with phosphatase and protease inhibitors was used to lyse the cells. Lysates were then added on top of various GST tagged XIAP mutants purified in the lab and incubated for 2 h at 4 °C. The beads were subsequently washed and finally lysed in Laemmli buffer. Samples were taken for Western Blot analysis and the GST tagged XIAP mutants were visualized using anti-GST antibody (Santa Cruz), while Cdc42 was visualized using anti-Cdc42 antibody (BD).

### **Interaction between XIAP and Cdc42 mutants**

To check for the nucleotide dependence of binding, GST protein or GST tagged XIAP was first immobilized on Glutathione Sepharose beads and rotated at 4 degrees for 1 hour. 1 microgram of GST tagged XIAP was used for this experiment per sample. The samples were then blocked using 1 % BSA in Binding Buffer (25 mM Tris-HCl pH 7.2, 150 mM NaCl, 0.5 % NP-40, 1 mM MgCl<sub>2</sub>, 5 % Glycerol). After 1 h of rotation at 4 °C, the samples were washed thrice with Binding Buffer and cleaved protein was added on the beads. In all cases, either 1 or 2 microgram of protein was used. Samples were rotated for 1.5 h at 4°C and then washed 3 times with Binding Buffer. In this step, 250 mM NaCl is used to minimize background binding. Laemmli buffer was added and samples were heated at 100 °C for 5 min. The interaction between the proteins of interest was then observed by SDS-PAGE and immunoblot analysis.

#### **2.3.4. Immunoprecipitation:**

To immunoprecipitate endogenous WAVE2 or Rac1, cells were seeded on 10 cm dishes, transfected with XIAP siRNAs after 24 h and then lysed 48 h post transfection. The cells were lysed with RIPA buffer (50 mM Tris-HCl, pH 7.5,

250 mM NaCl, 1% Triton X-100, 1 mM NaVO<sub>3</sub>, 25 mM NaF, 1.5 mM MgCl<sub>2</sub>, 1 mM PMSF, β-mercaptoethanol (1:1000 dilution, Applichem), protease inhibitor cocktail (1:100 dilution, Calbiochem), 10% Glycerol) for 30 min on ice. The lysates were cleared by centrifugation at 14,000 rpm for 15 min. Endogenous proteins were then immunoprecipitated with respective antibodies for 15 h at 4°C. The antigen-antibody complexes were precipitated by sepharose coupled protein A/G beads (Roche, #11-134-515-001 and 11-243-233-001). The proteins bound to the beads were washed thrice with the lysis buffer, dissolved in 5X Laemmli and analyzed by SDS-PAGE and immunoblotting.

### **2.3.5. HIS-TUBE pull down**

HeLa cells were transfected in 24 well plates with XIAP siRNA using Lipofectamine RNAiMAX as per manufacturer's instruction. Cells were transferred to 100 mm tissue culture plates 24 h later. Two days post transfection, cells were treated with MG132 (10 μM) for 6 h. Then cells were lysed in RIPA buffer (250 mM NaCl, 50 mM Tris HCl, 10% Glycerine, 1% Triton X-100, pH 7.5), supplemented with EDTA free Protease Cocktail inhibitor (Roche, 64693159001), and N-ethyl maleimide (5 mM). Equal amounts of pre-cleared lysates were incubated with 100 μg/ml His6-TUBE1 (LifeSensors, UM201) for 15 min on ice. After collecting total cell lysates, the remaining lysate were incubated in Ni-NTA beads (Qiagen, Ni-NTA Superflow, 30410) and rotated overnight (at 4 °C). Samples were washed three times with RIPA buffer containing 50 mM imidazole and eluted in SDS buffer containing Laemmli buffer and analysed by SDS-PAGE and immunoblotted for Cdc42 using anti-Cdc42 antibody.

### **2.3.6. F-actin assay - FACS analysis**

HeLa cells were seeded on 24-well plates and treated with IAC for 15 h. Then, they were fixed with 3.7 % PFA for 10 min, washed with PBS and permabilized using 0.1% Triton X-100 in PBS for 10 min. This was followed by washing the cells thrice with PBS. 1% BSA/PBS was then added to each well



and cells were blocked for 30 min. The cells were again washed with PBS and 1:40 dilution of phalloidin (Oregon Green® 488 phalloidin; Invitrogen) in 1% BSA/PBS was added to stain the cells. After 30 min of incubation, cells were washed thrice with PBS and subsequently trypsinized to detach them from their wells. Finally, 450 µl of HEPES buffer (20 mM HEPES, 115 mM NaCl, 1.2 mM CaCl<sub>2</sub>, 1.2 mM MgCl<sub>2</sub>, 2.4 mM K<sub>2</sub>HPO<sub>4</sub>, pH=7.4) was added to the cells, and the cells were sorted using Flow Cytometry.

## **2.4. Proteomics**

### **2.4.1. Determination of Ubiquitin sites on proteins**

In gel trypsin digestion of the proteins was performed as described in Shevchenko et al., 2007. Chloroacetamide was used for alkylation to minimize formation of lysine modifications isobaric to Gly-Gly (Nielsen et al., 2008). After peptide desalting on C18 StageTips, LC-MS analyses were performed using an Easy-LC system (ProxeonBiosystems) coupled to an LTQ-Orbitrap XL mass spectrometer (Thermo Fisher Scientific) as described previously in Borchert et al., 2010. Peptides were eluted using a segmented gradient of 5–80% of solvent B (80% ACN in 0.5% acetic acid) with a constant flow of 200 nl min<sup>-1</sup> over 60 min. Full scan MS spectra were acquired in a mass range from m/z 300 to 2000 with a resolution of 60,000 in the Orbitrap mass analyser using the lock mass option for internal calibration. The five most intense ions were sequentially isolated for CID fragmentation in the linear ion trap. Inclusion list containing 9 ions of special interest (ubiquitinated Cdc42 peptides) was used and up to 500 precursor ion masses selected for MS/MS were dynamically excluded for 90 s. Mass spectra were processed using the MaxQuant software suite (Cox and Mann, 2008) (version 1.0.14.3) and the data were searched using Mascot search engine (Matrix Science) against a decoy human database (ipi.HUMAN.v3.64) containing 168,584 protein entries. Carbamidomethylation (Cys) was defined as fixed-, and protein N-terminal acetylation, oxidation (Met) and Gly-Gly (Lys) were defined as variable modifications. Initial mass tolerance was set to 7 p.p.m. for precursor

ions, and to 0.5 Da for fragment ions. The GlyGly (Lys) modification sites were considered localized if the localization probability (calculated by MaxQuant software) was higher than 0.75. Spectra of modified peptides were manually validated.

#### **2.4.2. Whole Proteome Analysis**

For the whole proteome analysis in which RhoB was subsequently identified, a SILAC experiment was performed. Briefly, HeLa cells were cultured in both unlabeled as well as heavy (K8R10) labeled medium independently. Cells were checked for successful incorporation of the heavy amino acids and then expanded to multiple 15 cm dishes. Once around 40% confluent in the 15cm dishes, unlabeled cells were transfected with Control siRNA while the heavy labeled cells were transfected with XIAP siRNA. After 48 h, cells were lysed in Lysis Buffer (8 M Urea, 75 mM NaCl, 50 mM Tris, pH 8.2, 1 mM NaF, 1 mM Beta-Glycerophosphate, 1 mM Sodium Orthovanadate, 10 mM Sodium Pyrophosphate, 1 mM PMSF and 1 tablet of Protease Inhibitor Cocktail (Roche). In-solution protein digestion was performed. Briefly, lysates were normalized to the same concentration using a BCA assay, then disulphide bonds were reduced, IAA was added to prevent reformation of disulphide bonds and finally LysC and Trypsin were added to facilitate Lysine and Arginine cleavage. Trypsin was quenched using 10 % Trifluoro acetic acid (TFA) and peptide desalting was performed to remove Urea and other detergents from the protein solution. Freeze drying was performed to reduce sample volumes before a cation exchange chromatography (SCX) step wherein fractionation of protein samples was done in order to prevent overloading columns when shooting samples into the mass spectrometer. Samples were again freeze dried and peptide desalting was again performed to remove the SCX buffer. Perform TiO<sub>2</sub> enrichment for phosphoenrichment and with 1/20<sup>th</sup> of the sample, take it for whole proteome analysis. Finally, the samples were stage tipped, eluted and then shot into the mass spectrometer. Data analysis was performed using Max Quant software and various thresholds were set to identify both upregulated and downregulated proteins

upon XIAP knockdown.

## **2.5. Phenotypical studies**

### **2.5.1. Immunofluorescence and Counting of Filopodia**

Cells were seeded and transfected in 12 well plates. One day post transfection, they were split and re-seeded upon coverslips in a new 12 well plate. The confluency of cells on the cover slip was maintained below 30 %. 2 days post transfection, cells were taken and washed thrice with PBS before being fixed in 4 % paraformaldehyde for 10 min. They were then permeabilised using 0.1 % Triton X-100 for 3 min and then blocked for 20 min at RT using 1 % BSA in PBS. The actin cytoskeleton was then labeled with 1:50 Alexa Fluor 488 Phalloidin (Invitrogen) in blocking buffer for 20 min in the dark. For staining of Cdc42 protein, cells were incubated in 1:250 dilution of Cdc42 antibody (BD) overnight in 0.5 % BSA in PBS. Cells were then incubated with secondary Cy3 antibody in Blocking Buffer for 1 h at RT in the dark. Between each step, the cover slip was always washed thrice with PBS. Finally, the cells were mounted on glass slides using Moviol (Sigma) and examined using a Confocal microscope (Leica TCS SP8). Cells were normally viewed at 63X magnification and digital zooming was done in case single cells were focused on. Filopodia were then counted manually using the KatiKati software which has an in-built zoom function to enlarge the images. This was done for all the cell types, tumor and primary cell lines employed in the studies.

### **2.5.2. Wound healing assay**

HeLa control or XIAP depleted cells were seeded onto 12 well plates and scratches were made on confluent monolayers with a pipette tip. Cells were then washed and the extent of wound closure was assessed for 24 h. The images were acquired with a Leica DMI8 microscope using a 10x objective (Live Cell Imaging System) and the percentage of wound closure was

calculated from the width of the wound formed after time using IMAGEJ software tools <sup>11</sup>.

### 2.5.3. Lung colonization experiments

HeLa cells were transfected with the desired siRNAs. Two days post transfection, cells were detached from culture plates, and  $10^6$  cells were suspended in 100  $\mu$ l of PBS before injection into the tail veins of NOD-SCID mice. After 5 weeks, the mice were sacrificed and their lungs were fixed in 4% PFA and analysed for the presence of surface metastatic foci. Three independent pairs of eyes counted the foci to ensure impartiality of counts. Lungs were then sliced with microtomes and hematoxylin and eosin staining was performed. Light microscopy evaluation was performed to confirm the presence of lung nodules.

## 2.6. Appendix- material

### Chemicals and special reagents

Acetonitrile Mass Spec grade	Thermo Fisher Scientific
Acrylamide/Bis solution, 40%	Bio Rad
APS	Applichem
Albumine bovine fraction V	Sigma, Taufkirchen, Germany
Bromphenolblue	Roth, Karlsruhe, Germany
$\beta$ -mercaptoethanol	Applichem
$\beta$ -Glycerophosphate	Sigma, Taufkirchen, Germany
Calcium Chloride	Sigma, Taufkirchen, Germany
DTT	MP biomedical, France
Ethanol	Roth, Karlsruhe, Germany
HEPES	Roth, Karlsruhe, Germany
Hydrochloric acid (HCl)	Sigma, Taufkirchen, Germany
Low melting point agarose	Sigma, Taufkirchen, Germany
Glycerol	Roth, Karlsruhe, Germany
Glycine	Applichem

Iodoacetamide (IAA)	Sigma, Taufkirchen, Germany
Magnesium Chloride (MgCl <sub>2</sub> )	Applichem
Methanol	Sigma, Taufkirchen, Germany
NP-40	Applichem
PMSF	Sigma, Taufkirchen, Germany
Dipotassium Phosphate	Merck, Darmstadt, Germany
Protease inhibitor cocktail	Roche, Mannheim, Germany
Proteinase K	Roth, Karlsruhe, Germany
SDS	Sigma, Taufkirchen, Germany
Sodium Chloride (NaCl)	Roth, Karlsruhe, Germany
Sodium Orthovanadate (NaVO <sub>3</sub> )	Sigma, Taufkirchen, Germany
Sodium Fluoride (NaF)	Sigma, Taufkirchen, Germany
Sodium Hydroxide (NaOH)	Riedel-de-Haën,
T-EDTA, 10x	Sigma, Taufkirchen, Germany
Temed	Sigma, Taufkirchen, Germany
Tris-base	Applichem
Trypsin/EDTA	PAA Laboratories, Austria
Triton X-100	Applichem

All chemicals, reagents and materials that have been used are listed or marked in the appropriate method section; detailed buffer constitutions are given in parentheses.

## 3. Results

### 3.1. Ubiquitin-mediated regulation of Cdc42 by XIAP

#### 3.1.1. Role of XIAP in regulating Cdc42 stability and activity

##### 3.1.1.1. Depletion of XIAP leads to Cdc42 upregulation

Previous studies have implicated IAPs in controlling the actin cytoskeleton by regulation of Rac1 stability <sup>7</sup>. Interestingly, over the course of those experiments, it was observed that XIAP depleted cells exhibited actin rich protrusions on their surface. While lamellipodia formation is associated with Rac1 activity, fine finger like actin protrusions were detected on these cells irrespective of the matrix on which the cells were cultured. It was thus hypothesized that XIAP might regulate other Rho GTPases apart from Rac1. Due to its integral role in filopodia formation, we first checked for differences in Cdc42 levels upon XIAP depletion (**Figure 3.1 A**). A siRNA targeting the 3'-UTR of XIAP was utilized in this experiment with an aim to perform complementation studies. With the same set of siRNAs, XIAP was depleted in a panel of cell lines – BT474 breast cancer cells, HeLa cervical cancer cells, NCI-H226 lung cancer cells and the highly metastatic MDA-MB231 breast cancer cells. As shown in **Figure 3.1 A**, depletion of XIAP led to an increase in Cdc42 protein levels in all cell types. To confirm this observation, multiple siRNAs targeting XIAP mRNA were used to knockdown the protein (**Figure 3.1 B**). Further, complementation experiments revealed that expression of XIAP in trans prevented the increase in Cdc42 levels observed in cells depleted of XIAP using the 3'-UTR XIAP siRNA (**Figure 3.1 B**). Interestingly, while a consistent increase in Cdc42 levels is observed upon XIAP knockdown, there was no linear correlation between the extent of XIAP depletion and increase in Cdc42 levels (**Figure 3.1 C**). On an average a 1.5-2 fold increase was detected in HeLa cells with XIAP depletion. Thus, further corroboration was sought and Mouse Embryonic Fibroblasts (MEFs) derived

from XIAP deficient mice were tested. XIAP deficient MEFs exhibited high Cdc42 protein levels and this is reduced upon complementation of the same cells with exogenously expressed XIAP cDNA (**Figure 3.1 D**). Taken together, these results confirm the specificity of the observed phenotype.

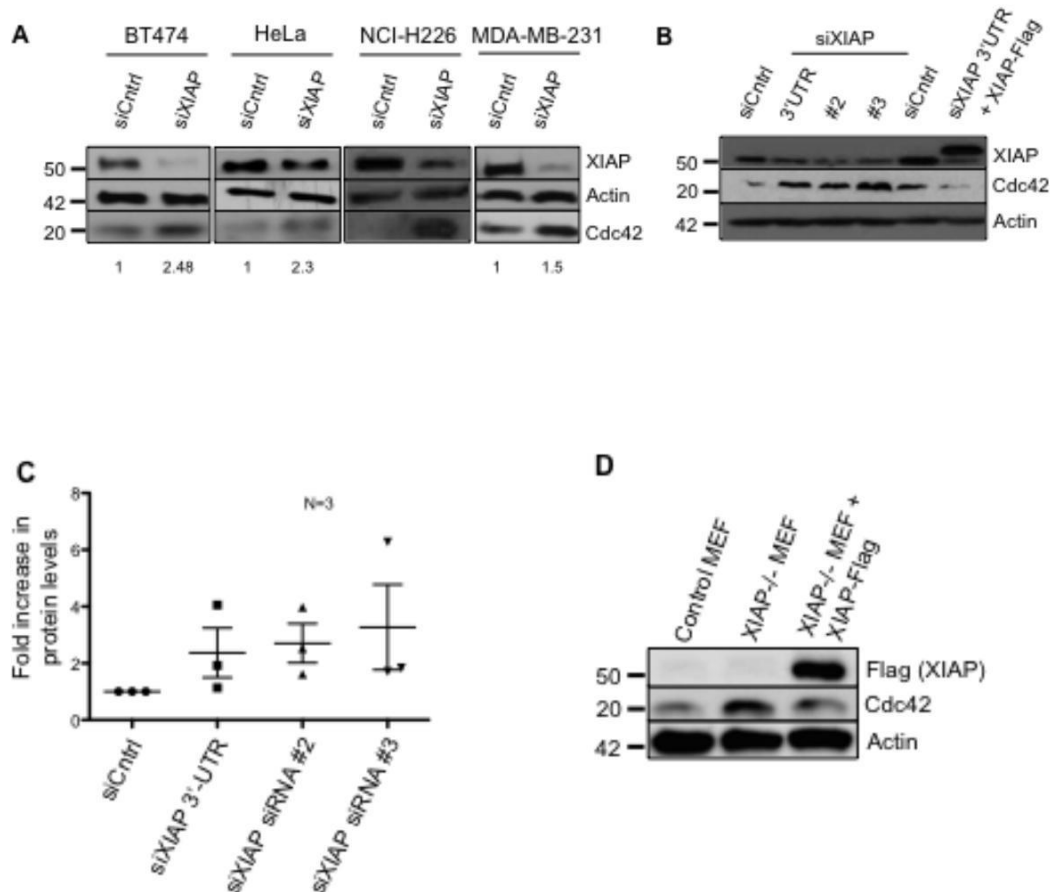
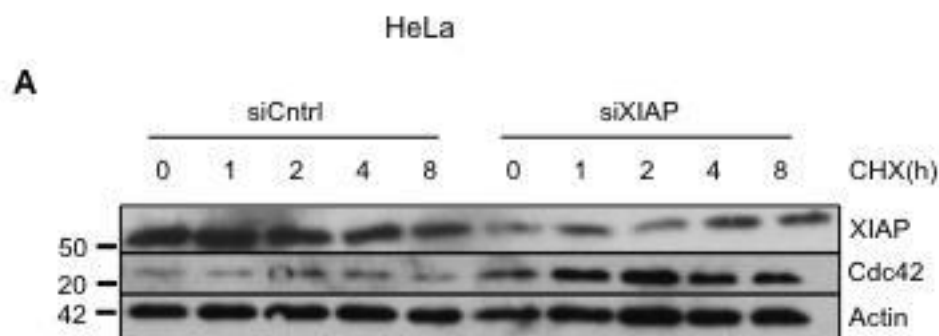


**Figure 3.1: Depletion of XIAP leads to Cdc42 upregulation** - BT474, HeLa, NCI-H226 and MDA-MB231 cells were transfected with Control or XIAP siRNA for 48 h and lysates were then collected for immunoblotting. The levels of total Cdc42 were monitored in the immunoblots. Quantification was performed by densitometry. (B) HeLa cells were transfected with three different XIAP siRNAs and Cdc42 levels were monitored. Further, HeLa cells transfected with the 3'-UTR XIAP siRNA were complemented with the XIAP-Flag vector and Cdc42 levels were observed. (C) Quantification of three independent experiments where 3 different XIAP siRNAs were used and Cdc42 protein expression was checked 48 h post transfection (D) Mouse embryonic fibroblasts (MEFs) were cultured and lysed to check for Cdc42 levels. Control MEFs and XIAP knockout MEFs stably complemented with Flag tagged XIAP were employed.

### 3.1.1.2. XIAP contributes to the proteostasis of Cdc42

Cycloheximide chase experiments were performed in a panel of cell types to determine whether XIAP depletion contributed to the stability of Cdc42 on a translational level. Two tumor cell lines used previously, HeLa (**Figure 3.2 A**) and MDA-MB231 (**Figure 3.2 B**) were employed in this study and a kinetics experiments was performed with cycloheximide in the presence or absence of XIAP. The half-life of the protein was monitored and it was quite clear that while the half-life of Cdc42 under control conditions was between 4-6 hours, it increased to over 8 h upon depletion of XIAP. Curiously, we also observed in many of these cycloheximide experiments that the levels of protein detected upon immunoblotting increased upon cycloheximide treatment. We speculate that this could be due to factors like DMSO (in which the cycloheximide in prepared) that may have off target effects. Overall though, these experiments revealed that depletion of XIAP enhanced protein stability of Cdc42.

Due to the interesting observations in different breast cancer cell lines, primary HMEC (Human Mammary Epithelial Cells) were used and the Cycloheximide chase experiment repeated as mentioned earlier (**Figure 3.2 C**). Again, it was observed that Cdc42 levels were indeed stabilized upon XIAP knockdown. To confirm whether the observed phenomenon was on an mRNA or protein level, qPCR was then performed on cell samples transfected with control or XIAP siRNAs in HeLa cells (**Figure 3.2 D**). However, loss of XIAP did not lead to an increase in the mRNA levels of Cdc42, suggesting that XIAP directly contributes to the proteostasis of Cdc42.





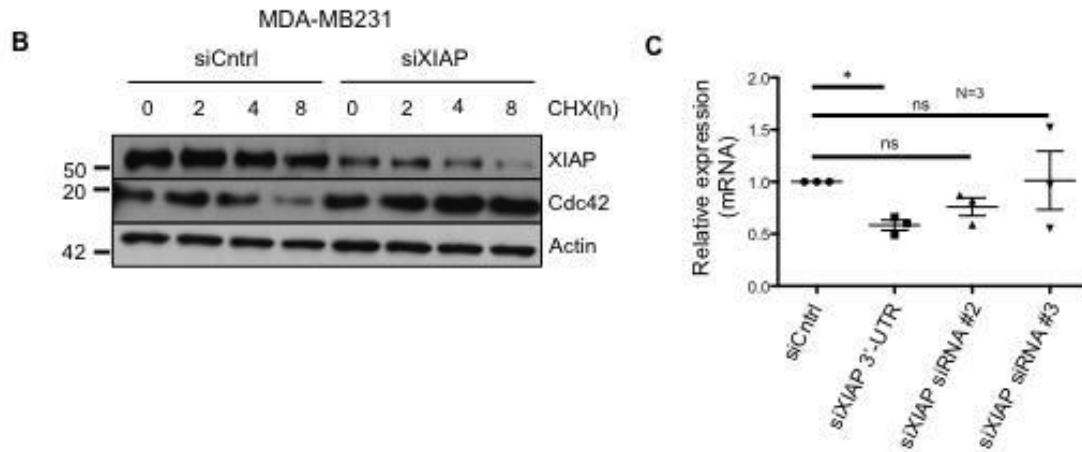


**Figure 3.2: XIAP contributes to the proteostasis of Cdc42** - (A) and (B) Cycloheximide chases were performed in HeLa (A), MDA-MB231 (B) (C) qPCR was performed with the three different XIAP siRNAs to observe the transcriptional regulation of Cdc42 in HeLa cells. Shown here are data from three independent experiments. The Y-axis represents the relative mRNA expression normalized to the Control, which has been set to 1 for all experiments.

### 3.1.1.3. Depletion of XIAP leads to basal and EGF induced Cdc42 activation

It was often detected that stimulation of either HeLa cells or primary HMEC cells with EGF kinetically led to an increase in the protein levels of Cdc42 (**Figure 3.3 A and B**) without much changes in XIAP levels. These data suggest that EGF controls Cdc42 levels perhaps in a XIAP independent manner. Further, in XIAP depleted cells there was no additive increase in Cdc42 levels upon EGF stimulation (**Figure 3.3A and B**). The next point addressed was whether the observed increase in Cdc42 levels also translated to an Increased Cdc42 activity in these cells. CRIB pull down assays employing PAK-PBD in control and XIAP depleted cells showed that the loss of XIAP also led to an increase in the GTP-bound active form of Cdc42 in tumor as well as in primary cells (**HeLa Figure 3.3 C and HMEC Figure 3.3 D**). Interestingly, XIAP co-precipitated with active Cdc42 suggesting that Cdc42 and XIAP co-existed in a protein complex in these cell types and further these is no linear correlation between the amounts of active Cdc42 and co-precipitated XIAP (**Figure 3.3 C and D**). This could possibly due to the

interaction between Rac1 and XIAP as active Rac1 is also precipitated with PAK-PBD proteins (Please see Discussion for further details).

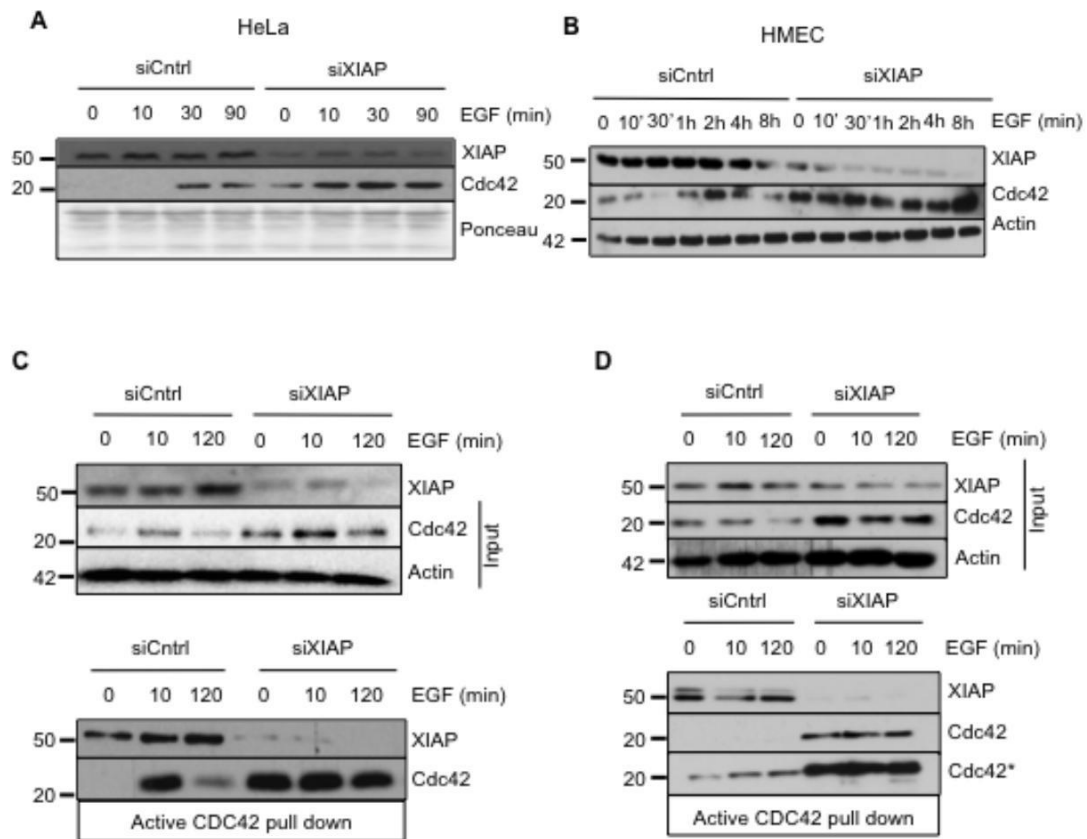


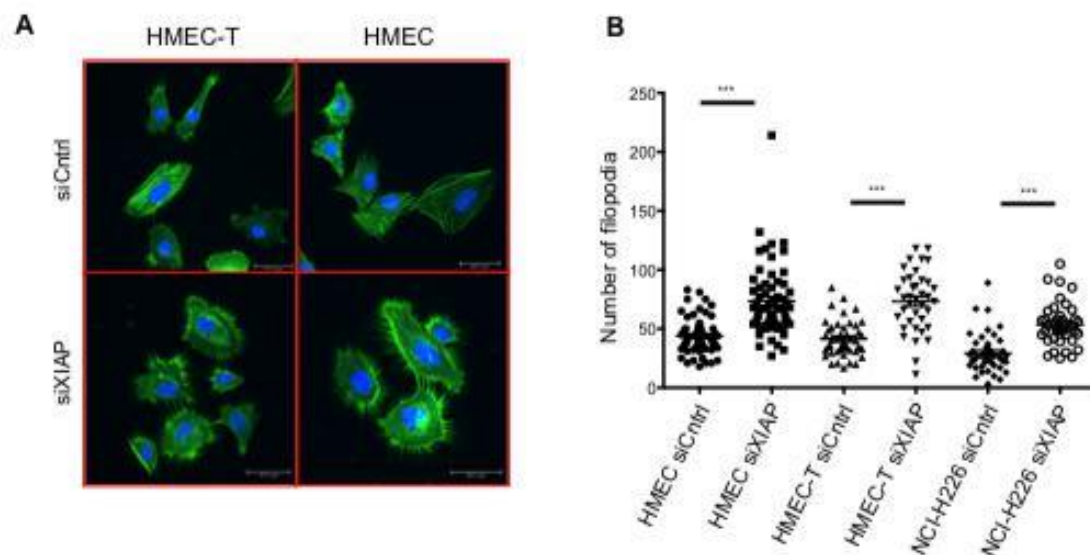
**Figure 3.3: Depletion of XIAP leads to basal and EGF induced Cdc42 activation** - (A) HeLa cells and (B) HMECs were transfected with XIAP siRNA and treated with EGF 48 h post transfection for the times indicated in the figure. The levels of Cdc42 were monitored via immunoblotting. (C) & (D) Active Cdc42 pulldown using GST PAK-PBD protein was performed in HeLa (C) and HMECs (D) to test for levels of the active protein upon EGF treatment at times indicated in the figure. \* denotes a higher exposure of Cdc42 in Figure 3.3 D.

### 3.1.2. Role of XIAP in filopodia formation

#### 3.1.2.1. Depletion of XIAP enhances number of filopodia

Results thus far showed that XIAP depletion stabilized and activated Cdc42 in cells independent of EGF stimulation. To confirm these observations, immunofluorescence experiments were performed in a panel of cell lines and

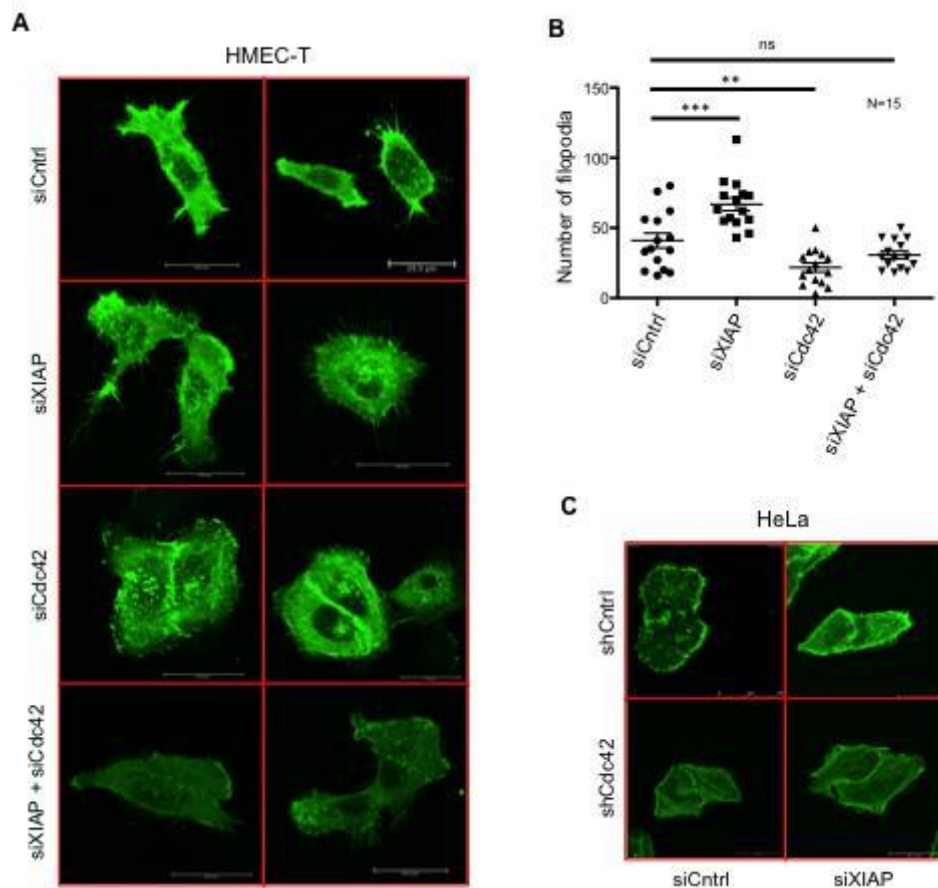
polymerized F-actin was stained with phalloidin. As expected, XIAP depletion led to profuse filopodia formation in both primary as well as tumor cell lines (**Figure 3.4 A and C**). Primary HMEC, immortalized HMEC and NCI-H226 cells were employed for these experiments. While control HMEC and HMEC-T cells had on an average 40 filopodia per cell, XIAP depleted HMEC and HMEC-T cells displayed close to 70 filopodia per cell. Similarly, NCI-H226 cells showed an increase from around 40 to over 60 filopodia per cell. These observations were quantified and statistical significance was assigned (**Figure 3.4 B**). The same experiments were also repeated in HeLa cells, and the observations were replicated, however Control HeLa cells on average had only around 10 filopodia per cell, hence the other cell lines were used for better quantification purposes.



**Figure 3.4: Depletion of XIAP enhances number of filopodia** - (A) & (C) HMEC, NCI-H226 and HMEC-T cells were depleted of XIAP and immunofluorescence staining was performed using Phalloidin AlexFluor 488 to look for differences in actin structures. (B) Quantification of the number of filopodia in the three cell lines of (A) upon depletion of XIAP. Data shown are from 3 independent experiments with a total of 40-60 cells counted per condition,  $p < 0.001$

### 3.1.2.2. XIAP regulates filopodia formation through Cdc42

To verify the dependence of this phenomenon on Cdc42, Cdc42 was co-depleted both transiently (**Figure 3.5 A**) and stably (**Figure 3.5 C**). Immunofluorescence experiments were performed similar to those in 3.1.2.1. HeLa cells were first stably depleted of Cdc42 and then transiently depleted of XIAP in both Control and Cdc42 stable knockdown conditions. Similarly, HMEC cells were transiently co-depleted of XIAP and Cdc42. Clearly, co-depletion of Cdc42 reduced the number of filopodia in both Control and XIAP-depleted cells thus confirming the specificity of this phenotype. These observations were quantified in **Figure 3.5 B and D**.



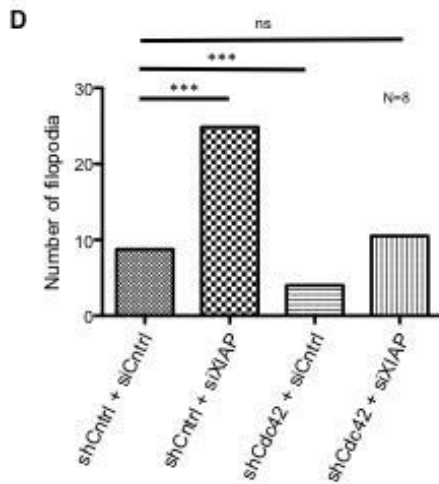


**Figure 3.5: XIAP regulates filopodia formation through Cdc42** – (A) HMEC-T cells were transiently depleted of XIAP as well as Cdc42 siRNA to look for the dependency of filopodia formation on the two proteins. Cells were fixed and stained (as described in Materials and Methods) with phalloidin. (B) The quantification of the number of filopodia is shown, n=15 cells. (C) Cdc42 was stably knocked down in HeLa cells and a transient depletion of XIAP was performed to check for the dependence of filopodia formation on Cdc42. Cells were lysed 48 h post transfection and fixed and stained as described in Materials & Methods (D) Quantification of Figure (C), 7-8 cells were counted per condition, p<0.001

### 3.1.2.3. EGF stimulation mimics XIAP depletion

Due to the similar increase in Cdc42 levels upon EGF stimulation and XIAP depletion, it was tested whether this led to a similar phenotype in both cases as well. To perform these experiments, we performed validation studies employing Cdc42 knock down in HMEC-T cells. Immunocytochemical studies using a validated Cdc42 antibody revealed that Cdc42 is strongly upregulated in XIAP depleted cells and specifically localizes to the filopodial protrusions in immortalized HMEC cells (**Figure 3.6 A**). Further, XIAP depleted cells phenocopied EGF stimulated cells with an increased Cdc42 activity observed along the periphery of the cells. These observations were quantified in **Figure 3.6 B** and confirmed that the increase in total and active Cdc42 levels observed upon depletion of XIAP contributed to the enhanced actin rich protrusions in these cells.

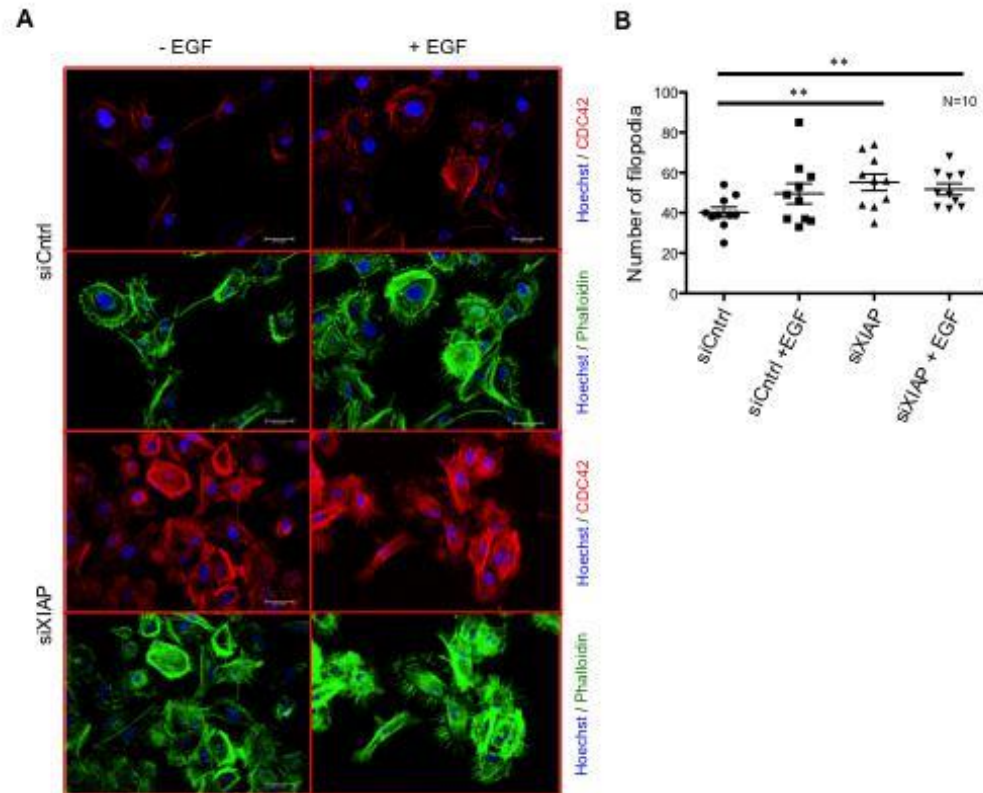


**Figure 3.6: EGF stimulation mimics XIAP depletion** - (A) HMEC-T cells were treated with EGF stimulation after Control or XIAP siRNA treatment and immunofluorescence was performed using three different stains: Phalloidin for Actin, Hoechst for the nucleus and a Cdc42 primary antibody followed by Cy3 mouse secondary to check for localization of Cdc42 protein in the cell (B) Quantification of the number of filopodia seen in Figure (A) with  $n = 10$  cells counted per condition,  $p < 0.01$ .

### 3.1.3. Molecular mechanisms of XIAP-mediated Cdc42 degradation

#### 3.1.3.1. XIAP directly binds to Cdc42

Given that XIAP was observed to co-precipitate along with Cdc42 in the CRIB pulldown assays shown in **3.1.1.3**, we hypothesized that XIAP might directly bind to Cdc42. Recombinant proteins containing various mutants of XIAP were generated (**Figure 3.7 C**). By employing these proteins, we tested which domains of XIAP were vital for Cdc42 binding. The IAPs being traditionally sticky proteins, were GST tagged while the Cdc42 was either pulled down from cells (**Figure 3.7 A**) or purified from a bacterial system (**Figure 3.7 B**) as



described in Materials and Methods. GST tagged Rho GTPases were cleaved using Thrombin, also described in Materials and Methods.

Cells overexpressing Cdc42 were added on to various XIAP mutants and pulled down. These experiments revealed that XIAP binds to Cdc42 in a RING dependent manner. While the BIR1-XIAP mutant also retains some binding efficiency, the XIAP RING mutant completely ablated all binding (**Figure 3.7 A**). In-vitro binding assays were then performed to test whether XIAP binds to Cdc42 in a nucleotide dependent manner. Cdc42 Wild Type (WT), Q61L (Active) and T17N (Inactive) mutants were employed in this assay and interestingly, XIAP failed to interact with the Cdc42T17N mutant, suggesting that this interaction was dependent on the activation status of Cdc42 (**Figure 3.7 B**). This experiment also conclusively proved that XIAP does indeed bind directly to Cdc42 in an activation dependent manner.

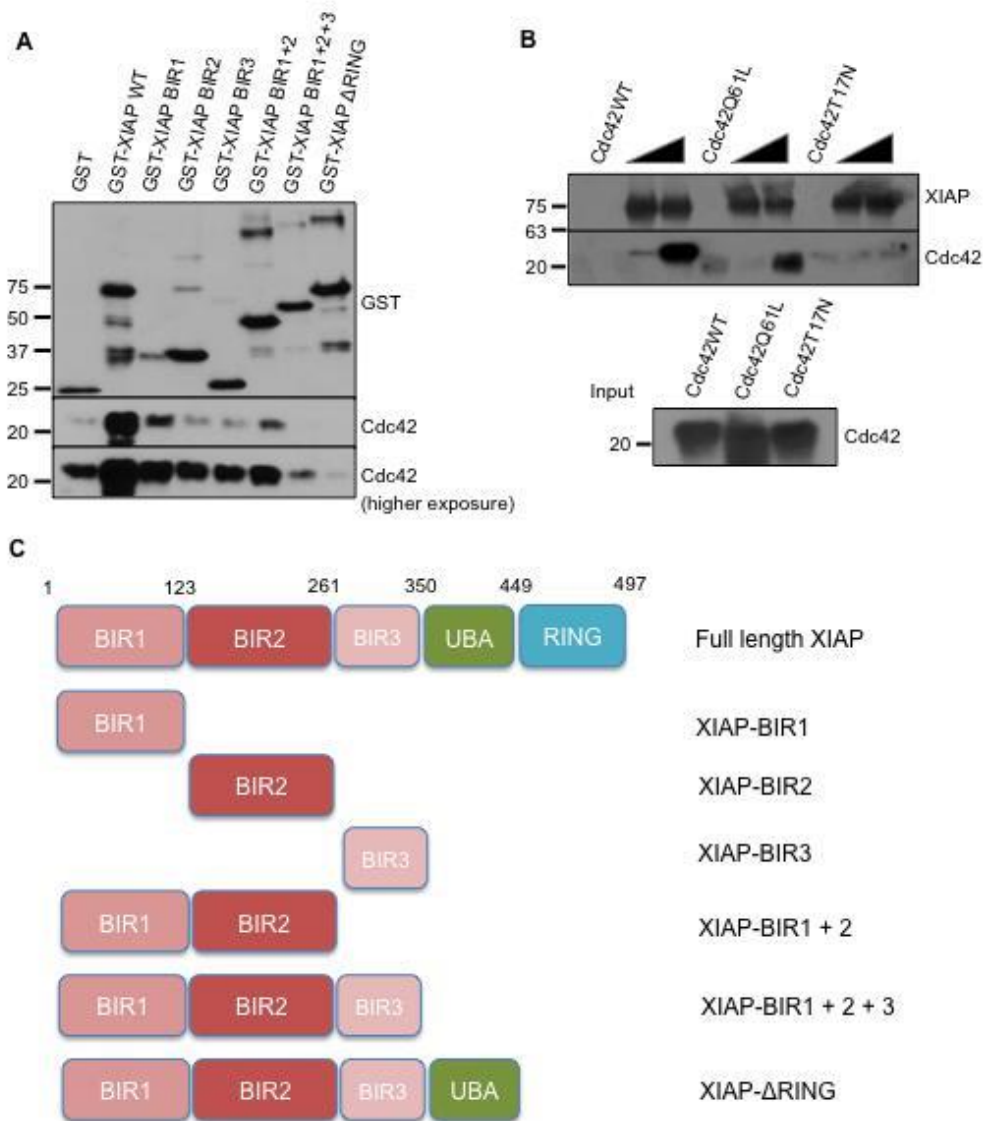


**Figure 3.7: XIAP directly binds to Cdc42** - (A) 293T cells were overexpressed with Cdc42 WT plasmid. Cells were lysed 48 h post overexpression and the lysates were added on different mutants of XIAP (GST tagged). A GST Pulldown was then performed to check for interaction between Cdc42 and the XIAP mutants (B) Interaction between XIAP and different Cdc42 mutants was tested via an in-vitro GST Pulldown assay. With GST protein as a control, two different concentrations of cleaved Cdc42 mutants were used to test the binding to GST tagged XIAP. (C) Various recombinant mutants of XIAP were generated to perform the GST pulldown assay in Figure (A). The various domains are listed in the figure.

### 3.1.3.2. XIAP is an E3 ubiquitin ligase of Cdc42

Due to the importance of the RING domain in the XIAP-Cdc42 interaction (**Figure 3.7 A**) and the previous history of IAPs excelling in their role as E3 ubiquitin ligases through their RING domain, it was speculated that XIAP



could possibly function as a direct E3 ubiquitin ligase of Cdc42. In-vitro ubiquitination experiments revealed that XIAP directly conjugated ubiquitin chains to both the WT and the Q61 active mutant but not the inactive T17N mutant (**Figure 3.8 A**), consistent with the results observed in the interaction experiments. Further in-vitro ubiquitination experiments also revealed that XIAP and not cIAP-1 could directly conjugate ubiquitin chains to the active Cdc42Q61L mutant (**Figure 3.8 B**). To test whether XIAP could influence the ubiquitination and proteasomal degradation at physiological levels in cells, pull down experiments were performed employing TUBEs (Tandem Ubiquitin Binding Entity). TUBEs were used to enrich ubiquitinated proteins from both Control and XIAP depleted cell lysates. It was observed that loss of XIAP reduced the polyubiquitination of Cdc42 at endogenous levels (**Figure 3.8 C**). As XIAP can directly ubiquitinate Cdc42, it was then tested if the RING domain of XIAP is required for modulating the protein levels of Cdc42 in vivo. To perform these studies, MEFs derived from XIAP deficient mice were employed and complimented with either wild type or RING (XIAPH467A) mutants. Interestingly, expression of wild type XIAP but not the RING mutant of XIAP reduced the Cdc42 levels in XIAP deficient MEFs (**Figure 3.8 D**). In fact expression of the RING mutant of XIAP augmented the protein levels of Cdc42 under these settings (**Figure 3.8 D**). These results further confirm that XIAP directly influences the protein stability of Cdc42 through its E3 ligase activity.

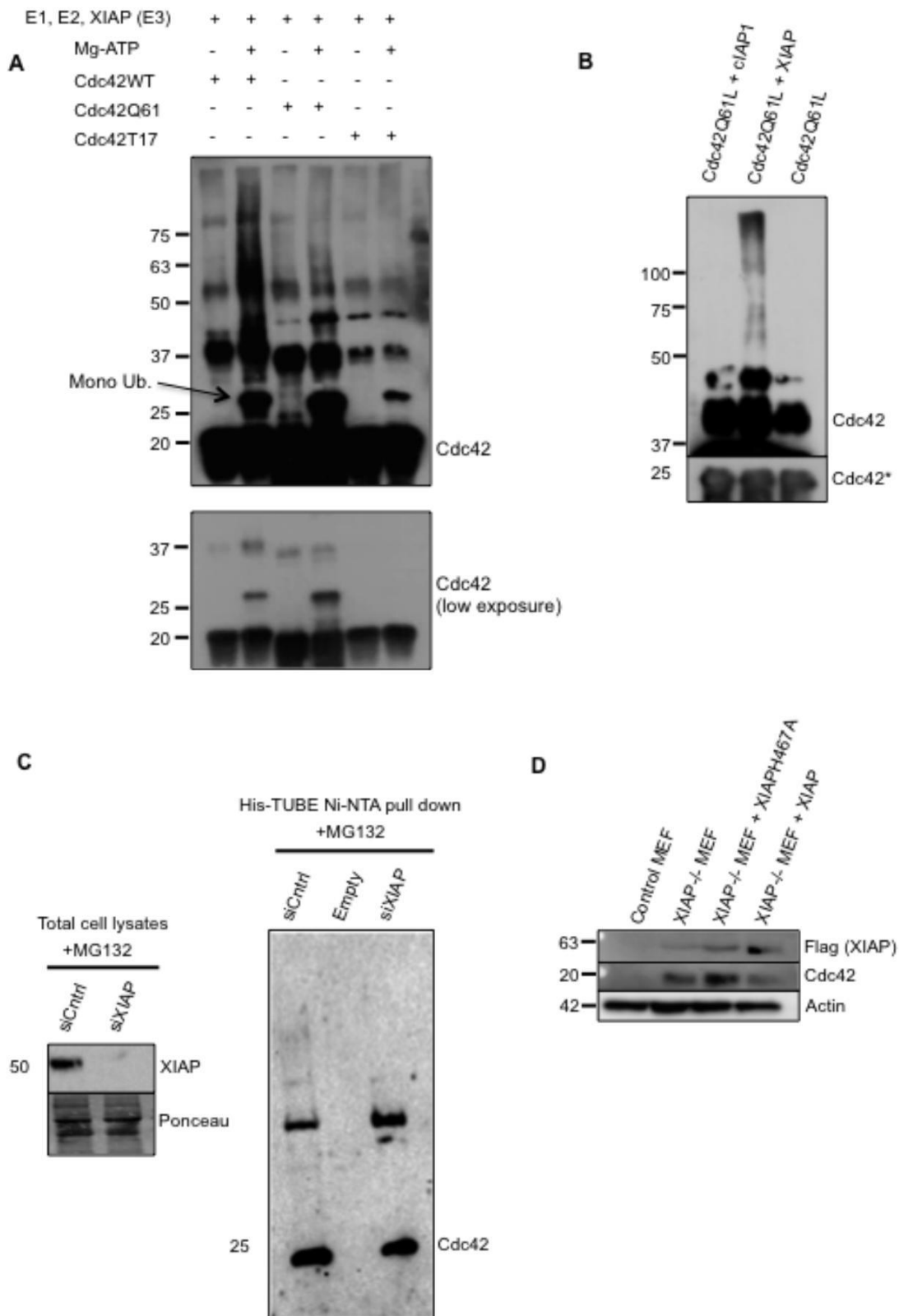


**Figure 3.8: XIAP is an ubiquitin ligase of Cdc42** - (A) In-vitro ubiquitination of Cdc42 mutants by XIAP. Purified recombinant Cdc42 Wild Type, Q61L and T17N were subjected to in-vitro ubiquitination by recombinant human XIAP (B) In-vitro ubiquitination of Cdc42 by XIAP. Purified recombinant Cdc42Q61L was subjected to in-vitro ubiquitination by XIAP and

clAP1 recombinant proteins (protocol described in Materials and Methods). (C) HeLa cells were transfected with XIAP siRNA for 48 h and treated with MG132 for 6 h. The cells were lysed in RIPA buffer and His-TUBE immobilized on NiNTA beads were employed to enrich the ubiquitinated proteins. The samples were loaded onto a gel and the presence of Cdc42 was monitored by immunoblots. The efficiency of XIAP knock down was tested in the lysates control. (D) Mouse embryonic fibroblasts (MEFs) were cultured and lysed to check for Cdc42 levels. Control MEFs and XIAP knockout MEFs stably complemented with different XIAP constructs were used for this experiment. \* denotes lower exposure of Cdc42.

### 3.1.3.3. XIAP ubiquitinates Cdc42 on Lysine 166

Mass spectrometric techniques were employed to determine the ubiquitination sites of Cdc42. These analyses revealed that XIAP conjugated ubiquitin chains to the Lysine 166 of Cdc42, which is localized to the C-terminus of the Rho GTPase (**Figure 3.9 A**). To test whether this mutation has any physiological relevance, we performed cycloheximide chase experiments employing various mutants of Cdc42. We first attempted to understand the degradation kinetics of different Cdc42 mutants. For this, we mutated the Cdc42 Wild Type (WT) plasmid at two spots to generate two separate mutations – the active Q61L and the T17N mutant. Previous research showed that CNF1 toxin deamidates the Q61 of Rac1 thus activating it and making it susceptible for degradation<sup>293</sup>. Similarly, the T17N mimics the GDP bound form and is thus more stable. Thus, cycloheximide chases were performed upon overexpression of the three Cdc42 mutants to check whether similar degradation kinetics was followed. These experiments proved that the Cdc42Q61L active mutant was the least stable of the three mutants (**Figure 3.9 B**). To check whether the Lysine 166 had an impact on protein stability, the Cdc42Q61L mutant was chosen and the Lysine 166 mutated on this construct into an Alanine. Cycloheximide chase experiments performed with this mutant revealed that the protein stability of Cdc42Q61L was significantly enhanced upon mutation and suggested that ubiquitination at this site by XIAP is relevant to the proteolysis of activated Cdc42 (**Figure 3.9 C**)

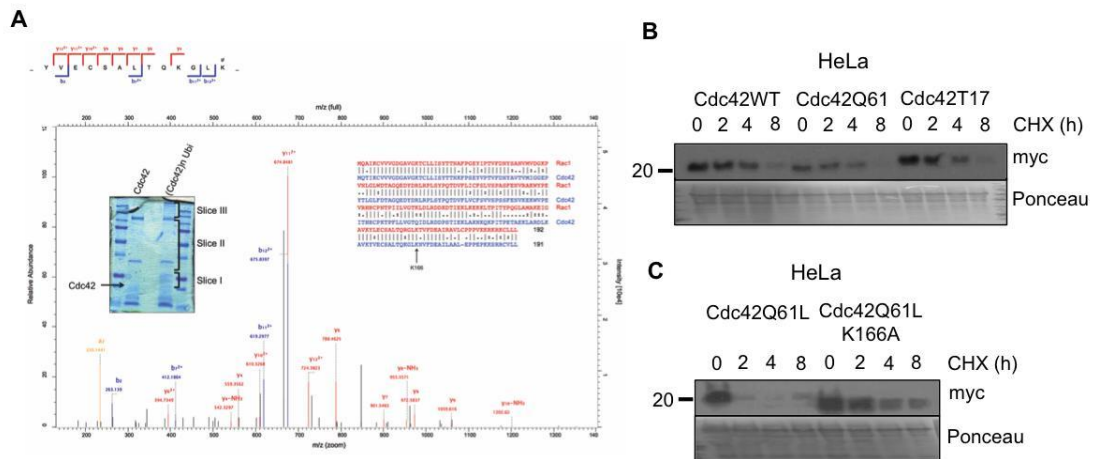


**Figure 3.9: XIAP ubiquitinates Cdc42 at Lysine 166** – (A) Gel slices of the in-vitro ubiquitination reaction were subjected to mass spectrometric analysis to determine the Lysine(s) responsible for the ubiquitination. Inset shows the gel slices taken for the analysis as well as a comparison between the sequences of Rac1 and Cdc42. (B) Different myc tagged Cdc42 mutants were overexpressed in HeLa cells and a cycloheximide chase was performed to check for half life of protein expression. (C) Myc tagged Cdc42Q61L and Cdc42Q61LK166A mutants were overexpressed in HeLa cells and Cycloheximide chases were performed to check for the half-life of Cdc42 protein.

### 3.1.3.4. Molecular modeling of the XIAP-Cdc42 interface

Molecular modeling studies were performed based on the published crystal structures of Cdc42 and PAK6 leading to the prediction that the conjugation of Ubiquitin to K166 could disrupt the interaction between Cdc42 and its effector protein PAK2 (**Figure 3.10 A**). Since the PBD domains of PAK2 and PAK6 are highly conserved, a model of PAK6 was used for this simulation. Models were made in the absence of Ubiquitin as well as in its presence. Conjugation of di ubiquitin to K166 was attempted and these studies suggested ubiquitin binding could possibly interfere with the effector binding. To test this hypothesis, CRIB pull down experiments were performed involving the p21 Binding Domain (PBD) of PAK2. Cdc42 was first subjected to an in-vitro ubiquitination assay and GST PAK-PBD was subsequently added to the reaction mix and the CRIB pull down was performed as described in the methods. Three different controls were employed – First, a sample wherein there was no energy to drive the ubiquitination reaction; second, a sample with no XIAP thus also preventing ubiquitination; and a third control with all

the ingredients thus ensuring that the ubiquitination reaction was working as intended. The first three lanes were pulled down with PAK-PBD to check for ubiquitination, while the 4<sup>th</sup> lane did not involve any pulldown with PAK-PBD and was just an ubiquitination control. It was observed that ubiquitinated Cdc42 failed to interact with PAK-PBD suggesting that conjugation of ubiquitin to K166 directly prevented the interaction of Cdc42 with its downstream effector (**Figure 3.10 B**). While the percentage of ubiquitinated Cdc42 was less (around 10%), it is clear that upon ubiquitination, Cdc42 does not interact with its downstream effector.

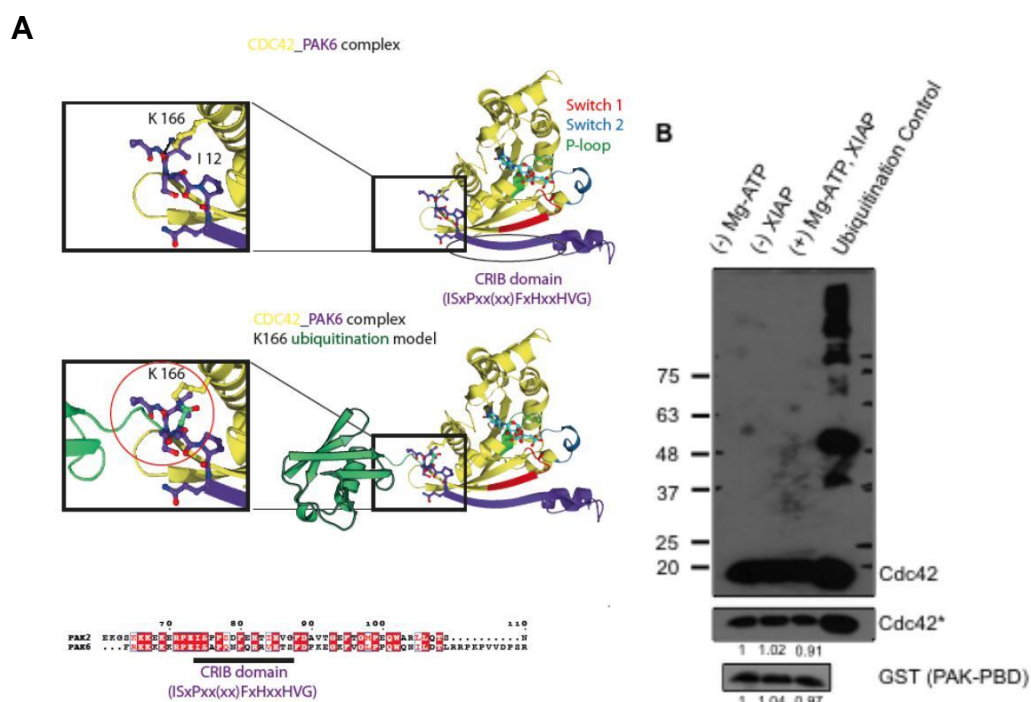


**Figure 3.10: Molecular modeling of the XIAP-Cdc42 interface:** (A) Ribbon model of crystal structure of CDC42 (Yellow) in complex with PAK6 (Purple) (PDB: 2ODB). P-loop (residues 10-17), Switch I (residues 32–40), and switch II (residues 60–67) of Cdc42 are green, red and cyan, respectively. Nucleotide (cyan), K166 of CDC42 and residues 11-16 of PAK6 are shown in ball-and-stick representation. Hydrogen bond between K166 of CDC42 and PAK6 (carbonyl oxygen of I12) is shown as black dashed line. The second figure shows a model of ubiquitinated (Green) CDC42 (Yellow) in complex with PAK6 (Purple). Finally, a sequence alignment of CRIB domain of PAK2 and PAK6. (B) The same in-vitro ubiquitination assay as in Figure 3.8A was performed and the reaction was then subjected to a PAK-PBD GST pull-down (as described in Materials and Methods) to check for interaction of ubiquitinated Cdc42 and its downstream effector PAK. The ubiquitination of Cdc42 was confirmed in the samples employed for PAK-PBD pull down (lane 4).

### 3.1.4. Role of XIAP in tumor cell metastases

Previous studies have shown that Cdc42 plays a crucial role in the metastases of tumor cells<sup>272</sup>. To evaluate the pathophysiological significance of XIAP-Cdc42 interaction in vivo, an experimental metastases model was used employing NOD/SCID mice. Control or XIAP depleted HeLa cells were injected into the tail vein of mice, and an increase in the number of nodules in the surface of the lung was detected at 4-5 weeks post injection in mice injected with XIAP depleted cells (**Figure 3.11 A**). Co-depletion of Cdc42 strongly reduced the number of lung nodules confirming that loss of XIAP led to an increase in the number of lung nodules in a Cdc42 dependent manner (**Figure 3.11 B**). Hemotoxylin and Eosin staining confirmed the presence of nodules in the lungs of the mice (**Figure 3.11 C**).

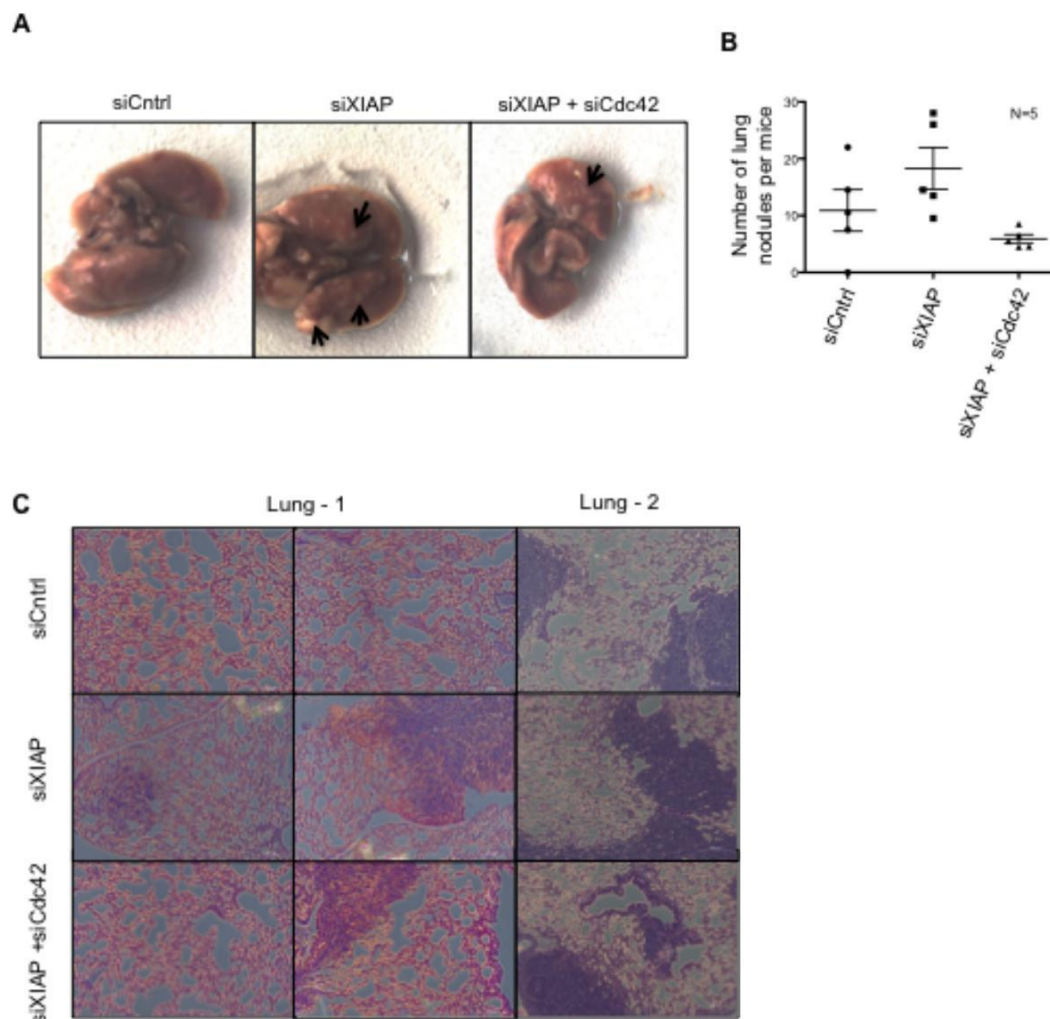




**Figure 3.11: Depletion of XIAP enhances tumor cell metastases** - (A) NOD-SCID mice were injected through the tail vein with 1 million tumor cells treated with different siRNAs as indicated. Mice were sacrificed after 4-5 weeks of injection and the lungs were isolated. Shown are pictures of the whole lung (B) Metastatic nodules were counted manually on each lung by three independent pairs of eyes, with 5 mice lungs counted per condition (C) Lungs were fixed and H&E stained and representative images of the lungs are shown.

## 3.2. Regulation of RhoA, Rac1 and RhoB by IAPs

### 3.2.1. XIAP binds to but does not ubiquitinate RhoA

Oberoi et al had shown that IAP depletion led to a decrease in active RhoA levels whilst simultaneously activating Rac1<sup>11</sup>. Thus, it was prudent to check whether XIAP indeed bound to RhoA or whether the inactivation was indirectly through Rac1. Cells overexpressed with RhoA were lysed and added on to various XIAP GST tagged mutants and a GST pulldown assay was performed. Similar to the interactions between Cdc42 and XIAP, the deletion of the RING domain completely abrogated interaction between RhoA and XIAP (**Figure 3.12 A**). Further, a combination of the BIR domains was not sufficient in restoring this interaction. In-vitro ubiquitination experiments were performed to check whether RhoA is ubiquitinated by XIAP. Interestingly, while XIAP ubiquitinated Rac1 in the control sample, there was no ubiquitination observed on RhoA by XIAP (**Figure 3.12 B**). Thus, it is likely that the interaction between XIAP and RhoA is non-ubiquitin RING mediated in nature.

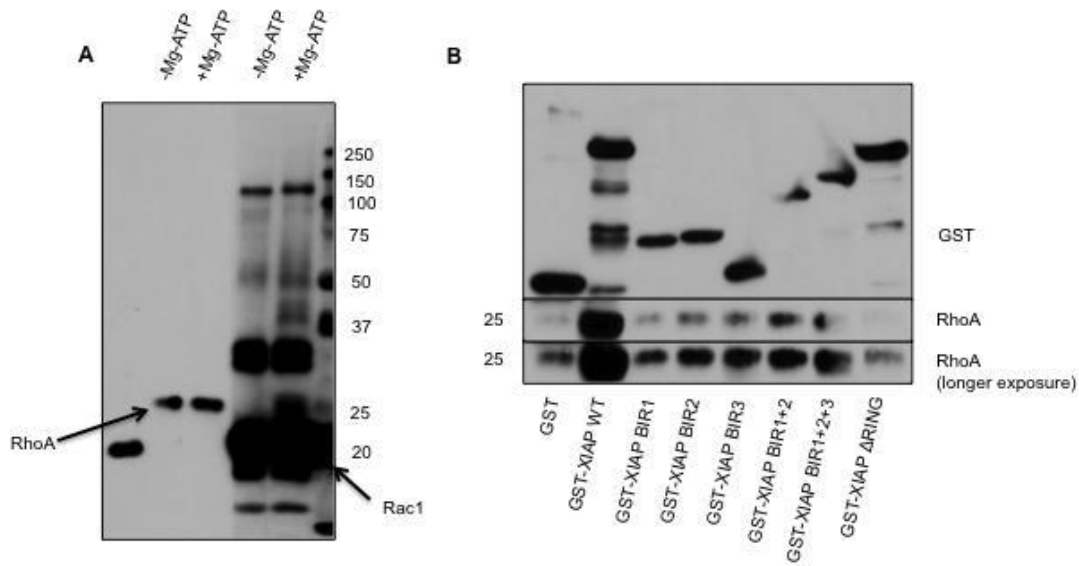


**Figure 3.12: RhoA binds to but isn't ubiquitinated by XIAP** – (A) Both RhoA and Rac1 Wild Type were subjected to an in-vitro ubiquitylation reaction with XIAP. The modification of the proteins (or lack thereof) was monitored by immunoblots. (B) 293T cells were overexpressed with RhoA WT plasmid. Cells were lysed 48 h post overexpression and the lysates were added on different mutants of XIAP (GST tagged). A GST Pull-down was then performed to check for interaction between RhoA and the XIAP mutants. Samples were taken for Western Blot analysis and the GST tagged XIAP mutants were visualized using GST antibody, while RhoA was visualized using RhoA antibody.

### 3.2.2. Control of Rac1 and WAVE2 complex by IAPs

#### 3.2.2.1. cIAP1 synthesises possibly K11/K48 polyubiquitin chains on Rac1

Earlier studies by Oberoi et al had demonstrated that cIAP1 and XIAP act as E3 ligases for Rac1 and target it for proteasomal degradation<sup>11</sup>. As cIAP1/XIAP-mediated ubiquitination of Rac1 led to proteasomal degradation, it was speculated that the IAPs could potentially synthesize K-48 linked degradative ubiquitin chains on this Rho GTPase. This hypothesis was confirmed by an in-vitro Ubiquitin assay followed by a pull-down of Rac1. Finally, the sample was loaded and probed with chain-specific Ubiquitin



antibodies. Intriguingly, a mixture of K11 and K48 chains were deemed to be formed on Rac1 in vitro (**Figure 3.13 A**).

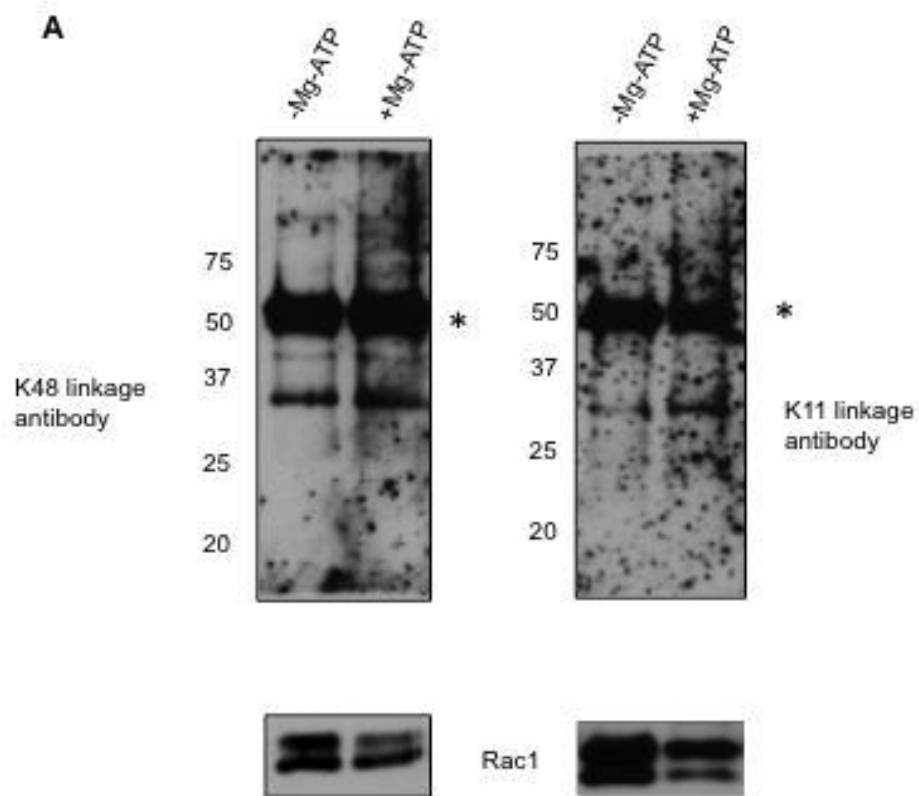


**Figure 3.13: K11/48 chains are synthesized on Rac1** – (A) In-vitro ubiquitination reactions were performed using Rac1 and recombinant human cIAP1 and after the reaction, the reaction mix was pulled down using a Rac1 antibody. Linkage specific antibodies were used to probe for ubiquitin smears upon Western Blotting.

### 3.2.2.2. IAP-mediated cell morphology is dependent on the WAVE regulatory complex

Previous results had shown that knockdown of IAPs via siRNAs or by treatment with IAP antagonist compounds (IAC; BV6) led to Rac1-dependent elongated, mesenchymal morphology in various primary and tumor cell lines. The WAVE2 complex, as mentioned in the introduction is a pentameric complex downstream of Rac1 which upon activation, binds to the Arp2/3 protein thus leading to actin polymerization. The WAVE2 regulatory complex (WRC) consists of 5 proteins, Sra1, Nap1, WAVE2, Abi1/2 and HSPC300, the first two and the last three proteins forming sub complexes respectively that

come together to form the WRC. The loss of even one protein renders the other components unstable and the complex non functional <sup>294</sup>. To test whether this morphology is reliant on the WAVE2 regulatory complex (WRC), the complex was destabilized by stably knocking down Nap1. Knocking down other components HeLa cells were stably depleted of Nap1 using lentiviral particles and then transiently depleted of XIAP and immunofluorescence experiments were performed wherein the actin cytoskeleton was stained (**Figure 3.14 A**). Further, experiments were also performed with IACs and circularity of cells was measured (**Figure 3.14 B**) and this data clearly show that the WRC is integral in IAP-mediated elongated morphology (**Figure 3.14 A**).

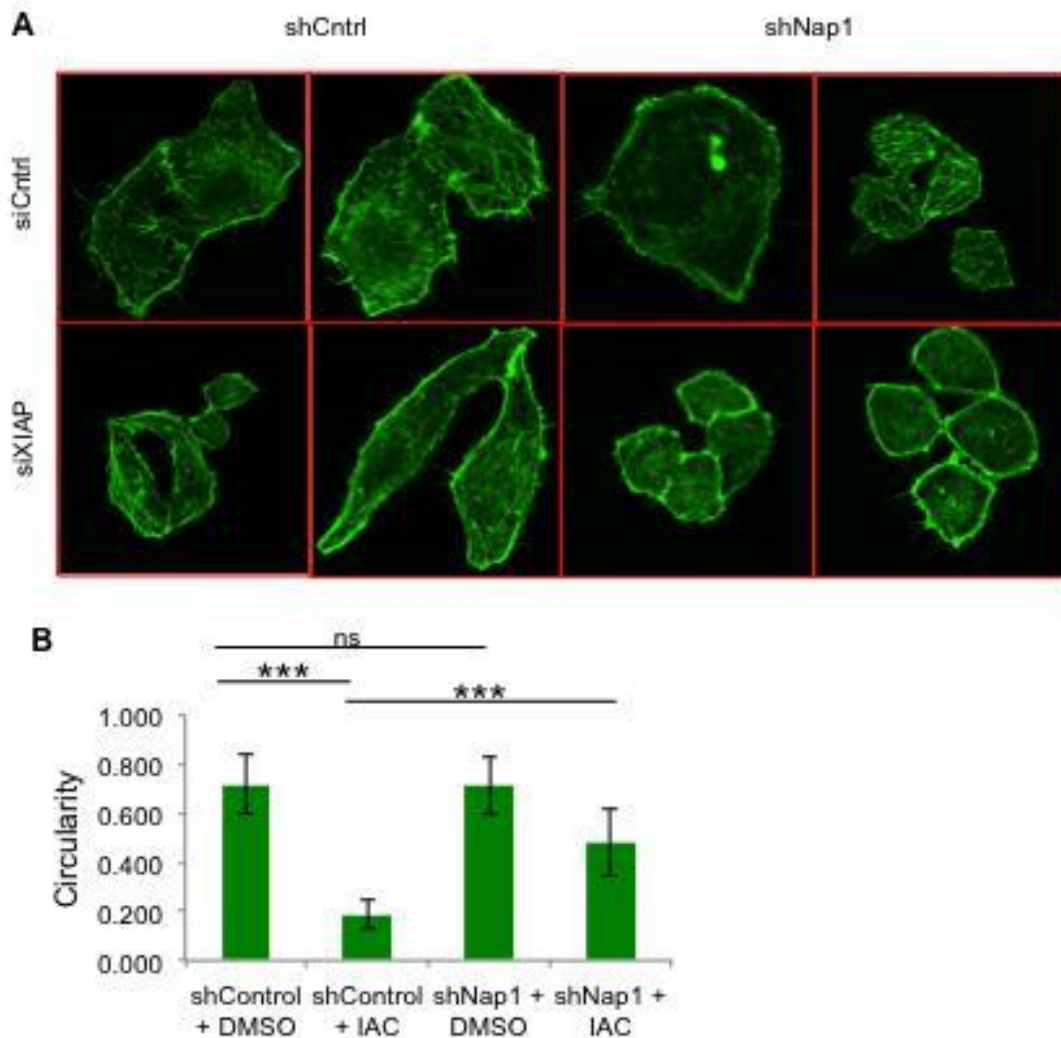


**Figure 3.14: Depletion of IAPs influence WRC regulated morphology** - (A) shControl and shNap1 cells were seeded on coverslips after depletion of XIAP for 48 h and then fixed and

stained with phalloidin for detecting filamentous actin. Shown in (B) is quantification of Circularity for cells upon IAC depletion. 50 cells per condition were assessed for the measurement of circularity by ImageJ software and depicted graphically. Student's t test was performed to check for significance. (\*\*\*,  $p < 0.005$ ).

### **3.2.2.3. Depletion of IAPs promote actin polymerization**

Due to the integral role of the WRC in actin polymerization through its downstream partner, Arp2/3, it was tested whether depletion of IAPs led to an increase in overall actin polymerization in the cell. Cells were treated with both IAP antagonists (**Figure 3.15 A**) as well as depleted of XIAP using siRNA techniques (**Figure 3.15 B**). Cells were stained with Phalloidin which bound to filamentous actin and were then sorted using FACS analysis. Thus termed an F-actin assay, this assay was graded on two parameters – the average intensity of Phalloidin staining as well as the percentage of cells above a particular preset threshold intensity. Jasplakinolide, a cyclo-depsipeptide, is a commonly used actin filament polymerizing and stabilizing compound and was used in this assay as a positive control, while Latrunculin B, was used to disrupt the actin cytoskeleton and was used as a negative control. The time points for these controls was optimized and fixed at 1 h and 30 min respectively. These results clearly revealed an increase in the actin polymerization upon IAC treatment.

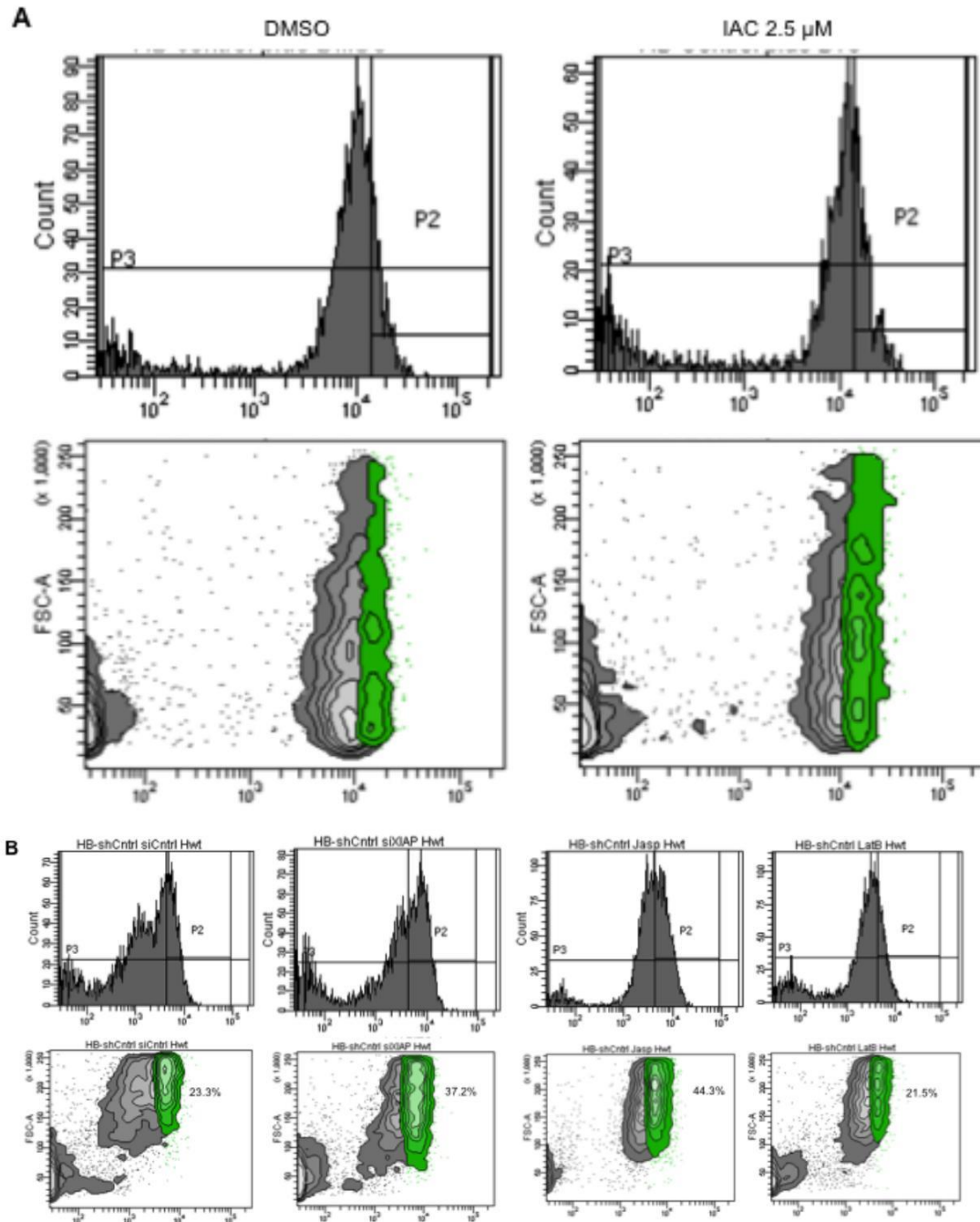


**Figure 3.15: IAP antagonists promote actin polymerization - (A)** HeLa cells treated with DMSO or IAC for 15 h were fixed and stained with phalloidin and then FACS analysis was performed. Two parameters were assessed – (1) the average intensity of the phalloidin stain (P3) and (2) the percentage of cells beyond a threshold intensity (P2; shown in green in the dot blot), both of which directly co-relate to the amount of polymerized F-actin in cells. **(B)** HeLa cells were depleted of XIAP for 48 h and were fixed and stained with Phalloidin as in **(A)**. 50 nM Jasplakinolide and 1  $\mu$ M Latrunculin B were added at mentioned time points prior to the F-Actin Assay.

#### 3.2.2.4. IAP depletion influences WAVE2 phosphorylation

Groups in the past had demonstrated that ERK1/2/ could phosphorylate WAVE2 and Abi1, components of the WRC, thus stimulating WRC activity and promoting actin-driven edge protrusion and cell migration *in vivo*<sup>207</sup>. We have previously shown that loss of XIAP and cIAPs led to an increase in active CRAF levels thus leading to an enhanced ERK1/2 activation in these cells. Having shown that IAP depletion promoted WRC mediated elongation as well as actin polymerization in cells; we tested if WAVE2 is phosphorylated in IAP depleted cells in a MAPK dependent manner. XIAP depleted HeLa cells were either untreated or treated with MEK inhibitor, UO126, an inhibitor that blocked the MEK1/2 kinase. NSC23766, a Rac1 inhibitor was also employed independently in this study to test the dependence of WAVE2 phosphorylation on Rac1 activity. WAVE2 protein was immunoprecipitated and phosphorylation of WAVE2 on known ERK1/2 target residues, S308 and T346, was assessed. It was observed that both these residues were phosphorylated upon depletion of XIAP in a MAPK dependent, Rac1 independent manner (**Figure 3.16 A and B**). The experiments were performed in two different HeLa clones A and B. These results show that IAPs modulate WRC activation in a synergistic manner – through Rac1 as well as via the CRAF-MEK-ERK pathway.

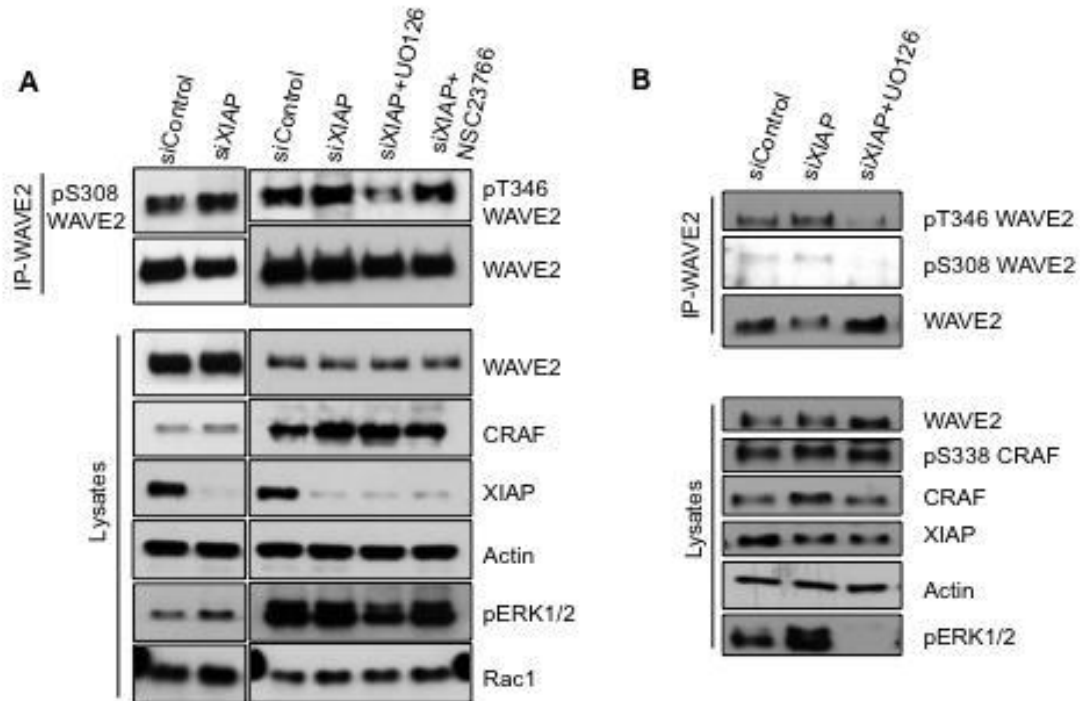


**Figure 3.16: IAP depletion promotes WAVE2 phosphorylation** - (A) HeLa cells were transfected with Control and XIAP siRNA. Either 10  $\mu$ M UO126 was added to block ERK activation via MAPK pathway or 50  $\mu$ M NSC -23766 was added to prevent Rac1 activation. WAVE2 was immunoprecipitated and phosphorylations on S308 and T346 were analyzed by western blotting. As shown, IAP depletion leads to an increase in WAVE2 phosphorylation in a RAF-MAPK pathway-dependent manner. (B) A second clone of HeLa cells was used to reproduce the findings in (A). siRNA-mediated knockdown of XIAP from these cells also show an increase in phosphorylation of S308 and T346 of WAVE2 as observed by western blotting.

### 3.2.3. RhoB stability is influenced by XIAP

Employing quantitative mass spectrometry based approaches we identified several factors that are regulated by XIAP (**Table 1**). Preliminary validation of these results revealed that XIAP influence the stability of RhoB, another member of the Rho GTPase family. Depletion of XIAP was observed to increase RhoB levels in both primary HMEC cells and in NCI-H226 lung cancer cells (**Figure 3.17 A**). Cycloheximide experiments performed with and in the absence of XIAP revealed that RhoB stability is enhanced upon cycloheximide chase (**Figure 3.17 C**). As RhoB has been implicated in cell adhesion, adhesion assays were performed to test for changes in adhesion

properties of cells in response to IAP depletion. However, these assays performed revealed no significant changes in adhesion levels of cells.

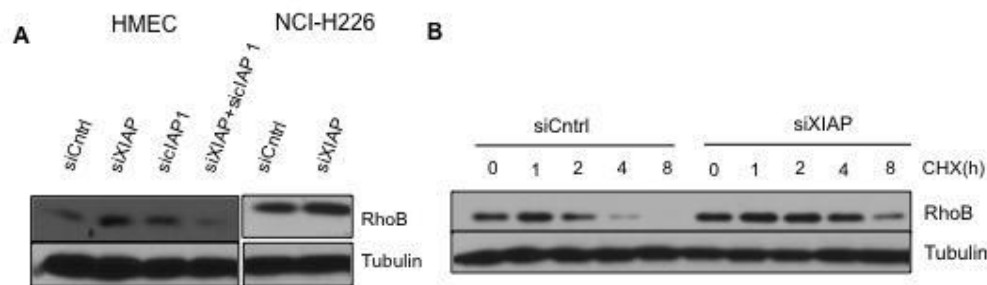


**Figure 3.17: RhoB stability is influenced by XIAP** – (A) Depletion of XIAP, but not cIAP1 results in upregulation of RhoB. HMEC cells and NCI-H226 cells were transfected with Control or XIAP siRNA for 48 h and lysates were then collected for immunoblotting. The levels of total Cdc42 were monitored in the immunoblots. (B) A cycloheximide chase was performed for 8 h to check for RhoB stability over time upon depletion of XIAP for 48 h.

**TABLE 1**

Gene	Name of the protein identified	Fold change
RGSL1	Regulator of G-protein signaling protein-like	13.7
TBL1XR1	F-box-like/WD repeat-containing protein TBL1XR1	4.7
SLC6A9	Sodium- and chloride-dependent glycine transporter 1	3.3
ZFP106	Zinc finger protein 106 homolog	3.27
TUBA4A	Tubulin alpha-4A chain	2.67
SLC2A3	Solute carrier family 2, facilitated glucose transporter member 3	2.6
NCOR2	Nuclear receptor	2.45



	corepressor 2	
RPS19BP1	Active regulator of SIRT1	2.19
MPG;PIG16	DNA-3-methyladenine glycosylase	2.1
MRPL28	39S ribosomal protein L28, mitochondrial	2.08
RPS6KA3	Ribosomal protein S6 kinase alpha-3	2,0719
PPP2R5E	Serine/threonine-protein phosphatase 2A 56 kDa regulatory subunit epsilon isoform	2.06
RhoB	Ras homolog gene family, member B	1.32
FARP1	FERM, RhoGEF and pleckstrin domain-containing protein 1	0.48

This preliminary data with RhoB suggests that IAPs could play a prominent role in controlling intercellular adhesion, cell shape, cell migration and invasion and associated phenotypes. We have thus far validated RhoB, because of the connection to Rho GTPases. The other factors identified in the screen needs further studies and perhaps open an as yet unknown side of IAPs in other physiological processes.



## 4. Discussion

### 4.1. Loss of XIAP promotes filopodia formation in a Cdc42 dependent manner

There has been debate in the field as to the exact mechanism of filopodia formation. While Cdc42 has been primarily implicated in this process, various other Rho GTPases, including but not limited to RhoU, RhoV and Rif have all been shown to play a role in a context specific manner. Neither the convergent elongation model nor the tip nucleation models have successfully deciphered the role of downstream proteins in this process. Thus, it comes as no surprise that there are conflicting reports regarding filopodium formation in the literature. Further, studies suggested that both the Arp2/3 complex as well as mDia2 co-exist in a multi-molecular complex along with WAVE2 thus inhibiting the actions of mDia2. Only when mDia2 disengages itself from the complex does filopodia formation get promoted <sup>295</sup>. Recent studies also showed that ARPC3(-/-) fibroblasts (ARPC3 encodes the p21 subunit of the Arp2/3 complex) were unable to form lamellipodia but did form mDia1 and 2 enriched filopodia like protrusions at the leading edges <sup>296</sup>. Another recent study furthered the tip nucleation model and the role of formins by showing that viral filopodia formation was dependent on the formin diaphanous 2 and not Arp2/3 <sup>297</sup>. However, regardless of the downstream pathways influencing this phenomenon, Cdc42 plays a crucial role in a context and cell type dependent manner. For instance, Cdc42-null mouse embryonic fibroblasts (MEFs) completely lack filopodia activity <sup>298</sup>, Cdc42-null neurons show reduced filopodia <sup>262</sup>, while fibroblastoid cells derived from Cdc42-null embryonic stem cells form normal filopodia <sup>299</sup>.

Over the course of our studies, we worked with both primary as well as tumor cells. We detect a clear role for Cdc42 in filopodia formation in the cell lines we worked with as depletion of Cdc42 almost completely inhibited basal as well as EGF induced filopodia formation in multiple cell types (**Figure 3.5 A and 3.6 A**). As depletion of XIAP promoted the activity of Cdc42, we expected

a strong effect on the number of filopodia in these cells. As expected, depletion of XIAP enhanced filopodia formation in both primary and tumor cell types. Co-depletion of Cdc42 prevented filopodia formation both in control and XIAP depleted cells suggesting that the effect observed is indeed dependent on Cdc42. Unlike HMEC and NCI-H226 cells, which form long, striking, almost spike like filopodia, HeLa cells displayed far fewer number of filopodial protrusions and the protrusions were much shorter than that with other cell types, and consequently tougher to visualize and perform further analysis.

While we did not study the detailed molecular mechanisms regarding filopodium formation, one could hypothesize that our data fits the convergent elongation model better than the tip nucleation model. Previous studies in our group have shown that XIAP depletion increases Rac1 levels as well as Cdc42 activity in cells. Further, in this thesis, we showed that IAP depletion led to enhanced actin polymerization through phosphorylation of the WAVE2 complex and Arp2/3 activation. Finally, having performed CRIB pulldowns with both Rac1 and Cdc42 and seeing both proteins come down with the PAK-PBD domain, one could visualize a multi-protein complex where XIAP normally controls both Rac1 and Cdc42 and prevents binding to its downstream effectors. Upon depletion of XIAP, both Rac1 and Cdc42 are “released” from this complex thus leading to a sustained activation of both Rho GTPases and subsequent downstream signaling. Inhibition of Arp2/3 using Arp2/3 inhibitors did not confirm our hypothesis, as the Arp2/3 complex is far too vital for the cells to survive without it. Attempted wound healing assays with the Arp2/3 inhibitors were unsuccessful due to pronounced cell death. Thus, we can only speculate that the phenomenon of filopodia formation is an Arp2/3 dependent one. Interactome analyses of Cdc42 under basal as well as stimulated conditions, and control and XIAP knockdown conditions would help shed light on as yet undiscovered partners of the Rho GTPase. It could yet be that formins play a role in this process, however we focused more on the factors influencing Cdc42 rather than downstream signaling.

#### 4.2. XIAP directly binds to Cdc42

XIAP possesses BIR domains that are classical protein-protein interaction motifs and thus it was prudent to hypothesize that XIAP directly binds to Cdc42. Indeed, Oberoi et al demonstrated that XIAP binds to Rac1/2 and Rac3 in a nucleotide independent manner <sup>11</sup>. Given the extremely high sequence homology and the evolutionarily conserved nature of the Rac subfamily members, this didn't come as much of a surprise. Experiments using structural mutants of XIAP revealed that the binding of the IAP to Rac1 was BIR3, UBA and RING independent. However, the exact residues responsible for driving the interaction between XIAP and Rac1 were not studied in detail at the time. However, studies from Lemmichez group suggested that HACE1 binds to only the activated form of Rac1. Given that Rac1 and Cdc42 share a high degree of homology (almost 70%), we hypothesized that XIAP also bound directly to Cdc42 thus influencing its stability. We also wondered whether any potential interaction would be nucleotide dependent and if so, which domains of XIAP were responsible for the interaction. This gains further importance in the light that Liu et al showed in 2011 that XIAP bound to RhoGDI, a sequestering protein for Rho GTPases in a RING dependent manner <sup>284</sup>. This interaction was independent of its E3 ligase activity. The E3 ligase activity was shown to be responsible for cell migration, but surprisingly, RhoGDI was not ubiquitinated by XIAP. Further, XIAP negatively regulated SUMOylation of RhoGDI at Lys 138 and that this SUMOylation was crucial for inhibiting cancer cell motility.

Literature suggests that Cdc42 is normally present at the leading edge of the cell in tumor cell migration in response to various stimuli. Growth factors like Epidermal Growth Factor (EGF) are known activators of Cdc42 and also promote its phosphorylation in cells <sup>186</sup>. Similarly, Hepatocyte Growth Factor (HGF) stimulates Cdc42, RhoA and Rac1 thus contributing to epithelial cell colony spreading and dissociation <sup>300</sup>. While there are no mutation hotspots known for Cdc42, there is increasing evidence that Cdc42 deregulation

frequently occurs in different human cancers due to molecular alterations in the genes encoding Cdc42 regulatory proteins and/or downstream effectors. This includes upregulation of GEFs upstream of Cdc42 or deregulation of GAPs thus preventing GTP hydrolysis. The Cdc42 GEFs Vav2, Vav3, ITSN-1, P-Rex and FGD1 exemplify this phenomenon, as their overexpression and/or hyperactivity has been directly linked to different types of human cancers, including leukemia, breast, prostate and brain tumors<sup>301–303</sup>. The DOCK family, another family of GEFs was recently identified to activate Rho GTPases by a DH-unrelated domain named the DOCKER, CZH2 or DHR2 domain. The DOCK family has been implicated in a number of cellular events such as cell migration, phagocytosis of apoptotic cells, T-cell activation and neurite outgrowth<sup>304</sup>. Interestingly, the Cdc42-specific activator DOCK8 has been linked to a human disease, specifically to primary immune deficiency<sup>305</sup>. Considering the above studies, and given that we noticed that a Rac1 GEF, FARP1 was downregulated upon XIAP depletion in our mass spectrometric screen, this also opens up the possibility of XIAP regulating Rac1/Cdc42 through proteins upstream of the Rho GTPases. Whether XIAP negatively regulates GEFs or targets GAPs by other means, one cannot rule out the hypothesis that the IAPs regulate the same Rho GTPases on multiple levels. One could theorize that the IAPs behave as a scaffold for GEFs, Rho GTPases and downstream targets (the former two binding in distinct domains of the Rho GTPase) in a multi-protein complex and react to various growth factors or cellular triggers to modulate protein levels in cells. In the light of these studies and the results they demonstrate, it is imperative that we understand further the interaction dynamics of Cdc42 in different cell types as well as identify context specific roles for the Rho GTPase.

In this study, we first showed that XIAP and active Cdc42 are present in one complex at endogenous levels (**Figure 3.3 C and D**). Interestingly, XIAP bound to the activated but not the inactivated form of Cdc42 (Figure 4.1). This suggests that XIAP could possibly function as an effector protein though XIAP does not possess any Rho GTPase binding domains. Abrogation of the RING domain prevented XIAP–Cdc42 interaction. It is currently unclear if the RING

domain directly mediates the interaction or deletion of RING domain confers conformational changes on XIAP that would not favour Cdc42 binding. Further experiments are clearly warranted to substantiate these claims. For instance, it would be interesting to test if the RING domain of XIAP alone can bind to activated Cdc42 at high affinity and that this interaction could be abrogated by mutating the  $Zn^{2+}$  ion coordinating residues. However, the observation that the RING domain was crucial for interaction with activated Cdc42 led us to test the possibility whether XIAP could potentially function as an E3 Ub-ligase of Cdc42. It is also unclear if Cdc42 binding triggers the RING activity of XIAP.

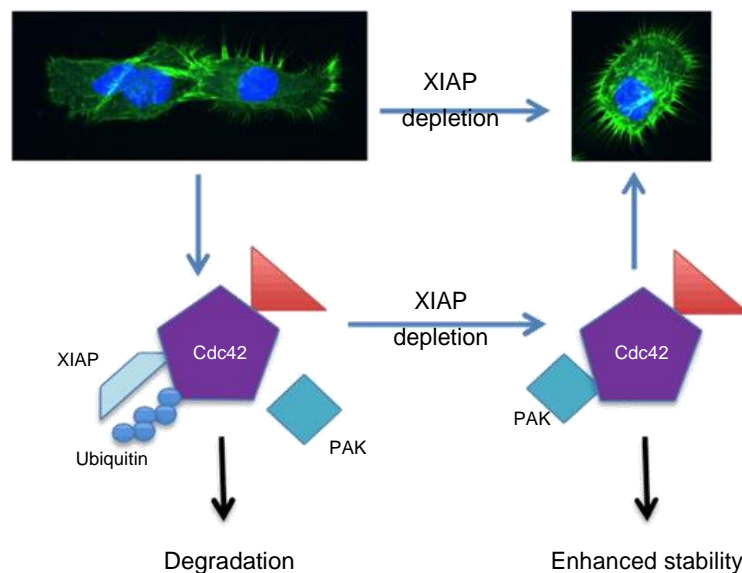


**Figure 4.1:** XIAP binds to Cdc42 resulting in enhanced stability of the protein. Our results show that XIAP binds preferentially to the activated form of Cdc42 and conjugate ubiquitin chains to K166, thus preventing PAK binding and causing degradation of the protein. Upon depletion of XIAP, PAK binds to Cdc42 in the same domain that XIAP does leading to enhanced stability and more filopodia formation.

The functional interplay between XIAP, Cdc42 and RhoGDI was not explored in detail in this study. However, it is tempting to propose that binding to RhoGDI also regulates the interaction of Cdc42 with XIAP and its consequent ubiquitination. Each member of this trio of proteins has been shown to interact with the other in independent studies<sup>288,306</sup>. Given that our data suggests that XIAP binds only to the active GTP bound form of Cdc42, a very

interesting question would be whether XIAP-RhoGDI and XIAP-CDC42 interactions are mutually exclusive and if so, what are the cellular triggers influencing each state. Structural studies of the RhoGDI-Cdc42 complex have shown that there are various interaction surfaces on Cdc42, both polar and hydrophobic. First, the amino-terminal regulatory arm of the GDI binds to the switch I and II domains of Cdc42 causing the inhibition of both GDP dissociation and GTP hydrolysis. Second, the geranylgeranyl moiety of Cdc42 inserts into a hydrophobic pocket within the immunoglobulin-like domain of the GDI molecule leading to membrane release. Given that we observe XIAP interacting with Cdc42, it is likely that preferential binding of one molecule over the other with Cdc42 leads to different downstream signaling events. There is also the question of cellular localization that was not addressed in this study. Rho GTPases, depending on their activation status are either sequestered in the cytosol in an inactive form or are tethered to the plasma membrane upon activation. RhoGDI utilizes the post-translational modifications to extract Cdc42 from the plasma membrane, while XIAP is traditionally a cytosolic protein. One could envisage that both RhoGDI and XIAP compete to bind to active Cdc42 and detach the Rho GTPase from the plasma membrane. To this end, it would be interesting to check whether isoprenylated or geranylgeranylated Cdc42 is ubiquitinated. XIAP binding directly to RhoGDI could be another event which influences binding of one of these proteins to Cdc42. PAK binding is another event that adds to the complexity of this interaction and one that was explored in this thesis in context with XIAP. Further studies are warranted to understand the spatiotemporal dynamics of Cdc42-XIAP interaction. Lastly, it would be interesting to see how Cdc42-XIAP interaction contrasts with the Rac1-XIAP interaction – and the potential upstream stimuli and post-translational modification(s) that govern these interactions.

### **4.3. XIAP is a direct E3 ligase of Cdc42**

Advances in our understanding of E3 ligases that catalyze ubiquitylation of Rho GTPases has shed new light on the importance of ubiquitination in

regulating Rho GTPase activity spatiotemporally. In the last 10 years, various novel degradative pathways have been discovered for the Rho GTPase family. Beginning with Smurf1 acting as an E3 ligase for RhoA, there are multiple E3 ligases known for both RhoA and Rac1 to date. Overexpression of Smurf1 was shown to cause a loss of stress fibres and reduced cell motility in epithelial cells<sup>192,307,308</sup>. aPKC $\zeta$ -mediated recruitment of Smurf1 to the leading edge of cells led to RhoA degradation and ensured cell polarity. Unlike Smurf1, CRL3<sup>BACURD</sup>, the second Rho GTPase discovered for RhoA targets inactive RhoA for degradation<sup>195</sup>. The third E3 ligase for RhoA, Skp1-Cul1-Fbox (SCF) FBXL19 (SCF<sup>FBXL19</sup>) ubiquitinates RhoA at Lysine 135 and targets it for proteasomal degradation in an Erk2-dependent manner. In short, Erk2-mediated phosphorylation of RhoA was necessary for ubiquitylation of RhoA. This interesting interplay between PTMs adds a greater level of fine-tuning to Rho GTPase regulation. Similar to RhoA, RhoB is also ubiquitylated by Smurf1 at Lysine 6/7 and is consequently marked for proteasomal degradation<sup>309</sup> while reduction in Smurf1 levels in response to DNA damage promotes RhoB-mediated apoptosis.

Similarly, various E3 ligases were identified for Rac1. XIAP, cIAP1 and Hace1 were all observed to ubiquitinate Rac1 at Lysine 147. SCF<sup>FBXL19</sup>, a fourth E3 ligase ubiquitinated Rac1 at Lysine 166 and intriguingly also targets Rac3 at the same position<sup>310,311</sup>. It is not yet clear how the same E3 ligase functions for three different target proteins – RhoA, Rac1 and Rac3, all having their own unique and at times contradictory functions, but it is likely that is a cell type specific phenomenon which is also governed by their expression levels.

Our discovery that the interaction between XIAP and Cdc42 is RING dependent made us question whether ubiquitination was involved in this interaction. After initial validation that XIAP did indeed ubiquitinate the Cdc42 wild type protein, we checked further whether this ubiquitination was also nucleotide dependent. This led to further in-vitro ubiquitination experiments (**Figure 3.8 A**) where we showed clearly that XIAP ubiquitinated both the Wild Type and the Cdc42Q61L mutant while the Cdc42T17N mutant wasn't,



consistent with our binding experiments. As previous studies had shown that Rac1 was ubiquitinated by both XIAP and cIAP1, it was a natural progression to check whether cIAP1 ubiquitinated Cdc42 as well. Interestingly enough, unlike Rac1, it was only XIAP and not cIAP1 which ubiquitinated Cdc42 (**Figure 3.8 B**). While these results fall in line with those from our collaborators who showed that cIAP1 does not ubiquitinate Cdc42<sup>282</sup>, it differs from the IAP-Rac1 interaction we observed in the past. Having shown direct binding as well as ubiquitination in vitro, we went into cells and performed TUBE assays (**Figure 3.8 C**) to check for endogenous ubiquitination of Cdc42. These TUBE assays showed that depletion of XIAP reduced ubiquitin smears compared to control cells upon inhibition of proteasomal degradation by MG132 further confirming our hypothesis that XIAP functions as an E3 ubiquitin ligase of Cdc42. Finally, experiments in Mouse Embryonic Fibroblasts (**Figure 3.8 D**) demonstrated that the RING activity of XIAP was crucial in regulating levels of Cdc42 as the RING mutant of XIAP was not able to influence Cdc42 levels in MEFs.

Mass spectrometric analyses for the ubiquitination sites of Rac1 revealed one ubiquitination site on Cdc42 – the Lysine 166 (Figure 4.2). Conserved with Rac1, we performed molecular modeling to further understand this interaction. What we observed was that the XIAP-Cdc42 interaction was in direct opposition to the Cdc42-PAK interaction. Our modeling suggested that ubiquitination of Cdc42 by XIAP would sterically hinder Cdc42 binding to PAK, its downstream effector (**Figure 3.10 A**). To confirm this hypothesis, we performed further binding studies with PAK-PBD, the domain of PAK that binds to Cdc42. These experiments (**Figure 3.10 B**) confirmed that ubiquitination of Cdc42 did indeed affect PAK-Cdc42 interaction. **Figure 2.1** summarizes the above-described interactions with an emphasis on the downstream inactivation of PAK as a result of XIAP binding to Cdc42.

Almost nothing was known to date regarding the ubiquitin-mediated regulation of Cdc42. Cdc42, however, is linked to RhoA because of its association with the aPKC $\zeta$ -Par complex, which controls Smurf1<sup>192</sup>. This suggests a spatio-



temporal regulation for controlling RhoA levels at the leading edge during protrusion dependent movements by Cdc42. This thesis advanced the role for XIAP as an E3 ligase of Cdc42. Interestingly, XIAP ubiquitinates Cdc42 at Lysine 166, which is the same site for SCF<sup>FBXL19</sup> on Rac1. Cdc42 shares almost 70% sequence homology with Rac1 (see **Inset Figure 3.9 A**). However, despite this high degree of homology, Cdc42 does not contain a Lysine at 147. It would be interesting to understand how the same E3 ligase performs its duties on two different, yet structurally similar proteins, at different positions. Further, it might be interesting to study whether mutation of the Lysine 166 affects the stability of the protein upon overexpression of XIAP.

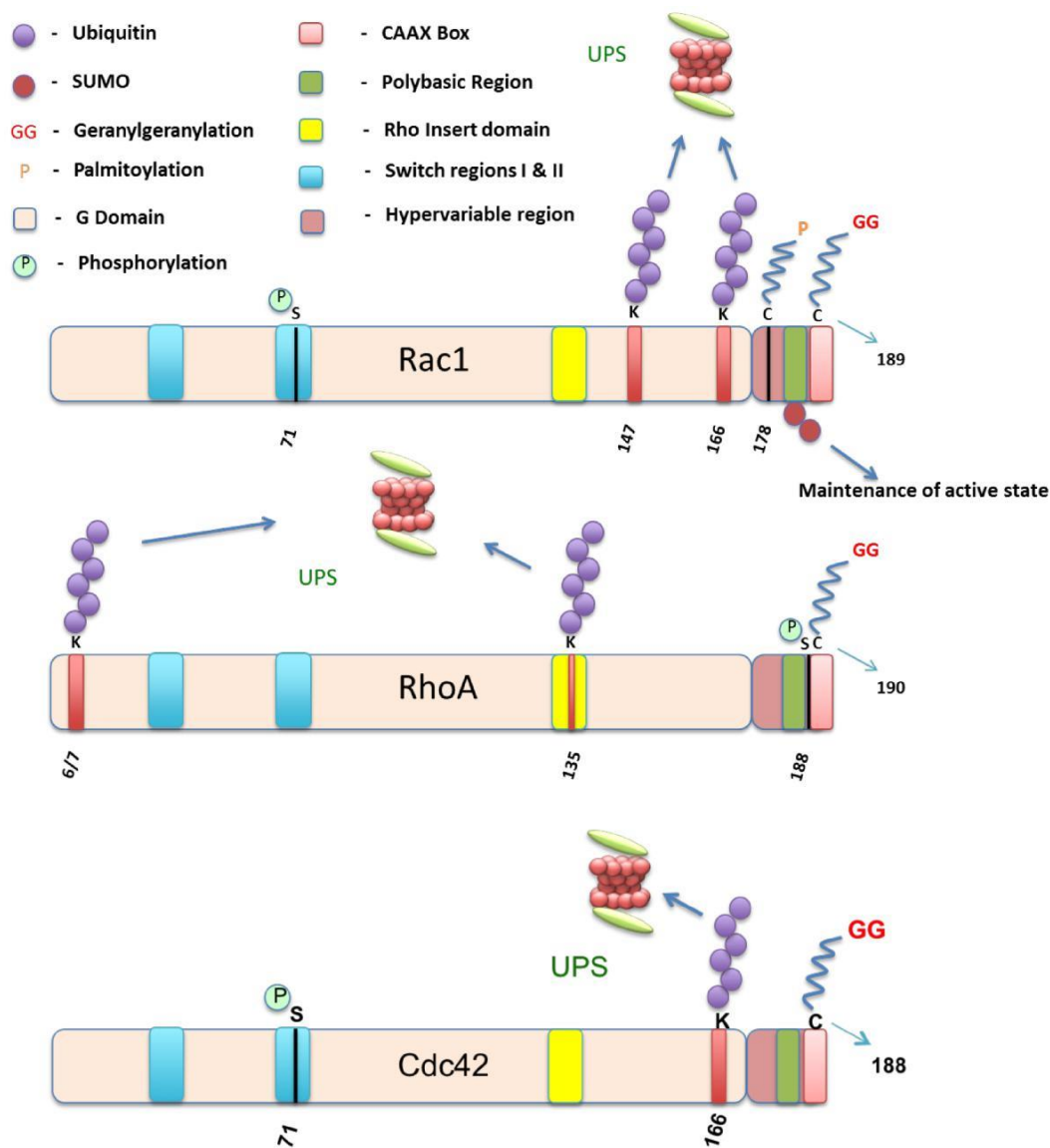


**Figure 4.2:** Cdc42 is ubiquitinated on Lysine 166 and targeted for proteasomal degradation similar to the other Rho GTPases Rac1 and RhoA, which are ubiquitinated at different sites – K147 and K166 for Rac1, and K6/7 and K135 for RhoA. Various domains are represented for each Rho GTPase along with the post translational modifications

As the activated form of Cdc42 is targeted for ubiquitination and proteasomal degradation, it is possible that interaction with XIAP and ubiquitination is also regulated by interaction with RhoGDI. Another observation made was that depletion of XIAP enhanced the active-GTP bound form of Cdc42 with a concomitant increase in actin rich filopodial protrusions in normal and tumor cells. As XIAP binds to the activated Cdc42 and promotes ubiquitination, loss of XIAP led to the accumulation of activated Cdc42 in cells. These observations further support the model that XIAP-mediated ubiquitination could serve as a non-canonical way of Cdc42 inactivation. Finally, it would also be very interesting to test if any other effectors of Cdc42 trigger the RING activity of XIAP directly or indirectly by inflicting a PTM on Cdc42.

We observed with Rac1 that cIAP1 synthesized a mixture of K11/K48 chains on the Rho GTPase (**Figure 3.12**). However, further studies are warranted if these chains are detected in vivo at endogenous levels. Nevertheless, these preliminary observations do fit in to the prevailing understanding in the field that both K11 and K48 ubiquitin chains are signals targeting proteins for proteasomal degradation. While we did not check in the case of Cdc42, we hypothesize that this may again be the case as we shown the ubiquitination to be of a degradative nature. In addition to the canonical conjugates, homogenous chains are also formed by modification of M1, K6, K11, K27, K29, or K33<sup>312</sup>. Several of these linkages can mediate proteasomal degradation, but the reason for this redundancy is unclear<sup>312–314</sup>. Normally, the E2 enzyme strongly influences the selection of the correct modifier, ubiquitin, and a suitable E3<sup>57</sup>. The UBC domain provides the E2 with a structural framework to communicate with the correct E1 to pick up ubiquitin and to engage with an E3. The E2 also helps to determine length of the attached ubiquitin chain. Some E2s preferentially transfer ubiquitin to a Lys in the substrate to initiate ubiquitin chain formation, whereas others are powerful

chain-elongating factors. While some E2s only synthesize a particular kind of ubiquitin chain, others are not as selective. In the case of the IAPs, the E2 UbcH5a synthesizes different kind of chains. Moreover, IAPs have also been shown to synthesize all kinds of ubiquitin chains, including linear chains on their target substrates<sup>315</sup>, thus leaving open the possibility that mixed chains may be synthesized on Cdc42 as well.

#### **4.4. Loss of XIAP promotes tumor cell metastases *in vivo***

XIAP is a legitimate caspase inhibitor and thus efforts have been made to target XIAP–caspase inhibition to promote tumor cell apoptosis. Further, IAPs are found to be upregulated in various tumor types and therefore IAP antagonists (IACs) are being developed and tested on cancer patients. IAPs are also up-regulated in response to chemotherapy and radiotherapy thus contributing to the notion that IAPs are responsible for resistance of these cancer cells<sup>316,317</sup>. Several drugs have been developed to achieve these goals and some of them have reached the clinics. However it is not clear to this date the role for individual IAPs in malignancies. While cIAP1 has been classified as an oncogene in specific cancers, in other cancers, high expression of IAPs correlates to a better outcome<sup>101</sup>. Further, studies by our group and others have shown a contradictory role for IAPs in regulating cell migration and tumor metastasis. Our studies revealed the other side of XIAP in the control of Rho GTPases (especially Rac1 and Cdc42), the prime drivers of tumor cell migration and invasion. Anne Ridley's group in 2012 showed that Cdc42 activity is critical for transendothelial migration and lung metastasis formation *in vivo* in a  $\beta$ 1 integrin dependent fashion<sup>276</sup>. This suggests that targeting Cdc42 in the early steps of endothelial layer interaction could potentially decrease cancer cell colonization and metastasis. Marivin et al showed in 2014 that cIAP1 regulates Cdc42 activation in response to EGF and HRas-V12 expression. Downregulation of cIAP1 reduced tumor cell intercalation and adhesion to endothelial cells as well as cell polarization - all Cdc42-dependent processes. Deletion of cIAP1 also delayed and caused reduction in experimental lung metastasis in HRas-V12-transformed cells<sup>286</sup>.

Our observation that loss of XIAP increases seeding of tumor cells in the lung and cause enhanced micro metastases is of concern, as XIAP antagonists are also in clinical development for the treatment of cancer. However, these experiments need to be substantiated with more physiologically relevant, immunocompetent, preclinical models. In fact, studies from Colin Duckett's group with immunocompetent mice in 2008 showed that loss of XIAP led to an aggressive form of disease<sup>318</sup>. They generated transgenic adenocarcinoma of the mouse prostate (TRAMP) mice that lack XIAP and observed that there was no protective effect of lack of XIAP in these mice. In fact, these mice unexpectedly had a more aggressive form of disease. Further, the knowledge that IAPs interact with various Rho GTPases means that combinatorial therapeutics are likely to be the way forward in order to avoid off target effects. A recent work by Ong et al. targeted p21-activated kinase 1 (PAK1) and XIAP together and managed to efficiently increase effector caspase activation and consequent apoptosis of NSCLC cells<sup>319</sup>. The apoptotic phenotype resulting from combined inhibition of PAK1 and IAP differs substantially from the antiproliferative effect that is observed after single-agent inhibition of PAK1 in squamous NSCLC cell lines. In the light of our studies, which show IAP depletion increases Cdc42 and Rac1 activity and thus enhance PAK activity downstream (both PAK1 and 2), dual inhibition of PAK1 and XIAP would in principle block the migratory effects IAPs exert on Rac1 and Cdc42, whilst also removing the apoptotic checkpoint safeguards that the IAPs provide in cells.

#### **4.5. Synergistic activation of WAVE complex upon IAP depletion**

WAVE2 complex is a well-established target for active Rac1 but apart from Rac1-mediated activation, WAVE2 is highly regulated by various phosphorylation events. WAVE2 contains 4 conserved domains: the N-terminus WAVE homology domain (WHD), a basic region, a proline-rich domain (PRD) and a C-terminus VCA domain. The majority of negative regulatory phosphorylation sites of WAVE2 are located in the VCA domain,

phosphorylated by CK2<sup>320</sup>. However, Y150 phosphorylation of WAVE2 by Abl in WHD and S308, S343, S351 and T346 of WAVE2 by ERK1/2 in the PRD are required for activation of the WAVE2 complex<sup>211,320</sup>.

In this thesis, we demonstrate that IAPs limit WAVE2 phosphorylation and WRC-mediated changes in cell morphology and migration by a two-pronged approach. Apart from limiting Rac1 stability and activation, IAPs can also prevent C-RAF induced MAPK pathway activation, thereby hampering WAVE2 phosphorylation by ERK1/2 and membrane recruitment of WRC (Figure 4.3). This debilitates WRC function and inhibits it from downstream recruitment and activation of Arp2/3 complex preventing actin polymerization (**Figure 3.15 A and B**). Conversely, knockdown of IAPs, either by IAC or siRNAs can promote WAVE2 complex phosphorylation by positive signaling via Rac1 and ERK/MAPK cascades (**Figure 3.16**). These triggers reinforce WRC-mediated Arp2/3 activation and actin polymerization (**Figure 3.15**). Disrupting the WAVE complex by stably knocking down a component (Nap1) clearly reversed the elongated morphology and directional migration observed upon IAP depletion by both siRNAs and IACs (**Figure 3.14**).

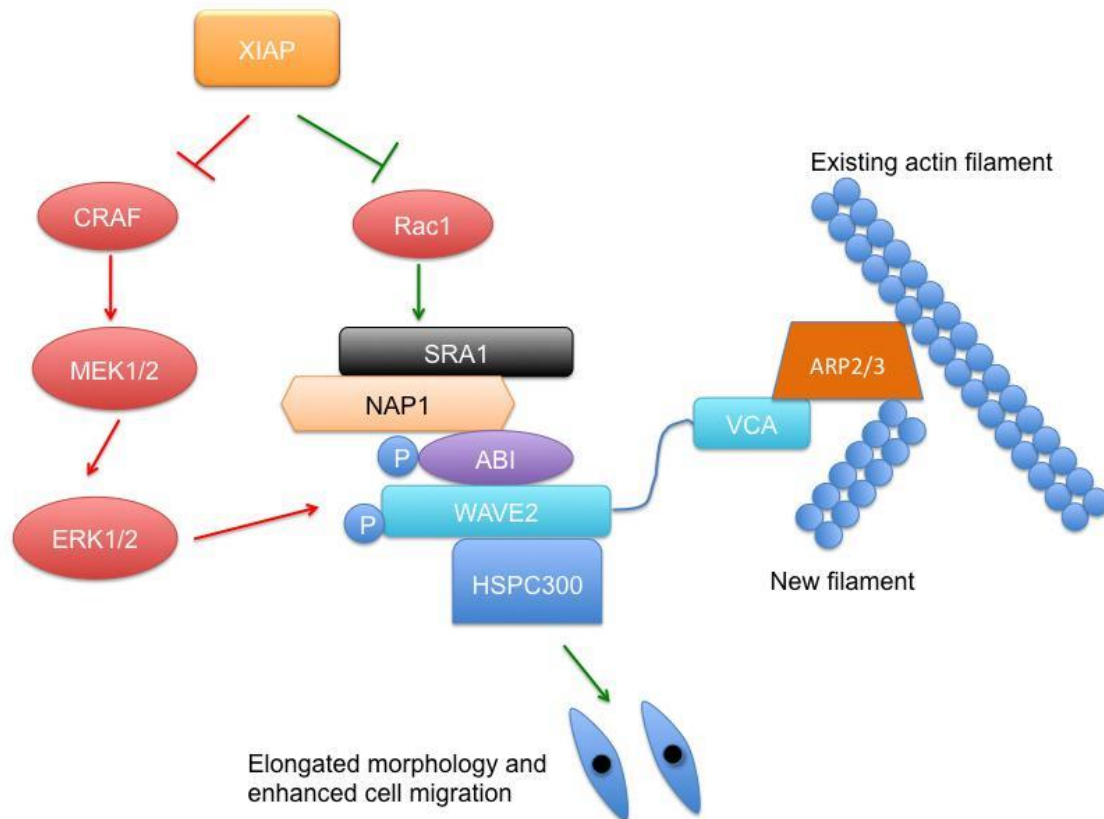


**Figure 4.3:** Synergistic activation of the WAVE complex due to XIAP depletion - Depletion of XIAP leads to elongated cell morphology, increased actin polymerisation and enhanced migration through the MAP Kinase pathway as well as Rac1 downstream signaling.

The WAVE family of proteins has shown a context-dependent role in carcinogenesis. While it was initially assumed WASPs and WAVEs would promote cancer invasion and metastasis because they positively regulate cell motility through actin polymerization; this was later revealed to be partially true<sup>321</sup> but oversimplified. Depletion of the WAVE2 complex inhibited Arp2/3 driven elongated morphology, but it also simultaneously promoted round morphology in a RhoA independent manner in certain cell types<sup>322</sup>. Silva and colleagues<sup>323</sup> found that reduced expression of the WAVE complex subunit Sra1/CYFIP1 causes loss of epithelial cell adhesion and promotes tumor progression, which implicates Sra1 as a suppressor of invasion in epithelial cancers. Thus it was concluded that WAVE2 suppresses cancer in the early stages but promotes invasion and metastasis at the later stages<sup>324</sup>. This study furthers the notion that the WAVE2 complex contributes to enhanced actin polymerization and migration and introduces a new factor that contributes to this phenomenon, namely XIAP. Further, this work also

provides a link between the C-RAF/MAPK module and Rac1 signaling pathways in controlling IAP-mediated cell morphology and migration phenotypes.

#### 4.6. Outlook and Future Perspectives - IAPs and Rho GTPases

While Geisbrecht and Montell demonstrated in 2004 for the first time that IAPs could play a role in influencing Rho GTPase function and cell migration with their experiments with DIAP1 and Rac1<sup>285</sup>, in the last 10 years, IAPs have slowly evolved from caspase inhibitors to pleiotropic proteins involved in a multitude of signaling pathways. Initial reports of IAPs playing a role in tumor cell migration came with Dogan et al, who showed that IAPs negatively regulate CRAF kinase activity and stability<sup>9</sup>. Since then, studies expanded to the field of Rho GTPases as scientists followed up on the seminal Geisbrecht Montell paper of 2004 and yearned to understand how IAPs influenced the morphology of tumor cells and the plasticity of cell migration. It was then that the first mammalian IAP-Rho GTPase link was made – also with Rac1<sup>11</sup>. Hornburger et al showed in 2013 that RhoA was regulated by XIAP thus implicating these proteins in endothelial barrier function<sup>243</sup>. Both XIAP, and to a lesser extent, cIAP1 were found to interact with RhoA independent of its activation status. In endothelial cells, downregulation of IAPs prevented thrombin-evoked RhoA activation, stress fiber formation, activation of contractile machinery and disassembly of adherens junctions<sup>243</sup>. It was suggested that IAP inhibition be used as a novel way to treat endothelial barrier dysfunction. This could in turn have an impact on tumor cell metastases as endothelial barrier permeability is a crucial early step in the facilitation of transendothelial migration of cancer cells during metastasis.

As IAPs have played a crucial role in regulating Rho GTPase stability, along with the added observations that XIAP depletion led to filopodia like protrusions on tumor cells irrespective of the matrices on which they were grown, it was a natural extension for us to check whether other members of the Rho GTPase family were also involved with IAPs. This study showed that



the XIAP-ubiquitin-Cdc42 axis plays a vital role in regulating filopodia formation and that depletion of XIAP led to an increase in lung metastases of NOD-SCID mice in a Cdc42 dependent manner. Further, an indirect role was observed for IAPs in regulating cell migration with the discovery that they can regulate the WAVE regulatory complex (WRC) indirectly through the MAP kinase signaling pathway. Finally, preliminary data from the validation of a mass spectrometric screen suggests that XIAP influences the stability of RhoB as well, though traditional RhoB phenotypes like adhesion are not affected as a result of XIAP depletion.

All of this adds up to a bigger picture wherein IAPs, especially XIAP, play a central role in Rho GTPase stability and their respective phenotypes (Figure 4.4). Not all IAP-Rho GTPase interactions are the same however – while cIAP1 and XIAP both ubiquitinate Rac1 and cIAP1 synthesizes a possible mixture of K11 and K48 linked chains on the Rho GTPase, only XIAP and not cIAP1 ubiquitinates Cdc42. However, these experiments were done in an in vitro system and would have to be replicated in an in vivo scenario to confirm these observations. cIAP1 controls Cdc42 activity in response to TNF alpha. Neither cIAP1 nor XIAP ubiquitinate RhoA, however, both of them interact with RhoA. Finally, depletion of XIAP also stabilized RhoB levels in cell lines. While it is possible that each of these effects could be cell line specific, it is more likely that these interactions are regulated tightly on a spatiotemporal basis. For example, while it has not been explored, one can speculate that while IAP-Rac1/Cdc42 interaction would be localized to the leading edge of a migrating cell, the IAP-RhoA interaction is likely near the trailing edge. The IAP-RhoB interaction could be localized to focal adhesion complexes where integrins and other ECM proteins play a vital role in maintaining these junctions. Advanced microscopic techniques to observe spatio-temporal localization of these proteins in response to triggers like growth factors like EGF or directional migration assays would help shed light on the interplay between these proteins in different parts of the cell. Another interesting question would be whether IAPs preferentially bind to particular Rho GTPases spatially or whether it all adds up to give a synergistic effect. For example,



depletion of XIAP activates Rac1 and Cdc42 while it inactivates RhoA. This could translate phenotypically to a cell changing its mode into a mesenchymal like one and form various protrusions at the leading edge thus allowing it to navigate through a matrix. The role of both RhoA and Cdc42 in endothelial cell permeability also adds an additional layer of complexity as regulation of IAPs could also lead to differences in tumor cells permeating through an endothelial layer of cells.

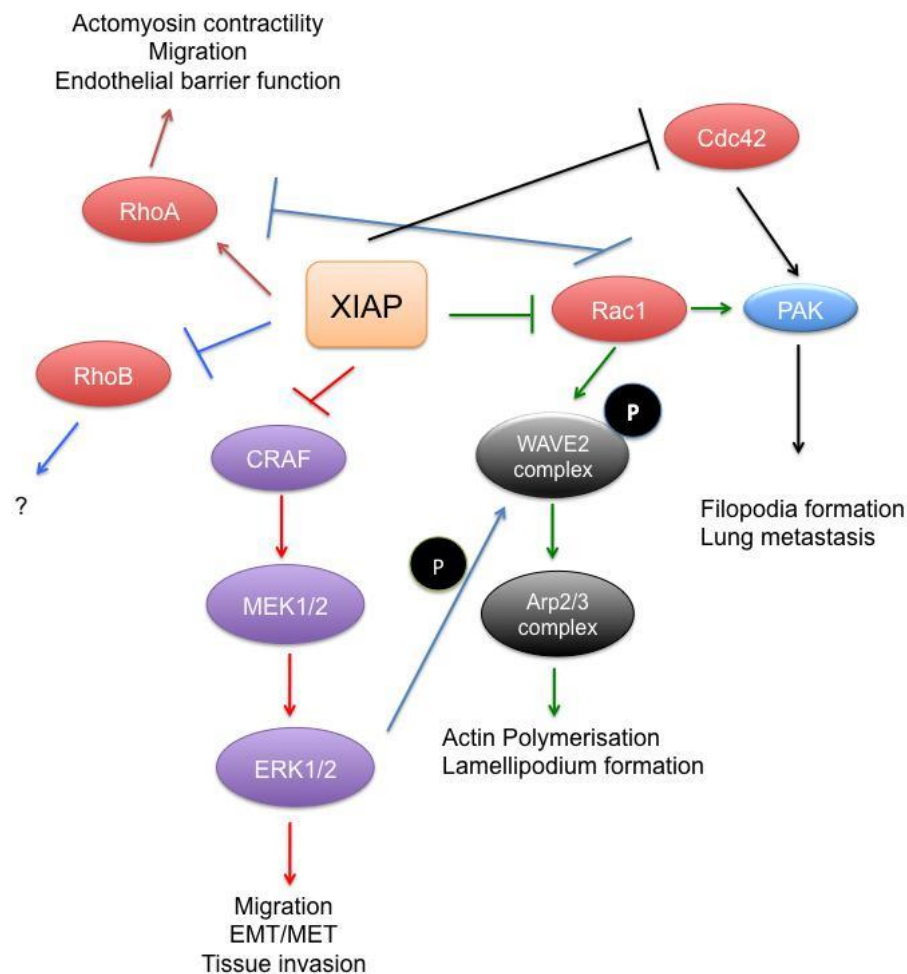


**Figure 4.4:** XIAP and Rho GTPases – The various roles of XIAP are explained in this figure. As is clear from the figure, XIAP plays a central role in regulating cell migration by interacting with different Rho GTPases as well as the MAP kinase pathway resulting in a variety of phenotypes in a context dependent manner

Given the deregulation of these Rho GTPases in cancer, it would be interesting to understand how IAP-Rho GTPase interactions are affected in these cases. Also of interest would be to determine whether IAPs are

expressed abnormally themselves in these cancers. This is true especially in the case of Cdc42 where no hotspot mutations are known and the most common features involve deregulation of Cdc42 regulatory proteins or downstream effectors of the Rho GTPase. It is also clear that various oncogenic pathways are linked intricately in tumors. For example, both the Ras influenced MAP kinase pathway and the Rho GTPases are connected to each other. Genetic deletion of Cdc42 in Ras-transformed cells caused a block in cell proliferation<sup>325</sup>. Similarly, blocking RhoA suppressed Ras-induced transformation while activating RhoA led to a synergistic cooperation with Raf to promote cell transformation<sup>326–328</sup>. Thus it makes sense to investigate whether there is a link between IAP expression and Rho GTPase expression in various cancers.

Overall, this thesis provided novel insights on Rho GTPase regulation and also advanced our knowledge on actin cytoskeleton modulation. It identified a novel non-canonical degradative pathway for Cdc42, whilst extending our knowledge on pathways downstream of Rac1. We could also confirm that the E3 ligase activity of XIAP was not indiscriminate, as it did not ubiquitinate RhoA. It also placed XIAP firmly at the heart of the cell migration cascade, thus adding another feather to the IAP arsenal. While it is still unclear how exactly the IAPs regulate so many diverse processes in different cellular compartments, it is quite evident that given their pleiotropic nature, it is of paramount importance that we understand more about these proteins so as to also exploit them therapeutically.

## 5. References

1. Birnbaum, M. J., Clem, R. J. & Miller, L. K. An apoptosis-inhibiting gene from a nuclear polyhedrosis virus encoding a polypeptide with Cys/His sequence motifs. *J. Virol.* **68**, 2521–8 (1994).
2. Crook, N. E., Clem, R. J. & Miller, L. K. An apoptosis-inhibiting baculovirus gene with a zinc finger-like motif. *J. Virol.* **67**, 2168–2174 (1993).
3. Roy, N. *et al.* The gene for neuronal apoptosis inhibitory protein is partially deleted in individuals with spinal muscular atrophy. *Cell* **80**, 167–178 (1995).
4. Gyrd-Hansen, M. & Meier, P. IAPs: from caspase inhibitors to modulators of NF-kappaB, inflammation and cancer. *Nat. Rev. Cancer* **10**, 561–74 (2010).
5. Bertrand, M. J. M. *et al.* Cellular Inhibitors of Apoptosis cIAP1 and cIAP2 Are Required for Innate Immunity Signaling by the Pattern Recognition Receptors NOD1 and NOD2. *Immunity* **30**, 789–801 (2009).
6. Labbé, K., McIntire, C. R., Doiron, K., Leblanc, P. M. & Saleh, M. Cellular Inhibitors of Apoptosis Proteins cIAP1 and cIAP2 Are Required for Efficient Caspase-1 Activation by the Inflammasome. *Immunity* **35**, 897–907 (2011).
7. Dagenais, M. *et al.* A critical role for cellular inhibitor of protein 2 (cIAP2) in colitis-associated colorectal cancer and intestinal homeostasis mediated by the inflammasome and survival pathways. *Mucosal Immunol.* **9**, 146–158 (2016).
8. Ebert, G. *et al.* Cellular inhibitor of apoptosis proteins prevent clearance of hepatitis B virus. *Proc. Natl. Acad. Sci.* **112**, 5797–5802 (2015).
9. Dogan, T. *et al.* X-linked and cellular IAPs modulate the stability of C-RAF kinase and cell motility. *Nat. Cell Biol.* **10**, 1447–1455 (2008).
10. Oberoi-Khanuja, T. K., Karreman, C., Larisch, S., Rapp, U. R. & Rajalingam, K. Role of melanoma inhibitor of apoptosis (ML-IAP) protein, a member of the baculoviral IAP repeat (BIR) domain family, in the regulation of C-RAF kinase and cell migration. *J. Biol. Chem.* **287**, 28445–28455 (2012).
11. Oberoi, T. K. *et al.* IAPs regulate the plasticity of cell migration by directly targeting Rac1 for degradation. *EMBO J.* **31**, 14–28 (2011).
12. Takeda, A.-N. *et al.* Ubiquitin-dependent regulation of MEKK2/3-MEK5-ERK5 signaling module by XIAP and cIAP1. *EMBO J.* **33**, 1–18 (2014).
13. Hinds, M. G., Norton, R. S., Vaux, D. L. & Day, C. L. Solution structure of a baculoviral inhibitor of apoptosis (IAP) repeat. *Nat. Struct. Biol.* **6**, 648–51 (1999).
14. Miller, L. K. An exegesis of IAPs: Salvation and surprises from BIR motifs. *Trends in Cell Biology* **9**, 323–328 (1999).
15. Sun, C. *et al.* NMR structure and mutagenesis of the third Bir domain of the inhibitor of apoptosis protein XIAP. *J. Biol. Chem.* **275**, 33777–33781 (2000).
16. Liu, Z. *et al.* Structural basis for binding of Smac/DIABLO to the XIAP BIR3 domain. *Nature* **408**, 1004–1008 (2000).
17. Srinivasula, S. *et al.* A conserved XIAP-interaction motif in caspase-9 and Smac/DIABLO regulates caspase activity and apoptosis. *Nature* **410**, 112–116 (2001).

18. Lin, S. C., Huang, Y., Lo, Y. C., Lu, M. & Wu, H. Crystal Structure of the BIR1 Domain of XIAP in Two Crystal Forms. *J. Mol. Biol.* **372**, 847–854 (2007).
19. Verhagen, a M. *et al.* Identification of mammalian mitochondrial proteins that interact with IAPs via N-terminal IAP binding motifs. *Cell Death Differ.* **14**, 348–57 (2007).
20. Vaux, D. L. & Silke, J. Mammalian mitochondrial IAP binding proteins. *Biochem. Biophys. Res. Commun.* **304**, 499–504 (2003).
21. Lu, M. *et al.* XIAP Induces NF- $\kappa$ B Activation via the BIR1/TAB1 Interaction and BIR1 Dimerization. *Mol. Cell* **26**, 689–702 (2007).
22. Uren, A. G., Pakusch, M., Hawkins, C. J., Puls, K. L. & Vaux, D. L. Cloning and expression of apoptosis inhibitory protein homologs that function to inhibit apoptosis and/or bind tumor necrosis factor receptor-associated factors. *Proc Natl Acad Sci U S A* **93**, 4974–4978 (1996).
23. Rothe, M., Pan, M. G., Henzel, W. J., Ayres, T. M. & Goeddel, D. V. The TNFR2-TRAF signaling complex contains two novel proteins related to baculoviral inhibitor of apoptosis proteins. *Cell* **83**, 1243–1252 (1995).
24. Chai, J. *et al.* Structural basis of caspase-7 inhibition by XIAP. *Cell* **104**, 769–780 (2001).
25. Riedl, S. J. *et al.* Structural basis for the inhibition of caspase-3 by XIAP. *Cell* **104**, 791–800 (2001).
26. Shiozaki, E. N. *et al.* Mechanism of XIAP-mediated inhibition of caspase-9. *Mol. Cell* **11**, 519–527 (2003).
27. Blankenship, J. W. *et al.* Ubiquitin binding modulates IAP antagonist-stimulated proteasomal degradation of c-IAP1 and c-IAP2 1. *Biochem. J* **417**, 149–160 (2009).
28. Gyrd-Hansen, M. *et al.* IAPs contain an evolutionarily conserved ubiquitin-binding domain that regulates NF-kappaB as well as cell survival and oncogenesis. *Nat. Cell Biol.* **10**, 1309–1317 (2008).
29. Yang, Y., Fang, S., Jensen, J. P., Weissman, A. M. & Ashwell, J. D. Ubiquitin protein ligase activity of IAPs and their degradation in proteasomes in response to apoptotic stimuli. *Sci. (New York, NY)* **288**, 874–877 (2000).
30. Tse, M. K. *et al.* Structural analysis of the uba domain of x-linked inhibitor of apoptosis protein reveals different surfaces for ubiquitin-binding and self-association. *PLoS One* **6**, (2011).
31. Budhidarmo, R. & Day, C. L. The ubiquitin-associated domain of cellular inhibitor of apoptosis proteins facilitates ubiquitylation. *J. Biol. Chem.* **289**, 25721–25736 (2014).
32. Vaux, D. & Silke, J. IAPs, RINGs and ubiquitylation. *Nat Rev Mol Cell Biol.* **6**, 287–297 (2005).
33. Krieg, A. *et al.* XIAP mediates NOD signaling via interaction with RIP2. *Proc. Natl. Acad. Sci. U. S. A.* **106**, 14524–14529 (2009).
34. Dynek, J. N. *et al.* c-IAP1 and UbcH5 promote K11-linked polyubiquitination of RIP1 in TNF signalling. *EMBO J.* **29**, 4198–4209 (2010).
35. Fulda, S. & Vucic, D. Targeting IAP proteins for therapeutic intervention in cancer. *Nat. Rev. Drug Discov.* **11**, 109–24 (2012).
36. Lopez, J. *et al.* CARD-Mediated Autoinhibition of cIAP1's E3 Ligase Activity Suppresses Cell Proliferation and Migration. *Mol. Cell* **42**, 569–583 (2011).
37. J. F. R. KERR\*, A. H. W. A. A. R. Currie. APOPTOSIS: A BASIC BIOLOGICAL

- PHENOMENON WITH WIDE- RANGING IMPLICATIONS IN TISSUE KINETICS. *J. Intern. Med.* **258**, 479–517 (1972).
38. Wei, Y., Fan, T. & Yu, M. Inhibitor of apoptosis proteins and apoptosis. *Acta Biochim. Biophys. Sin. (Shanghai)*. **40**, 278–288 (2008).
  39. Trapani, J. A. Target cell apoptosis induced by cytotoxic T cells and natural killer cells involves synergy between the pore-forming protein, perforin, and the serine protease, granzyme B. *Aust. N. Z. J. Med.* **25**, 793–9 (1995).
  40. Denault, J. B. *et al.* Engineered Hybrid Dimers: Tracking the Activation Pathway of Caspase-7. *Mol. Cell* **23**, 523–533 (2006).
  41. Berger, A. B. *et al.* Identification of early intermediates of caspase activation using selective inhibitors and activity-based probes. *Mol Cell* **23**, 509–521 (2006).
  42. Salvesen, G. S. & Duckett, C. S. IAP proteins: blocking the road to death's door. *Nat. Rev. Mol. Cell Biol.* **3**, 401–10 (2002).
  43. Lisi, S., Mazzon, I. & White, K. Diverse domains of THREAD/DIAP1 are required to inhibit apoptosis induced by REAPER and HID in *Drosophila*. *Genetics* **154**, 669–678 (2000).
  44. Goyal, L., McCall, K., Agapite, J., Hartwig, E. & Steller, H. Induction of apoptosis by *Drosophila* reaper, hid and grim through inhibition of IAP function. *EMBO J.* **19**, 589–97 (2000).
  45. Wang, S. L., Hawkins, C. J., Yoo, S. J., Müller, H. A. J. & Hay, B. A. The *Drosophila* caspase inhibitor DIAP1 is essential for cell survival and is negatively regulated by HID. *Cell* **98**, 453–463 (1999).
  46. Rodriguez, A. *et al.* Dark is a *Drosophila* homologue of Apaf-1/CED-4 and functions in an evolutionarily conserved death pathway. *Nat. Cell Biol.* **1**, 272–9 (1999).
  47. Eckelman, B. P., Salvesen, G. S. & Scott, F. L. Human inhibitor of apoptosis proteins: why XIAP is the black sheep of the family. *EMBO Rep.* **7**, 988–94 (2006).
  48. Schile, A. J., García-Fernández, M. & Steller, H. Regulation of apoptosis by XIAP ubiquitin-ligase activity. *Genes Dev.* **22**, 2256–2266 (2008).
  49. Suzuki, Y., Nakabayashi, Y. & Takahashi, R. Ubiquitin-protein ligase activity of X-linked inhibitor of apoptosis protein promotes proteasomal degradation of caspase-3 and enhances its anti-apoptotic effect in Fas-induced cell death. *Proc. Natl. Acad. Sci. U. S. A.* **98**, 8662–7 (2001).
  50. Varshavsky, A. The early history of the ubiquitin field. *Protein Sci.* **15**, 647–54 (2006).
  51. Hochstrasser, M. Origin and function of ubiquitin-like proteins. *Nature* **458**, 422–429 (2009).
  52. Hershko, A. & Ciechanover, A. The ubiquitin system. *Annu. Rev. Biochem.* **67**, 425–479 (1998).
  53. Pickart, C. M. & Eddins, M. J. Ubiquitin: Structures, functions, mechanisms. *Biochimica et Biophysica Acta - Molecular Cell Research* **1695**, 55–72 (2004).
  54. Stewart, M. D., Ritterhoff, T., Klevit, R. E. & Brzovic, P. S. E2 enzymes: more than just middle men. *Nat. Publ. Gr.* **26**, 423–440 (2016).
  55. Shi, D. *et al.* CBP and p300 are cytoplasmic E4 polyubiquitin ligases for p53. *Proc. Natl. Acad. Sci. U. S. A.* **106**, 16275–80 (2009).
  56. Uchida, C. & Kitagawa, M. RING-, HECT-, and RBR-type E3 Ubiquitin



- Ligases: Involvement in Human Cancer. *Curr. Cancer Drug Targets* **16**, 157–74 (2015).
57. Komander, D. & Rape, M. The Ubiquitin Code. *Annu. Rev. Biochem.* **81**, 203–229 (2012).
  58. Kirisako, T. *et al.* A ubiquitin ligase complex assembles linear polyubiquitin chains. *EMBO J.* **25**, 4877–87 (2006).
  59. Clague, M. J. *et al.* Deubiquitylases from genes to organism. *Physiol. Rev.* **93**, 1289–315 (2013).
  60. Cheung, H. H., Plenchette, S., Kern, C. J., Mahoney, D. J. & Korneluk, R. G. The RING domain of cIAP1 mediates the degradation of RING-bearing inhibitor of apoptosis proteins by distinct pathways. *Mol. Biol. Cell* **19**, 2729–2740 (2008).
  61. Dueber, E. C. *et al.* Antagonists induce a conformational change in cIAP1 that promotes autoubiquitination. *Science* **334**, 376–80 (2011).
  62. Shin, H. *et al.* Identification of ubiquitination sites on the X-linked inhibitor of apoptosis protein. *Biochem. J.* **373**, 965–971 (2003).
  63. Du, C., Fang, M., Li, Y., Li, L. & Wang, X. Smac, a mitochondrial protein that promotes cytochrome c-dependent caspase activation by eliminating IAP inhibition. *Cell* **102**, 33–42 (2000).
  64. Creagh, E. M., Murphy, B. M., Duriez, P. J., Duckett, C. S. & Martin, S. J. Smac/Diablo antagonizes ubiquitin ligase activity of inhibitor of apoptosis proteins. *J. Biol. Chem.* **279**, 26906–26914 (2004).
  65. Yang, Q. H. & Du, C. Smac/DIABLO Selectively Reduces the Levels of c-IAP1 and c-IAP2 but Not That of XIAP and Livin in HeLa Cells. *J. Biol. Chem.* **279**, 16963–16970 (2004).
  66. Fu, J., Jin, Y. & Arend, L. J. Smac3, a Novel Smac/DIABLO Splicing Variant, Attenuates the Stability and Apoptosis-inhibiting Activity of X-linked Inhibitor of Apoptosis Protein. *J. Biol. Chem.* **278**, 52660–52672 (2003).
  67. Galbán, S. *et al.* Cytoprotective effects of IAPs revealed by a small molecule antagonist. *Biochem. J.* **417**, 765–71 (2009).
  68. Qiu, W. *et al.* An apoptosis-independent role of SMAC in tumor suppression. *Oncogene* 1–10 (2012). doi:10.1038/onc.2012.265
  69. Vucic, D. *et al.* Engineering ML-IAP to produce an extraordinarily potent caspase 9 inhibitor: implications for Smac-dependent anti-apoptotic activity of ML-IAP. *Biochem. J.* **385**, 11–20 (2005).
  70. Ma, L. *et al.* Livin promotes Smac/DIABLO degradation by ubiquitin-proteasome pathway. *Cell Death Differ.* **13**, 2079–88 (2006).
  71. MacFarlane, M., Merrison, W., Bratton, S. B. & Cohen, G. M. Proteasome-mediated degradation of Smac during apoptosis: XIAP promotes Smac ubiquitination in vitro. *J. Biol. Chem.* **277**, 36611–36616 (2002).
  72. Liu, W.-H., Hsiao, H.-W., Tsou, W.-I. & Lai, M.-Z. Notch inhibits apoptosis by direct interference with XIAP ubiquitination and degradation. *EMBO J.* **26**, 1660–9 (2007).
  73. Arora, V. *et al.* Degradation of survivin by the X-linked Inhibitor of Apoptosis (XIAP)-XAF1 complex. *J. Biol. Chem.* **282**, 26202–26209 (2007).
  74. Ben-Neriah, Y. & Karin, M. Inflammation meets cancer, with NF- $\kappa$ B as the matchmaker. *Nat. Immunol.* **12**, 715–723 (2011).
  75. Mufti, A. R., Burstein, E. & Duckett, C. S. XIAP: Cell death regulation meets copper homeostasis. *Archives of Biochemistry and Biophysics* **463**, 168–174

- (2007).
76. Micheau, O. & Tschopp, J. Induction of TNF receptor I-mediated apoptosis via two sequential signaling complexes. *Cell* **114**, 181–190 (2003).
  77. Haas, T. L. *et al.* Recruitment of the Linear Ubiquitin Chain Assembly Complex Stabilizes the TNF-R1 Signaling Complex and Is Required for TNF-Mediated Gene Induction. *Mol. Cell* **36**, 831–844 (2009).
  78. Kanayama, A. *et al.* TAB2 and TAB3 activate the NF- $\kappa$ B pathway through binding to polyubiquitin chains. *Mol. Cell* **15**, 535–548 (2004).
  79. Rahighi, S. *et al.* Specific Recognition of Linear Ubiquitin Chains by NEMO Is Important for NF- $\kappa$ B Activation. *Cell* **136**, 1098–1109 (2009).
  80. Tokunaga, F. *et al.* Involvement of linear polyubiquitylation of NEMO in NF- $\kappa$ B activation. *Nat. Cell Biol.* **11**, 123–32 (2009).
  81. Mahoney, D. J. *et al.* Both cIAP1 and cIAP2 regulate TNF  $\alpha$ -mediated NF- $\kappa$ B activation. *PNAS* **2–7** (2008). doi:10.1073/pnas.0711122105
  82. Bertrand, M. J. M. *et al.* cIAP1 and cIAP2 Facilitate Cancer Cell Survival by Functioning as E3 Ligases that Promote RIP1 Ubiquitination. *Mol. Cell* **30**, 689–700 (2008).
  83. Varfolomeev, E. *et al.* c-IAP1 and c-IAP2 are critical mediators of tumor necrosis factor alpha (TNF $\alpha$ )-induced NF- $\kappa$ B activation. *J. Biol. Chem.* **283**, 24295–9 (2008).
  84. Petersen, S. L. *et al.* Autocrine TNF $\alpha$  Signaling Renders Human Cancer Cells Susceptible to Smac-Mimetic-Induced Apoptosis. *Cancer Cell* **12**, 445–456 (2007).
  85. Wang, L., Du, F. & Wang, X. TNF- $\alpha$  Induces Two Distinct Caspase-8 Activation Pathways. *Cell* **133**, 693–703 (2008).
  86. Winkles, J. A. The TWEAK-Fn14 cytokine-receptor axis: discovery, biology and therapeutic targeting. *Nat. Rev. Drug Discov.* **7**, 411–25 (2008).
  87. Zarnegar, B. J. *et al.* Noncanonical NF- $\kappa$ B activation requires coordinated assembly of a regulatory complex of the adaptors cIAP1, cIAP2, TRAF2 and TRAF3 and the kinase NIK. *Nat. Immunol.* **9**, 1371–8 (2008).
  88. Vallabhapurapu, S. *et al.* Nonredundant and complementary functions of TRAF2 and TRAF3 in a ubiquitination cascade that activates NIK-dependent alternative NF- $\kappa$ B signaling. *Nat. Immunol.* **9**, 1364–70 (2008).
  89. Wharry, C. E., Haines, K. M., Carroll, R. G. & May, M. J. Constitutive non-canonical NF $\kappa$ B signaling in pancreatic cancer cells. *Cancer Biol. Ther.* **8**, 1567–1576 (2009).
  90. Yamaguchi, N. *et al.* Constitutive activation of nuclear factor- $\kappa$ B is preferentially involved in the proliferation of basal-like subtype breast cancer cell lines. *Cancer Sci.* **100**, 1668–1674 (2009).
  91. Annunziata, C. M. *et al.* Frequent Engagement of the Classical and Alternative NF- $\kappa$ B Pathways by Diverse Genetic Abnormalities in Multiple Myeloma. *Cancer Cell* **12**, 115–130 (2007).
  92. Keats, J. J. *et al.* Promiscuous Mutations Activate the Noncanonical NF- $\kappa$ B Pathway in Multiple Myeloma. *Cancer Cell* **12**, 131–144 (2007).
  93. Wright, C. W. & Duckett, C. S. Reawakening the cellular death program in neoplasia through the therapeutic blockade of IAP function. *Journal of Clinical Investigation* **115**, 2673–2678 (2005).

94. Dubrez, L. & Rajalingam, K. IAPs and cell migration. *Seminars in Cell and Developmental Biology* **39**, 124–131 (2015).
95. Imoto, I. *et al.* Identification of cIAP1 as a candidate target gene within an amplicon at 11q22 in esophageal squamous cell carcinomas. *Cancer Res.* **61**, 6629–6634 (2001).
96. Dai, Z. *et al.* A comprehensive search for DNA amplification in lung cancer identifies inhibitors of apoptosis cIAP1 and cIAP2 as candidate oncogenes. *Human Molecular Genetics* **12**, 791–801 (2003).
97. LaCasse, E. *et al.* IAP-targeted therapies for cancer. *Oncogene* **27**, 6252–75 (2008).
98. Zender, L. *et al.* Identification and Validation of Oncogenes in Liver Cancer Using an Integrative Oncogenomic Approach. *Cell* **125**, 1253–1267 (2006).
99. Hu, Y. *et al.* Antisense oligonucleotides targeting XIAP induce apoptosis and enhance chemotherapeutic activity against human lung cancer cells in vitro and in vivo. *Clin. Cancer Res.* **9**, 2826–36 (2003).
100. Yang, L. *et al.* Predominant suppression of apoptosome by inhibitor of apoptosis protein in non-small cell lung cancer H460 cells: Therapeutic effect of a novel polyarginine-conjugated Smac peptide. *Cancer Res.* **63**, 831–837 (2003).
101. Ferreira, C. G. *et al.* Expression of X-linked inhibitor of apoptosis as a novel prognostic marker in radically resected non-small cell lung cancer patients. *Clin. Cancer Res.* **7**, 2468–74 (2001).
102. Moubarak, R. S. *et al.* The death receptor antagonist FLIP-L interacts with Trk and is necessary for neurite outgrowth induced by neurotrophins. *J. Neurosci.* **30**, 6094–6105 (2010).
103. Sole, C. *et al.* The death receptor antagonist FAIM promotes neurite outgrowth by a mechanism that depends on ERK and NF- $\kappa$ B signaling. *J. Cell Biol.* **167**, 479–492 (2004).
104. Liang, Y., Mirnics, Z. K., Yan, C., Nylander, K. D. & Schor, N. F. Bcl-2 mediates induction of neural differentiation. *Oncogene* **22**, 5515–5518 (2003).
105. Fadó, R. *et al.* X-linked inhibitor of apoptosis protein negatively regulates neuronal differentiation through interaction with cRAF and Trk. *Sci. Rep.* **3**, 2397 (2013).
106. Hindi, S. M., Tajrishi, M. M. & Kumar, A. Signaling mechanisms in mammalian myoblast fusion. *Sci. Signal.* **6**, re2 (2013).
107. Dinev, D. *et al.* Extracellular signal regulated kinase 5 (ERK5) is required for the differentiation of muscle cells. *EMBO Rep.* **2**, 829–834 (2001).
108. Gilman, A. G. G proteins: transducers of receptor-generated signals. *Annual review of biochemistry* **56**, 615–649 (1987).
109. Hepler, J. R. & Gilman, A. G. G proteins. *Trends Biochem. Sci.* **17**, 383–387 (1992).
110. Hurowitz, E. H. *et al.* Genomic characterization of the human heterotrimeric G protein alpha, beta, and gamma subunit genes. *DNA Res.* **7**, 111–120 (2000).
111. Murayama, T., Kajiya, Y. & Nomura, Y. Histamine-stimulated and GTP-binding Proteins-mediated Phospholipase A2 activation in rabbit platelets. *J. Biol. Chem.* **265**, 4290–4295 (1990).
112. Maruko, T. *et al.* Involvement of the  $\beta\gamma$  subunits of G proteins in the cAMP response induced by stimulation of the histamine H1 receptor. *Naunyn.*



- Schmiedebergs. Arch. Pharmacol.* **372**, 153–159 (2005).
113. Smrcka, A. V. G protein???? subunits: Central mediators of G protein-coupled receptor signaling. *Cellular and Molecular Life Sciences* **65**, 2191–2214 (2008).
  114. Goitre, L., Trapani, E., Trabalzini, L. & Retta, S. F. The ras superfamily of small GTPases: The unlocked secrets. *Methods in Molecular Biology* **1120**, 1–18 (2014).
  115. Murali, A. & Rajalingam, K. Small Rho GTPases in the control of cell shape and mobility. *Cellular and Molecular Life Sciences* **71**, 1703–1721 (2014).
  116. Jaffe, A. B. & Hall, A. Rho GTPases: biochemistry and biology. *Annu. Rev. Cell Dev. Biol.* **21**, 247–69 (2005).
  117. Aspenström, P., Ruusala, A. & Pacholsky, D. Taking Rho GTPases to the next level: The cellular functions of atypical Rho GTPases. *Experimental Cell Research* **313**, 3673–3679 (2007).
  118. Madaule, P. & Axel, R. A novel ras-related gene family. *Cell* **41**, 31–40 (1985).
  119. Didsbury, J., Weber, R. F., Bokoch, G. M., Evans, T. & Snyderman, R. rac, a novel ras-related family of proteins that are botulinum toxin substrates. *J. Biol. Chem.* **264**, 16378–16382 (1989).
  120. Johnson, D. I. & Pringle, J. R. Molecular characterization of CDC42, a *Saccharomyces cerevisiae* gene involved in the development of cell polarity. *J. Cell Biol.* **111**, 143–52 (1990).
  121. Adams, A. E. M., Johnson, D. I., Longnecker, R. M., Sloat, B. F. & Pringle, J. R. CDC42 and CDC43, two additional genes involved in budding and the establishment of cell polarity in the yeast *Saccharomyces cerevisiae*. *J. Cell Biol.* **111**, 131–142 (1990).
  122. Munemitsu, S. *et al.* Molecular cloning and expression of a G25K cDNA, the human homolog of the yeast cell cycle gene CDC42. *Mol. Cell. Biol.* **10**, 5977–82 (1990).
  123. Evans, T., Brown, M. L., Fraser, E. D. & Northup, J. K. Purification of the major GTP-binding proteins from human placental membranes. *J. Biol. Chem.* **261**, 7052–7059 (1986).
  124. Polakis, P. G., Snyderman, R. & Evans, T. Characterization of G25K, a GTP-binding protein containing a novel putative nucleotide binding domain. *Biochem Biophys Res Commun* **160**, 25–32 (1989).
  125. Waldo, G. L. *et al.* Identification and purification from bovine brain of a guanine-nucleotide-binding protein distinct from Gs, Gi and Go. *Biochem. J.* **246**, 431–9 (1987).
  126. Bustelo, X. R., Sauzeau, V. & Berenjeno, I. M. GTP-binding proteins of the Rho/Rac family: Regulation, effectors and functions in vivo. *BioEssays* **29**, 356–370 (2007).
  127. Bourne, H. R., Sanders, D. A. & McCormick, F. The GTPase superfamily: conserved structure and molecular mechanism. *Nature* **349**, 117–127 (1991).
  128. Valencia, A., Chardin, P., Wittinghofer, A. & Sanders, C. The ras Protein Family: Evolutionary Tree and Role of Conserved Amino Acids. *Biochemistry* **30**, 4637–4648 (1991).
  129. Parri, M. & Chiarugi, P. Rac and Rho GTPases in cancer cell motility control. *Cell Commun. Signal.* **8**, 23 (2010).

130. Abdul-Manan, N. *et al.* Structure of Cdc42 in complex with the GTPase-binding domain of the 'Wiskott-Aldrich syndrome' protein. *Nature* **399**, 379–383 (1999).
131. Worthylake, D. K., Rossman, K. L. & Sondek, J. Crystal structure of Rac1 in complex with the guanine nucleotide exchange region of Tiam1. *Nature* **408**, 682–688 (2000).
132. Hirshberg, M., Stockley, R. W., Dodson, G. & Webb, M. R. The crystal structure of human rac1, a member of the rho-family complexed with a GTP analogue. *Nat. Struct. Biol.* **4**, 147–152 (1997).
133. Chen, Z. *et al.* Activated RhoA binds to the Pleckstrin Homology (PH) domain of PDZ-RhoGEF, a potential site for autoregulation. *J. Biol. Chem.* **285**, 21070–21081 (2010).
134. Rittinger, K. *et al.* Crystal structure of a small G protein in complex with the GTPase-activating protein rhoGAP. *Nature* **388**, 693–697 (1997).
135. Pai, E. F. *et al.* Refined crystal structure of the triphosphate conformation of H-ras p21 at 1.35 Å resolution: implications for the mechanism of GTP hydrolysis. *EMBO J.* **9**, 2351–9 (1990).
136. Karnoub, A. E., Symons, M., Campbell, S. L. & Der, C. J. Molecular basis for Rho GTPase signaling specificity. *Breast Cancer Research and Treatment* **84**, 61–71 (2004).
137. Wittinghofer, A. & Vetter, I. R. Structure-function relationships of the G domain, a canonical switch motif. *Annu. Rev. Biochem.* **80**, 943–971 (2011).
138. Cherfils, J. & Zeghouf, M. Regulation of small GTPases by GEFs, GAPs, and GDIs. *Physiol. Rev.* **93**, 269–309 (2013).
139. Flatau, G. *et al.* Toxin-induced activation of the G protein p21 Rho by deamidation of glutamine. *Nature* **387**, 729–33 (1997).
140. Schmidt, G. *et al.* Gln63 of Rho is deamidated by Escherichia coli cytotoxic necrotizing factor-1. *Nature* **387**, 725–729 (1997).
141. Vetter, I. R. & Wittinghofer, A. The guanine nucleotide-binding switch in three dimensions. *Science* **294**, 1299–1304 (2001).
142. Schaefer, A., Reinhard, N. R. & Hordijk, P. L. Toward understanding RhoGTPase specificity: structure, function and local activation. *Small GTPases* **5**, 1–11 (2014).
143. Thomas, C., Fricke, I., Scrima, A., Berken, A. & Wittinghofer, A. Structural Evidence for a Common Intermediate in Small G Protein-GEF Reactions. *Mol. Cell* **25**, 141–149 (2007).
144. Lammers, M., Meyer, S., Kühmann, D. & Wittinghofer, A. Specificity of interactions between mDia isoforms and Rho proteins. *J. Biol. Chem.* **283**, 35236–35246 (2008).
145. Zong, H., Kaibuchi, K. & Quilliam, L. A. The insert region of RhoA is essential for Rho kinase activation and cellular transformation. *Mol. Cell. Biol.* **21**, 5287–5298 (2001).
146. McCallum, S. J., Wu, W. J. & Cerione, R. A. Identification of a putative effector for Cdc42Hs with high sequence similarity to the RasGAP-related protein IQGAP1 and a Cdc42Hs binding partner with similarity to IQGAP2. *J. Biol. Chem.* **271**, 21732–21737 (1996).
147. Nisimoto, Y., Freeman, J. L. R., Motalebi, S. A., Hirshberg, M. & Lambeth, J. D. Rac binding to p67(phox). Structural basis for interactions of the Rac1 effector region and insert region with components of the respiratory burst

- oxidase. *J. Biol. Chem.* **272**, 18834–18841 (1997).
148. Hamel, B. *et al.* SmgGDS is a guanine nucleotide exchange factor that specifically activates RhoA and RhoC. *J. Biol. Chem.* **286**, 12141–12148 (2011).
149. Lanning, C. C., Daddona, J. L., Ruiz-Velasco, R., Shafer, S. H. & Williams, C. L. The Rac1 C-terminal polybasic region regulates the nuclear localization and protein degradation of Rac1. *J. Biol. Chem.* **279**, 44197–44210 (2004).
150. Ramos, S., Khademi, F., Somesh, B. P. & Rivero, F. Genomic organization and expression profile of the small GTPases of the RhoBTB family in human and mouse. *Gene* **298**, 147–157 (2002).
151. Gao, J., Liao, J. & Yang, G. Y. CAAX-box protein, prenylation process and carcinogenesis. *American Journal of Translational Research* **1**, 312–325 (2009).
152. ten Klooster, J. P. & Hordijk, P. L. Targeting and localized signalling by small GTPases. *Biol. Cell* **99**, 1–12 (2007).
153. Roberts, P. J. *et al.* Rho family GTPase modification and dependence on CAAX motif-signaled posttranslational modification. *J. Biol. Chem.* **283**, 25150–25163 (2008).
154. Berzat, A. C. *et al.* Transforming activity of the Rho family GTPase, Wrch-1, a Wnt-regulated Cdc42 homolog, is dependent on a novel carboxyl-terminal palmitoylation motif. *J. Biol. Chem.* **280**, 33055–33065 (2005).
155. Chenette, E. J., Abo, A. & Der, C. J. Critical and distinct roles of amino- and carboxyl-terminal sequences in regulation of the biological activity of the Chp atypical Rho GTPase. *J. Biol. Chem.* **280**, 13784–13792 (2005).
156. Smithers, C. C. & Overduin, M. Structural Mechanisms and Drug Discovery Prospects of Rho GTPases. *Cells* **5**, 1–15 (2016).
157. Michaelson, D. *et al.* Differential localization of Rho GTPases in live cells: Regulation by hypervariable regions and RhoGDI binding. *J. Cell Biol.* **152**, 111–126 (2001).
158. Bos, J., Rehmann, H. & Wittinghofer, A. GEFs and GAPs : Critical Elements in the Control of Small G Proteins. *Cell* 865–877 (2007). doi:10.1016/j.cell.200
159. DerMardirossian, C. & Bokoch, G. M. GDIs: Central regulatory molecules in Rho GTPase activation. *Trends Cell Biol.* **15**, 356–363 (2005).
160. Moon, S. Y. & Zheng, Y. Rho GTPase-activating proteins in cell regulation. *Trends in Cell Biology* **13**, 13–22 (2003).
161. del Pozo, M. a, Price, L. S., Alderson, N. B., Ren, X. D. & Schwartz, M. a. Adhesion to the extracellular matrix regulates the coupling of the small GTPase Rac to its effector PAK. *EMBO J.* **19**, 2008–14 (2000).
162. Del Pozo, M. A. *et al.* Integrins Regulate Rac Targeting by Internalization of Membrane Domains. *Sci. (New York, NY)* **303**, 839–842 (2004).
163. del Pozo, M. A. *et al.* Integrins regulate GTP-Rac localized effector interactions through dissociation of Rho-GDI. *Nat. Cell Biol* **4**, 232–239 (2002).
164. Olofsson, B. Rho guanine dissociation inhibitors: Pivotal molecules in cellular signalling. *Cellular Signalling* **11**, 545–554 (1999).
165. Jaiswal, M., Fansa, E. K., Dvorsky, R. & Ahmadian, M. R. New insight into the molecular switch mechanism of human Rho family proteins: shifting a paradigm. *Biol. Chem.* **394**, 89–95 (2013).

166. Visvikis, O., Maddugoda, M. P. & Lemichez, E. Direct modifications of Rho proteins: deconstructing GTPase regulation. *Biol. cell* **102**, 377–389 (2010).
167. Aktories, K. Bacterial protein toxins that modify host regulatory GTPases. *Nat. Rev. Microbiol.* **9**, 487–498 (2011).
168. Casey, P. J. & Seabra, M. C. Protein prenyltransferases. *Journal of Biological Chemistry* **271**, 5289–5292 (1996).
169. Lane, K. T. & Beese, L. S. Thematic review series: lipid posttranslational modifications. Structural biology of protein farnesyltransferase and geranylgeranyltransferase type I. *J. Lipid Res.* **47**, 681–699 (2006).
170. Basu, J. Protein palmitoylation and dynamic modulation of protein function. *Current Science* **87**, 212–217 (2004).
171. Casey, P. J., Solski, P. A., Der, C. J. & Buss, J. E. P21Ras Is Modified By a Farnesyl Isoprenoid. *Proc. Natl. Acad. Sci. U. S. A.* **86**, 8323–8327 (1989).
172. Hancock, J. F., Paterson, H. & Marshall, C. J. A polybasic domain or palmitoylation is required in addition to the CAAX motif to localize p21ras to the plasma membrane. *Cell* **63**, 133–139 (1990).
173. Hancock, J. F., Magee, A. I., Childs, J. E. & Marshall, C. J. All ras proteins are polyisoprenylated but only some are palmitoylated. *Cell* **57**, 1167–1177 (1989).
174. Hancock, J. F., Cadwallader, K., Paterson, H. & Marshall, C. J. A CAAX or a CAAL motif and a second signal are sufficient for plasma membrane targeting of ras proteins. *EMBO J.* **10**, 4033–4039 (1991).
175. Hancock, J. F., Cadwallader, K. & Marshall, C. J. Methylation and proteolysis are essential for efficient membrane binding of prenylated p21K-ras(B). *EMBO J.* **10**, 641–646 (1991).
176. Adamson, P., Marshall, C. J., Hall, A. & Tilbrook, P. A. Post-translational modifications of p21rho proteins. *J. Biol. Chem.* **267**, 20033–20038 (1992).
177. Katayama, M. *et al.* The posttranslationally modified C-terminal structure of bovine aortic smooth muscle rhoA p21. *J. Biol. Chem.* **266**, 12639–45 (1991).
178. Navarro-Lérida, I. *et al.* A palmitoylation switch mechanism regulates Rac1 function and membrane organization. *EMBO J.* **31**, 534–51 (2012).
179. Nishimura, A. & Linder, M. E. Identification of a novel prenyl and palmitoyl modification at the CaaX motif of Cdc42 that regulates RhoGDI binding. *Mol. Cell. Biol.* **33**, 1417–1429 (2013).
180. Boulter, E. & Garcia-Mata, R. RhoGDI: A rheostat for the Rho switch. *Small GTPases* **1**, 65–68 (2010).
181. Hornbeck, P. V. *et al.* PhosphoSitePlus, 2014: Mutations, PTMs and recalibrations. *Nucleic Acids Res.* **43**, D512–D520 (2015).
182. Forget, M.-A., Desrosiers, R. R., Gingras, D. & Béliveau, R. Phosphorylation states of Cdc42 and RhoA regulate their interactions with Rho GDP dissociation inhibitor and their extraction from biological membranes. *Biochem. J.* **361**, 243–54 (2002).
183. Ellerbroek, S. M., Wennerberg, K. & Burridge, K. Serine phosphorylation negatively regulates RhoA in vivo. *J. Biol. Chem.* **278**, 19023–19031 (2003).
184. Lehman, H. L. *et al.* Regulation of inflammatory breast cancer cell invasion through Akt1/PKB $\alpha$  phosphorylation of RhoC GTPase. *Mol. Cancer Res.* **10**, 1306–18 (2012).

185. Tillement, V. *et al.* Phosphorylation of RhoB by CK1 impedes actin stress fiber organization and epidermal growth factor receptor stabilization. *Exp. Cell Res.* **314**, 2811–2821 (2008).
186. Tu, S., Wu, W. J., Wang, J. & Cerione, R. A. Epidermal growth factor-dependent regulation of Cdc42 is mediated by the Src tyrosine kinase. *J. Biol. Chem.* **278**, 49293–49300 (2003).
187. Kwon, T., Kwon, D. Y., Chun, J., Kim, J. H. & Kang, S. S. Akt protein kinase inhibits Rac1-GTP binding through phosphorylation at serine 71 of Rac1. *J. Biol. Chem.* **275**, 423–428 (2000).
188. Schoentaube, J., Olling, A., Tatge, H., Just, I. & Gerhard, R. Serine-71 phosphorylation of Rac1/Cdc42 diminishes the pathogenic effect of *Clostridium difficile* toxin A. *Cell. Microbiol.* **11**, 1816–1826 (2009).
189. Tong, J., Li, L., Ballermann, B. & Wang, Z. Phosphorylation of Rac1 T108 by extracellular signal-regulated kinase in response to epidermal growth factor: a novel mechanism to regulate Rac1 function. *Mol. Cell. Biol.* **33**, 4538–51 (2013).
190. Castillo-Lluva, S. *et al.* SUMOylation of the GTPase Rac1 is required for optimal cell migration. *Nat. Cell Biol.* **12**, 1078–1085 (2010).
191. Lerm, M., Pop, M., Fritz, G., Aktories, K. & Schmidt, G. Proteasomal degradation of cytotoxic necrotizing factor 1-activated Rac. *Infect. Immun.* **70**, 4053–4058 (2002).
192. Wang, H.-R. *et al.* Regulation of cell polarity and protrusion formation by targeting RhoA for degradation. *Science* **302**, 1775–1779 (2003).
193. Ozdamar, B. *et al.* Regulation of the polarity protein Par6 by TGFbeta receptors controls epithelial cell plasticity. *Science* **307**, 1603–9 (2005).
194. Zimmerman, E. S., Schulman, B. A. & Zheng, N. Structural assembly of cullin-RING ubiquitin ligase complexes. *Current Opinion in Structural Biology* **20**, 714–721 (2010).
195. Chen, Y. *et al.* Cullin Mediates Degradation of RhoA through Evolutionarily Conserved BTB Adaptors to Control Actin Cytoskeleton Structure and Cell Movement. *Mol. Cell* **35**, 841–855 (2009).
196. Wei, J. *et al.* A new mechanism of RhoA ubiquitination and degradation: Roles of SCFFBXL19 E3 ligase and Erk2. *Biochim. Biophys. Acta - Mol. Cell Res.* **1833**, 2757–2764 (2013).
197. Torrino, S. *et al.* The E3 ubiquitin-ligase HACE1 catalyzes the ubiquitylation of active Rac1. *Dev. Cell* **21**, 959–965 (2011).
198. Heo, J., Raines, K. W., Mocanu, V. & Campbell, S. L. Redox regulation of RhoA. *Biochemistry* **45**, 14481–14489 (2006).
199. Hobbs, G. A., Zhou, B., Cox, A. D. & Campbell, S. L. Rho GTPases, oxidation, and cell redox control. *Small GTPases* **5**, e28579 (2014).
200. Aghajanian, A., Wittchen, E. S., Campbell, S. L. & Burrige, K. Direct Activation of RhoA by Reactive Oxygen Species Requires a Redox-Sensitive Motif. *PLoS One* **4**, (2009).
201. Rocha, C. L., Rucks, E. A., Vincent, D. M. & Olson, J. C. Examination of the coordinate effects of *Pseudomonas aeruginosa* ExoS on Rac1. *Infect. Immun.* **73**, 5458–5467 (2005).
202. Yarbrough, M. L. *et al.* AMPylation of Rho GTPases by *Vibrio* VopS Disrupts Effector Binding and Downstream Signaling. *Science (80-. )*. **323**, 269–272 (2009).



203. Sehr, P. *et al.* Glucosylation and ADP ribosylation of Rho proteins: Effects on nucleotide binding, GTPase activity, and effector coupling. *Biochemistry* **37**, 5296–5304 (1998).
204. Just, I. *et al.* Glucosylation of Rho proteins by *Clostridium difficile* toxin B. *Nature* **375**, 500–503 (1995).
205. Zhang, Y., Rosado, L. A. R., Moon, S. Y. & Zhang, B. Silencing of D4-GDI inhibits growth and invasive behavior in MDA-MB-231 cells by activation of Rac-dependent p38 and JNK signaling. *J. Biol. Chem.* **284**, 12956–12965 (2009).
206. Chen, L., Zhang, J. J. & Huang, X. Y. cAMP inhibits cell migration by interfering with Rac-induced lamellipodium formation. *J. Biol. Chem.* **283**, 13799–13805 (2008).
207. Sala, G. *et al.* Phospholipase Cgamma1 is required for metastasis development and progression. *Cancer Res.* **68**, 10187–96 (2008).
208. Mendoza, M. C. Phosphoregulation of the WAVE regulatory complex and signal integration. *Seminars in Cell and Developmental Biology* **24**, 272–279 (2013).
209. Nakanishi, O., Suetsugu, S., Yamazaki, D. & Takenawa, T. Effect of WAVE2 phosphorylation on activation of the Arp2/3 complex. *J. Biochem.* **141**, 319–325 (2007).
210. Danson, C. M., Pocha, S. M., Bloomberg, G. B. & Cory, G. O. Phosphorylation of WAVE2 by MAP kinases regulates persistent cell migration and polarity. *J. Cell Sci.* **120**, 4144–54 (2007).
211. Mendoza, M. C. *et al.* ERK-MAPK Drives Lamellipodia Protrusion by Activating the WAVE2 Regulatory Complex. *Mol. Cell* **41**, 661–671 (2011).
212. Mullins, R. D., Heuser, J. a & Pollard, T. D. The interaction of Arp2/3 complex with actin: nucleation, high affinity pointed end capping, and formation of branching networks of filaments. *Proc. Natl. Acad. Sci. U. S. A.* **95**, 6181–6186 (1998).
213. Rotty, J. D., Wu, C. & Bear, J. E. New insights into the regulation and cellular functions of the ARP2/3 complex. *Nat. Rev. Mol. Cell Biol.* **14**, 7–12 (2013).
214. Vadlamudi, R. K., Li, F., Barnes, C. J., Bagheri-Yarmand, R. & Kumar, R. p41-Arc subunit of human Arp2/3 complex is a p21-activated kinase-1-interacting substrate. *EMBO Rep.* **5**, 154–60 (2004).
215. Edwards, D. C., Sanders, L. C., Bokoch, G. M. & Gill, G. N. Activation of LIM-kinase by Pak1 couples Rac/Cdc42 GTPase signalling to actin cytoskeletal dynamics. *Nat Cell Biol.* **1**, 253–259 (1999).
216. Bokoch, G. M. Regulation of cell function by Rho family GTPases. *Immunol. Res.* **21**, 139–148 (2000).
217. Rayala, S. K., Molli, P. R. & Kumar, R. Nuclear p21-activated kinase 1 in breast cancer packs off tamoxifen sensitivity. *Cancer Research* **66**, 5985–5988 (2006).
218. Ong, C. C. *et al.* p21-activated kinase 1: PAK'ed with potential. *Oncotarget* **2**, 491–496 (2011).
219. Sugihara, K. *et al.* Rac1 is required for the formation of three germ layers during gastrulation. *Oncogene* **17**, 3427–3433 (1998).
220. Benvenuti, F. *et al.* Requirement of Rac1 and Rac2 expression by mature dendritic cells for T cell priming. *Science* **305**, 1150–3 (2004).
221. Wheeler, A. P. *et al.* Rac1 and Rac2 regulate macrophage morphology but

- are not essential for migration. *J. Cell Sci.* **119**, 2749–57 (2006).
222. Walmsley, M. J. *et al.* Critical roles for Rac1 and Rac2 GTPases in B cell development and signaling. *Science* **302**, 459–62 (2003).
223. Guo, F., Cancelas, J. A., Hildeman, D., Williams, D. A. & Zheng, Y. Rac GTPase isoforms Rac1 and Rac2 play a redundant and crucial role in T-cell development. *Blood* **112**, 1767–1775 (2008).
224. Benninger, Y. *et al.* Essential and distinct roles for cdc42 and rac1 in the regulation of Schwann cell biology during peripheral nervous system development. *J. Cell Biol.* **177**, 1051–1061 (2007).
225. Wu, Y. I. *et al.* A genetically encoded photoactivatable Rac controls the motility of living cells. *Nature* **461**, 104–108 (2009).
226. Wu, Y. I., Wang, X., He, L., Montell, D. & Hahn, K. M. Spatiotemporal control of small GTPases with light using the LOV domain. *Methods Enzymol.* **497**, 393–407 (2011).
227. Wang, X., He, L., Wu, Y. I., Hahn, K. M. & Montell, D. J. Light-mediated activation reveals a key role for Rac in collective guidance of cell movement in vivo. *Nat. Cell Biol.* **12**, 591–7 (2010).
228. Kato, T., Kawai, K., Egami, Y., Takehi, Y. & Araki, N. Rac1-dependent lamellipodial motility in prostate cancer PC-3 cells revealed by optogenetic control of Rac1 activity. *PLoS One* **9**, (2014).
229. Hinde, E., Digman, M. A., Hahn, K. M. & Gratton, E. Millisecond spatiotemporal dynamics of FRET biosensors by the pair correlation function and the phasor approach to FLIM. *Proc. Natl. Acad. Sci. U. S. A.* **110**, 135–40 (2013).
230. Machacek, M. *et al.* Coordination of Rho GTPase activities during cell protrusion. *Nature* **461**, 99–103 (2009).
231. Liu, S. Y., Yen, C. Y., Yang, S. C., Chiang, W. F. & Chang, K. W. Overexpression of Rac-1 small GTPase binding protein in oral squamous cell carcinoma. *J. Oral Maxillofac. Surg.* **62**, 702–707 (2004).
232. Schnelzer, a *et al.* Rac1 in human breast cancer: overexpression, mutation analysis, and characterization of a new isoform, Rac1b. *Oncogene* **19**, 3013–20 (2000).
233. Lin, Y. & Zheng, Y. Approaches of Targeting Rho GTPases in Cancer Drug Discovery. *Expert Opin. Drug Discov.* **10**, 991–1010 (2015).
234. Engers, R. *et al.* Prognostic relevance of increased Rac GTPase expression in prostate carcinomas. *Endocr. Relat. Cancer* **14**, 245–256 (2007).
235. Pan, Y. *et al.* Expression of seven main Rho family members in gastric carcinoma. *Biochem. Biophys. Res. Commun.* **315**, 686–691 (2004).
236. Kamai, T. *et al.* Overexpression of RhoA, Rac1, and Cdc42 GTPases is associated with progression in testicular cancer. *Clin. Cancer Res.* **10**, 4799–4805 (2004).
237. Hodis, E. *et al.* A landscape of driver mutations in melanoma. *Cell* **150**, 251–263 (2012).
238. Krauthammer, M. *et al.* Exome sequencing identifies recurrent somatic RAC1 mutations in melanoma. *Nat. Genet.* **44**, 1006–14 (2012).
239. Halaban, R. RAC1 and Melanoma. *Clinical Therapeutics* **37**, 682–685 (2015).
240. Huang, M. & Prendergast, G. C. RhoB in cancer suppression. *Histology and Histopathology* **21**, 213–218 (2006).

241. Gómez Del Pulgar, T., Benitah, S. A., Valerón, P. F., Espina, C. & Lacal, J. C. Rho GTPase expression in tumourigenesis: Evidence for a significant link. *BioEssays* **27**, 602–613 (2005).
242. Friedl, P. & Wolf, K. Tumour-cell invasion and migration: diversity and escape mechanisms. *Nat. Rev. Cancer* **3**, 362–74 (2003).
243. Hornburger, M. C. *et al.* A novel role for inhibitor of apoptosis (IAP) proteins as regulators of endothelial barrier function by mediating RhoA activation. *FASEB J.* **28**, 1938–1946 (2014).
244. Kurokawa, K. & Matsuda, M. Localized RhoA Activation as a Requirement for the Induction of Membrane Ruffling. *Mol. Biol. Cell* **16**, 4294–4303 (2005).
245. El-Sibai, M. *et al.* RhoA/ROCK-mediated switching between Cdc42- and Rac1-dependent protrusion in MTLn3 carcinoma cells. *Exp. Cell Res.* **314**, 1540–1552 (2008).
246. Pertz, O., Hodgson, L., Klemke, R. L. & Hahn, K. M. Spatiotemporal dynamics of RhoA activity in migrating cells. *Nature* **440**, 1069–72 (2006).
247. Vega, F. M., Fruhwirth, G., Ng, T. & Ridley, A. J. RhoA and RhoC have distinct roles in migration and invasion by acting through different targets. *J. Cell Biol.* **193**, 655–665 (2011).
248. Kanai, M., Crowe, M. S., Zheng, Y., Vande Woude, G. F. & Fukasawa, K. RhoA and RhoC are both required for the ROCK II-dependent promotion of centrosome duplication. *Oncogene* **29**, 6040–50 (2010).
249. Fritz, G., Just, I. & Kaina, B. Rho GTPases are over-expressed in human tumors - Fritz - 1999 - International Journal of Cancer - Wiley Online Library. *Int. J. Cancer* (1999).
250. Li, X. R. *et al.* Overexpression of RhoA is associated with poor prognosis in hepatocellular carcinoma. *Eur. J. Surg. Oncol.* **32**, 1130–4 (2006).
251. Horiuchi, A. *et al.* Up-regulation of small GTPases, RhoA and RhoC, is associated with tumor progression in ovarian carcinoma. *Lab. Invest.* **83**, 861–870 (2003).
252. Kamai, T. *et al.* Significant association of Rho/ROCK pathway with invasion and metastasis of bladder cancer. *Clin. Cancer Res.* **9**, 2632–2641 (2003).
253. Faried, A., Faried, L. S., Usman, N., Kato, H. & Kuwano, H. Clinical and prognostic significance of RhoA and RhoC gene expression in esophageal squamous cell carcinoma. *Ann. Surg. Oncol.* **14**, 3593–601 (2007).
254. Sandilands, E. *et al.* RhoB and actin polymerization coordinate Src activation with endosome-mediated delivery to the membrane. *Dev. Cell* **7**, 855–869 (2004).
255. Fernandez-Borja, M., Janssen, L., Verwoerd, D., Hordijk, P. & Neefjes, J. RhoB regulates endosome transport by promoting actin assembly on endosomal membranes through Dia1. *J. Cell Sci.* **118**, 2661–2670 (2005).
256. Wheeler, A. P. & Ridley, A. J. RhoB affects macrophage adhesion, integrin expression and migration. *Exp. Cell Res.* **313**, 3505–3516 (2007).
257. Vega, F. M., Colomba, A., Reymond, N., Thomas, M. & Ridley, A. J. RhoB regulates cell migration through altered focal adhesion dynamics. *Open Biol* **2**, 120076 (2012).
258. Vega, F. M., Thomas, M., Reymond, N. & Ridley, A. J. The Rho GTPase RhoB regulates cadherin expression and epithelial cell-cell interaction. *Cell Commun. Signal.* **13**, 1–9 (2015).



259. Rodriguez, P. L., Sahay, S., Olabisi, O. O. & Whitehead, I. P. ROCK I-mediated activation of NF- $\kappa$ B by RhoB. *Cell. Signal.* **19**, 2361–2369 (2007).
260. Alfano, D., Ragno, P., Stoppelli, M. P. & Ridley, a. J. RhoB regulates uPAR signalling. *J. Cell Sci.* **125**, 2369–2380 (2012).
261. Thurnherr, T. *et al.* Cdc42 and Rac1 signaling are both required for and act synergistically in the correct formation of myelin sheaths in the CNS. *J. Neurosci.* **26**, 10110–9 (2006).
262. Garvalov, B. K. *et al.* Cdc42 regulates cofilin during the establishment of neuronal polarity. *J. Neurosci.* **27**, 13117–13129 (2007).
263. Lee, K. *et al.* Cdc42 promotes host defenses against fatal infection. *Infect. Immun.* **81**, 2714–2713 (2013).
264. Zhang, H. *et al.* Myosin-X provides a motor-based link between integrins and the cytoskeleton. *Nat. Cell Biol.* **6**, 523–531 (2004).
265. Kerber, M. L. *et al.* A Novel Form of Motility in Filopodia Revealed by Imaging Myosin-X at the Single-Molecule Level. *Curr. Biol.* **19**, 967–973 (2009).
266. Eilken, H. M. & Adams, R. H. Dynamics of endothelial cell behavior in sprouting angiogenesis. *Current Opinion in Cell Biology* **22**, 617–625 (2010).
267. Johnston, S. A., Bramble, J. P., Yeung, C. L., Mendes, P. M. & Machesky, L. M. Arp2/3 complex activity in filopodia of spreading cells. *BMC Cell Biol.* **9**, 65 (2008).
268. Cohen, M., Georgiou, M., Stevenson, N. L., Miodownik, M. & Baum, B. Dynamic Filopodia Transmit Intermittent Delta-Notch Signaling to Drive Pattern Refinement during Lateral Inhibition. *Dev. Cell* **19**, 78–89 (2010).
269. Lee, K., Gallop, J. L., Rambani, K. & Kirschner, M. W. Self-assembly of filopodia-like structures on supported lipid bilayers. *Science* **329**, 1341–5 (2010).
270. Brill-Karniely, Y., Ideses, Y., Bernheim-Groswasser, A. & Ben-Shaul, A. From branched networks of actin filaments to bundles. *ChemPhysChem* **10**, 2818–2827 (2009).
271. Steffen, A. *et al.* Filopodia formation in the absence of functional WAVE- and Arp2/3-complexes. *Mol. Biol. Cell* **17**, 2581–91 (2006).
272. Yang, C. *et al.* Novel roles of formin mDia2 in lamellipodia and filopodia formation in motile cells. *PLoS Biol.* **5**, 2624–2645 (2007).
273. Schirenbeck, A., Bretschneider, T., Arasada, R., Schleicher, M. & Faix, J. The Diaphanous-related formin dDia2 is required for the formation and maintenance of filopodia. *Nat. Cell Biol.* **7**, 619–625 (2005).
274. Peng, J., Wallar, B. J., Flanders, A., Swiatek, P. J. & Alberts, A. S. Disruption of the Diaphanous-related formin Drf1 gene encoding mDia1 reveals a role for Drf3 as an effector for Cdc42. *Curr. Biol.* **13**, 534–545 (2003).
275. Tucci, M. G. *et al.* Involvement of E-cadherin,  $\beta$ -catenin, Cdc42 and CXCR4 in the progression and prognosis of cutaneous melanoma. *Br. J. Dermatol.* **157**, 1212–1216 (2007).
276. Reymond, N. *et al.* Cdc42 promotes transendothelial migration of cancer cells through  $\beta$ 1 integrin. *J. Cell Biol.* **199**, 653–68 (2012).
277. Doyle, A. D., Petrie, R. J., Kutys, M. L. & Yamada, K. M. Dimensions in cell migration. *Current Opinion in Cell Biology* **25**, 642–649 (2013).
278. Petrie, R. J. & Yamada, K. M. At the leading edge of three-dimensional cell

- migration. *J. Cell Sci.* **125**, 5917–5926 (2012).
279. Linder, S., Wiesner, C. & Himmel, M. Degrading devices: invadosomes in proteolytic cell invasion. *Annu. Rev. Cell Dev. Biol.* **27**, 185–211 (2011).
280. Baker, B. M. & Chen, C. S. Deconstructing the third dimension - how 3D culture microenvironments alter cellular cues. *J. Cell Sci.* **125**, 3015–3024 (2012).
281. Wyckoff, J. B., Jones, J. G., Condeelis, J. S. & Segall, J. E. A critical step in metastasis: In vivo analysis of intravasation at the primary tumor. *Cancer Res.* **60**, 2504–2511 (2000).
282. Friedl, P. *et al.* Migration of Coordinated Cell Clusters in Mesenchymal and Epithelial Cancer Explants in Vitro. *Cancer Res.* **55**, 4557–4560 (1995).
283. Friedl, P., Hegerfeldt, Y. & Tusch, M. Collective cell migration in morphogenesis and cancer. *International Journal of Developmental Biology* **48**, 441–449 (2004).
284. Kalluri, R. EMT: When epithelial cells decide to become mesenchymal-like cells. *Journal of Clinical Investigation* **119**, 1417–1419 (2009).
285. Geisbrecht, E. R. & Montell, D. J. A role for Drosophila IAP1-mediated caspase inhibition in Rac-dependent cell migration. *Cell* **118**, 111–125 (2004).
286. Marivin, a *et al.* cIAP1 regulates TNF-mediated cdc42 activation and filopodia formation. *Oncogene* **33**, 1–12 (2013).
287. Liu, J. *et al.* E3 ligase activity of XIAP RING domain is required for XIAP-mediated cancer cell migration, but not for its RhoGDI binding activity. *PLoS One* **7**, (2012).
288. Liu, J. *et al.* X-linked Inhibitor of Apoptosis Protein (XIAP) mediates cancer cell motility via Rho GDP Dissociation Inhibitor (RhoGDI)-dependent regulation of the cytoskeleton. *J. Biol. Chem.* **286**, 15630–15640 (2011).
289. Yu, J. *et al.* RhoGDI SUMOylation at Lys-138 increases its binding activity to Rho GTPase and its inhibiting cancer cell motility. *J. Biol. Chem.* **287**, 13752–13760 (2012).
290. Ahn, S. & Park, H. XIAP is essential for shear stress-enhanced Tyr-576 phosphorylation of FAK. *Biochem. Biophys. Res. Commun.* **399**, 256–261 (2010).
291. Dohi, T. *et al.* An IAP-IAP complex inhibits apoptosis. *J. Biol. Chem.* **279**, 34087–34090 (2004).
292. Rajalingam, K. *et al.* IAP-IAP complexes required for apoptosis resistance of *C. trachomatis*-infected cells. *PLoS Pathog.* **2**, 1013–1023 (2006).
293. Doye, A. *et al.* CNF1 exploits the ubiquitin-proteasome machinery to restrict Rho GTPase activation for bacterial host cell invasion. *Cell* **111**, 553–564 (2002).
294. Dubielecka, P. M. *et al.* Essential role for Abi1 in embryonic survival and WAVE2 complex integrity. *Proc. Natl. Acad. Sci.* **108**, 7022–7027 (2011).
295. Beli, P., Mascheroni, D., Xu, D. & Innocenti, M. WAVE and Arp2/3 jointly inhibit filopodium formation by entering into a complex with mDia2. *Nat. Cell Biol.* **10**, 849–857 (2008).
296. Suraneni, P. *et al.* The Arp2/3 complex is required for lamellipodia extension and directional fibroblast cell migration. *J. Cell Biol.* **197**, 239–251 (2012).
297. Aggarwal, A. *et al.* Mobilization of HIV spread by diaphanous 2 dependent

- filopodia in infected dendritic cells. *PLoS Pathog.* **8**, (2012).
298. Linda Yang, Lei Wang, and Y. Z. Gene Targeting of Cdc42 and Cdc42GAP Affirms the Critical Involvement of Cdc42 in Filopodia Induction, Directed Migration, and Proliferation in Primary Mouse Embryonic Fibroblasts. *Mol. Biol. Cell* **18**, 986–994 (2007).
299. Czuchra, A. *et al.* Cdc42 Is Not Essential for Filopodium Formation, Directed Migration, Cell Polarization, and Mitosis in Fibroblastoid Cells □ D □ V. *Mol. Biol. Cell* **16**, 4473–4484 (2005).
300. Royal, I., Lamarche-Vane, N., Lamorte, L., Kaibuchi, K. & Park, M. Activation of Cdc42, Rac, PAK, and Rho-Kinase in Response to Hepatocyte Growth Factor Differentially Regulates Epithelial Cell Colony Spreading and Dissociation. *Mol. Biol. Cell* **11**, 1709–1725 (2000).
301. Lin, K. T. *et al.* Vav3-Rac1 signaling regulates prostate cancer metastasis with elevated Vav3 expression correlating with prostate cancer progression and posttreatment recurrence. *Cancer Res.* **72**, 3000–3009 (2012).
302. Chang, K. H. *et al.* Vav3 collaborates with p190-BCR-ABL in lymphoid progenitor leukemogenesis, proliferation, and survival. *Blood* **120**, 800–811 (2012).
303. Citterio, C. *et al.* The Rho Exchange Factors Vav2 and Vav3 Control a Lung Metastasis-Specific Transcriptional Program in Breast Cancer Cells. *Sci. Signal.* **5**, ra71-ra71 (2012).
304. Meller, N. CZH proteins: a new family of Rho-GEFs. *J. Cell Sci.* **118**, 4937–4946 (2005).
305. McGhee, S. A. & Chatila, T. A. DOCK8 immune deficiency as a model for primary cytoskeletal dysfunction. *Dis. Markers* **29**, 151–156 (2010).
306. Hoffman, G. R., Nassar, N. & Cerione, R. a. Structure of the Rho family GTP-binding protein Cdc42 in complex with the multifunctional regulator RhoGDI. *Cell* **100**, 345–356 (2000).
307. Sahai, E., Garcia-Medina, R., Pouysségur, J. & Vial, E. Smurf1 regulates tumor cell plasticity and motility through degradation of RhoA leading to localized inhibition of contractility. *J. Cell Biol.* **176**, 35–42 (2007).
308. Bryan, B. *et al.* Ubiquitination of RhoA by Smurf1 promotes neurite outgrowth. *FEBS Lett.* **579**, 1015–1019 (2005).
309. Wang, M. *et al.* ATR/Chk1/Smurf1 pathway determines cell fate after DNA damage by controlling RhoB abundance. *Nat. Commun.* **5**, 4901 (2014).
310. Zhao, J. *et al.* SCF E3 ligase F-box protein complex SCFFBXL19 regulates cell migration by mediating Rac1 ubiquitination and degradation. *FASEB J.* **27**, 2611–2619 (2013).
311. Dong, S. *et al.* F-box protein complex FBXL19 regulates TGFβ1-induced E-cadherin down-regulation by mediating Rac3 ubiquitination and degradation. *Mol. Cancer* **13**, 76 (2014).
312. Jin, L., Williamson, A., Banerjee, S., Philipp, I. & Rape, M. Mechanism of Ubiquitin-Chain Formation by the Human Anaphase-Promoting Complex. *Cell* **133**, 653–665 (2008).
313. Xu, P. *et al.* Quantitative Proteomics Reveals the Function of Unconventional Ubiquitin Chains in Proteasomal Degradation. *Cell* **137**, 133–145 (2009).
314. Koegl, M. *et al.* A Novel Ubiquitination Factor, E4, Is Involved in

- Multiubiquitin Chain Assembly. *Cell* **96**, 635–644 (1999).
315. Vandenabeele, P. & Bertrand, M. J. M. The role of the IAP E3 ubiquitin ligases in regulating pattern-recognition receptor signalling. *Nat. Rev. Immunol.* **12**, 833–844 (2012).
  316. Mansouri, A., Zhang, Q., Ridgway, L. D., Tian, L. & Claret, F.-X. Cisplatin resistance in an ovarian carcinoma is associated with a defect in programmed cell death control through XIAP regulation. *Oncol. Res.* **13**, 399–404 (2003).
  317. Holcik, M., Yeh, C., Korneluk, R. G. & Chow, T. Translational upregulation of X-linked inhibitor of apoptosis (XIAP) increases resistance to radiation induced cell death. *Oncogene* **19**, 4174–4177 (2000).
  318. Hwang, C. *et al.* X-linked inhibitor of apoptosis deficiency in the TRAMP mouse prostate cancer model. *Cell Death Differ.* **15**, 831–840 (2008).
  319. Ong, C. C. *et al.* Targeting p21-activated kinase 1 (PAK1) to induce apoptosis of tumor cells. *Proc. Natl. Acad. Sci. U. S. A.* **108**, 7177–82 (2011).
  320. Pocha, S. M. & Cory, G. O. WAVE2 is regulated by multiple phosphorylation events within its VCA domain. *Cell Motil. Cytoskeleton* **66**, 36–47 (2009).
  321. Kurisu, S., Suetsugu, S., Yamazaki, D., Yamaguchi, H. & Takenawa, T. Rac-WAVE2 signaling is involved in the invasive and metastatic phenotypes of murine melanoma cells. *Oncogene* **24**, 1309–1319 (2005).
  322. Yamazaki, D., Kurisu, S. & Takenawa, T. Involvement of Rac and Rho signaling in cancer cell motility in 3D substrates. *Oncogene* **28**, 1570–1583 (2009).
  323. Silva, J. M. *et al.* Cyfip1 Is a Putative Invasion Suppressor in Epithelial Cancers. *Cell* **137**, 1047–1061 (2009).
  324. Kurisu, S. & Takenawa, T. WASP and WAVE family proteins: Friends or foes in cancer invasion? *Cancer Science* **101**, 2093–2104 (2010).
  325. Stengel, K. R. & Zheng, Y. Essential role of cdc42 in Ras-Induced transformation revealed by gene targeting. *PLoS One* **7**, (2012).
  326. Prendergast, G. C. *et al.* Critical role of Rho in cell transformation by oncogenic Ras. *Oncogene* **10**, 2289–2296 (1995).
  327. Qiu, R. G., Chen, J., Kirn, D., McCormick, F. & Symons, M. An essential role for Rac in Ras transformation. *Nature* **374**, 457–9 (1995).
  328. Khosravi-Far, R., Soliski, P. A., Clark, G. J., Kinch, M. S. & Der, C. J. Activation of Rac1, RhoA, and mitogen-activated protein kinases is required for Ras transformation. *Mol. Cell. Biol.* **15**, 6443–6453 (1995).

## 6. List of Publications

- **Murali A**, Shin J, Yurugi H, Krishnan A, Akutsu M, Carpy A, Macek B, Rajalingam K. Ubiquitin mediated regulation of Cdc42 by XIAP; Cell Death Dis. 2017 (In press)
- **Murali A**, Rajalingam K. Small Rho GTPases in the control of cell shape and mobility; Cell Mol Life Sci. 2014 May; 71(9):1703-21. doi: 10.1007/s00018-013-1519-6. Epub 2013 Nov 26.
- Oberoi-Khanuja TK, **Murali A**, Rajalingam K. IAPs on the move: role of inhibitors of apoptosis proteins in cell migration; Cell Death Dis. 2013 Sep 5;4:e784. doi: 10.1038/cddis.2013.311
- Oberoi-Khanuja TK, **Murali A**, Dogan T, Karreman C, Rajalingam K. IAPs regulate cell shape changes and migration in a WAVE2-complex dependent manner (Manuscript in Revision)

